ASYMMETRIC BUSINESS CYCLES IN EMERGING MARKET ECONOMIES

Nadav Ben Zeev

Discussion Paper No. 19-09

September 2019

Asymmetric Business Cycles in Emerging Market Economies

Nadav Ben Zeev[*]

Ben-Gurion University of the Negev

September 26, 2019

Abstract

I document that business cycles in emerging market economies (EMEs) for pre-2008 data appear to be rather symmetric while being strongly asymmetric when post-2008 data is included. I then study this asymmetry through the lens of global risk appetite shocks, which are commonly viewed as central to the recent global recession and are implied by theory to have the potential of generating asymmetric business cycles. Using a nonlinear panel fixed-effects Bayesian framework that can identify sign-dependent impulse responses, I show that adverse global risk appetite shocks lead to much bigger declines in EMEs' output than the corresponding increases induced by favorable shocks. Financial frictions in EMEs seem to be an important mechanism underlying the strong asymmetry in impulse responses.

JEL classification: F41,F44

Key words: Emerging market economies; Asymmetric Business Cycles; Global risk appetite shocks; Sign-dependent impulse responses

---

[*]*Contact details:* Department of Economics, Ben-Gurion University of the Negev. P.O.B 653, Beer-Sheva 84105, Israel.
E-mail: nadavbz@bgu.ac.il.

1 Introduction

The issue of business cycle asymmetry in emerging market economies (EMEs), i.e., whether EMEs' economic activity behaves differently in recessions than in expansions, has mainly been studied in the context of Sudden Stops (see, e.g., Mendoza (2002), Durdu et al. (2009), Mendoza (2010), and Korinek and Mendoza (2014)).[1] However, as emphasized in Mendoza (2010), Sudden Stops are rare events nested within normal business cycles. Therefore, a better understanding of the potential asymmetry in EMEs business cycles necessarily requires research that goes beyond Sudden-Stops-induced business cycles and centers around the potentially asymmetric implications of the forces that generate more regular business cycles in these economies.

The Objective of this Paper.   The empirical questions this paper tries to address are the following: *i*) is the unconditional evidence on EMEs business cycles indicative of their being asymmetric?; *ii*) studying this potential asymmetry through the lens of a relevant candidate shock for producing such asymmetry, does the resulting conditional evidence point to significant asymmetry in EMEs' response to this shock?; and *iii*) what mechanism can explain the potential shock-induced asymmetry studied from addressing the previous question?

To address these questions, this paper unfolds in three parts. The first part provides unconditional evidence on business cycle asymmetry in EMEs which serves as motivation for studying the potentially asymmetric effects of shocks that are most closely related to the recent 2008-2009 global recession. The second part presents theoretical motivation for studying EMEs business cycle asymmetry through the lens of global risk appetite shocks, which have received increased attention recently following the 2008-2009 global recession as potential business-cycle-inducing shocks in EMEs (see, e.g., Carrire-Swallow and Cspedes (2013), Cesa-Bianchi et al. (2018), Ben Zeev (2017, 2019a), and Caballero and Kamber (2019)). And the third part conducts a thorough empirical investigation into the possibly asymmetric effects of these shocks on EMEs.

---

[1]The empirical classification of Sudden Stops normally defines them as severe and sudden falls in net capital inflows accompanied by sharp current account reversals (see, e.g., Ferretti and Razin (2000), Calvo and Reinhart (2000), and Calvo et al. (2006)).

Unconditional Evidence. In this part I establish unconditional evidence on significant business cycle asymmetry in a panel of 42 EMEs that encompasses the universe of EMEs with reasonable spans of quarterly macro data. However, this strong asymmetry is shown to be entirely driven by the recent 2008-2009 global recession, as it vanishes once post-2008 data is excluded from the sample. To obtain this unconditional evidence, I compute higher moments of trend-adjusted output growth rates accumulated at reasonable business cycle frequencies for the entire sample as well as separately for recessions and expansions, while differentiating between pre-2008 post-2008-inclusive samples. These calculations indicate that the distribution of the two-year cumulative growth rate in EMEs' output is highly asymmetric for the baseline 1986-2017 sample, exhibiting a significantly negative skewness of -0.85. Moreover, separating the sample into recessions and expansions, where recessions are defined as being characterized by at least two consecutive quarters of negative trend-adjusted output growth, I find that recessions defined as such (which account for 32% of the observations) exhibit -1.8% two-year average trend-adjusted output growth rate with a skewness of -1.3 compared to corresponding numbers of 1% and -0.6 for expansions.

Nevertheless, once only pre-2008 observations are included, the skewness becomes mildly positive at 0.17 with recessions- and expansions-specific skewness values of 0.1 and 0.3, respectively. I.e., the recent global recession of 2008-2009 is driving the observed negative skewness of output growth in EMEs. And this highlights that the shock that played a central role in generating this recession may have interesting asymmetric elements underlying its transmission into EMEs which go beyond the sheer size of this recession.

Theoretical Motivation. This part lays out a simple structural framework that builds on the costly state verification (CSV) problem between lenders and borrowers from Townsend (1979) (and as later used in Bernanke et al. (1999) (BGG)) with the aim of studying the potential sign-dependency of risk appetite shocks' effects. Specifically, my motivation centers around the risk underlying this problem, defined as the variance of idiosyncratic productivity shocks faced by the borrower. While it is well understood that the severity of the agency problem between the lender

and the borrower is increasing in this risk measure, with this severity measured by the elasticity of the external finance premium (EFP) and leverage, I highlight the asymmetric aspect of risk in this setting (which has not been explored to my knowledge): for given leverage, higher risk produces a larger upward shift in the EFP-leverage curve (and thus in borrowing costs) than the downward shift induced by lower risk.

I provide intuition for this asymmetry result that is based on the convexity of lenders' expected monitoring costs (in case of default) in risk and show in a simple, stochastic capital market equilibrium model that this asymmetry result implies a greater effect of positive risk shocks on EFP and investment than the corresponding effect of negative shocks. While very stylized and simple, the framework I use still serves as a conceptual base upon which to build the discussion of the empirical results (discussed next) and to help in motivating this paper's focus on global risk appetite shocks as a source of business cycle asymmetry in EMEs. More specifically, considering that EMEs are in general very reliant on credit from global lenders, with roughly a third of all external liabilities of EMEs being held by foreign banks (Bräuning and Ivashina (2019)), one can make the case that asymmetric implications of global risk appetite shocks for the financial frictions between global lenders and borrowers from EMEs may have the potential of producing business cycle asymmetry in these economies.

Conditional Evidence. Motivated by the results from the above-mentioned first two parts, this part aims to produce conditional evidence consistent with these results. The underlying fundamental I use to empirically measure global risk appetite shocks is the financial bond premium (FBP) series from Gilchrist and Zakrajšek (2011) and Gilchrist and Zakrajšek (2012a). Building on

the methodology from Gilchrist and Zakrajšek (2012b),[2] these papers use micro-level data for 193 financial intermediaries to construct a credit spread index which they decompose into a component that captures firm-specific information on expected defaults and a residual component that they termed as FBP which represents the shifts in financial intermediaries' risk attitudes. Since their FBP series serves as an exogenous and common global risk shock to EMEs that represents exogenous variation in the risk appetite of financial intermediaries, it can be employed to study whether impulse responses to global risk appetite shocks are sign-dependent (as explained next).

To identify the asymmetric effects of global risk appetite shocks, I perform a Bayesian estimation procedure which proceeds in three steps. First, I regress FBP on lags of its raw values and squared values as well as lags of raw and squared values of U.S. stock prices. Second, I regress the residual from the first step on its squared value and take the standardized residual from this regression to be the global risk appetite shock series. The second estimation step is meant to ensure that any contemporaneous, exogenous sign-dependent mechanism (as reflected in terms of squared values of the risk appetite shock) linking the global risk appetite shock and its associated fundamental (i.e., FBP) is not biasing my identified shock series. Indeed, the coefficient from the regression of the second step is significantly positive, indicating that there appears to be such contemporaneous mechanism; in accordance with this, as discussed on Page 26, the contemporaneous response of FBP to a positive shock is significantly larger than the corresponding response to a negative shock. Third, I estimate local projection regressions á la Jorda (2005) in a panel fixed-effects setting of outcome variables of interest on current raw and squared values of

---

[2]I also confirmed that the results of this paper are robust to using the excess bond premium (EBP) series from Gilchrist and Zakrajšek (2012b), which is the residual of non-financial firms (as opposed to financial) credit spreads left after controlling for firm-specific information on expected defaults. However, for the baseline analysis, I prefer to use the FBP series based on the following reasoning. For EMEs to respond asymmetrically to global risk shocks in a manner that goes beyond the asymmetry implied by a basic trade channel, the direct relationship between foreign lenders and EMEs-based borrowers needs to asymmetrically respond to foreign lenders' risk appetite shocks. Hence, to properly represent this reasoning from an empirical standpoint, one needs a good measure of foreign lenders' risk appetite. As argued in Gilchrist and Zakrajšek (2011), Gilchrist and Zakrajšek (2012a), and Gertler and Gilchrist (2018), such good measure arguably comes from FBP as this residual component is a good measure of financial intermediaries' risk appetite, which in turn reasonably reflects the degree of disruption (or tranquility) of global credit intermediation. (Also see related discussion on Page 38 on the superiority of the FBP measure for the purposes of this paper.)

4

the extracted shock series from the second step and construct impulse responses to positive and negative shocks from the first- and second-order polynomial coefficients. Ben Zeev (2019b) has shown that this approach to estimating impulse response sign-dependency does a good job of identifying the true response asymmetry when the true data generating process admits a second-order moving average process, as implied by a wide class of DSGE models (see, e.g., Lan and Meyer-Gohde (2013)).[3] I defer a more detailed description of the Bayesian estimation procedure to Section 4.2 and Appendix B.

My empirical findings can be summarized as follows. There is a statistically significant difference between the response of output to adverse and favorable global risk appetite shocks, with the former inducing output declines that are significantly larger in absolute terms than the corresponding output increases following favorable shocks. Response asymmetries are also economically significant. Specifically, the largest output response asymmetry for global risk appetite shocks takes place after six quarters reaching -1.1%, corresponding to a -1.4% output decline and 0.3% output increase produced by one standard deviation positive and negative global risk appetite shocks, respectively. Furthermore, the asymmetric behavior of consumption, investment, imports, and exports all follow closely that of output. Importantly, output's significant response asymmetry lasts for 13 additional quarters beyond the span of the significance of the response asymmetry of EMEs' exports to the U.S. (and 11 additional quarters beyond total exports' response

---

[3]For models with occasionally binding constraints (OBCs), which arise in many economic applications (including the Sudden Stops literature) and constitute an important part of the theoretical macroeconomics literature it is in general not necessarily the case that a smooth higher-order approximation would provide a sufficiently precise representation of their solution. The reason for this is that perturbation-based methods would generally lead to violation of the constraints. However, in practice, macroeconomic models containing such constraints have been found to be reasonably approximated by perturbation-based methods. Guerrieri and Iacoviello (2015) develop a piece-wise perturbation approach that gives a good approximation to the solution of these models. In a more recent paper, Holden (2016) develops an accurate and fast perturbation-based-algorithm that first solves the model via perturbation techniques while ignoring the potential violation of the constraints, and then imposes the constraints' bounds by adding endogenous news shocks that correct for potential violation of these bounds. The method from Holden (2016) improves on the method from Guerrieri and Iacoviello (2015) in being applicable to higher-order pruned perturbation solutions, which is especially relevant for my analysis as it implies that models with OBCs considered in the macroeconomics literature can be reasonably approximated by DGPs of the type assumed in my empirical analysis. This implication is also borne out by recent results from Benigno et al. (2017) and Binning and Maih (2017) which establish the validity of higher-order perturbation-based solutions of models with OBCs via the treatment of the constraints through the lens of an endogenous regime-switching framework.

asymmetry span), indicating that the former is not simply an artifact of the significantly stronger response of U.S. output to global risk appetite shocks; rather, there seems to be an additional mechanism driving EMEs output response asymmetry following global risk appetite shocks.

To shed light on the mechanism behind these results, I turn my analysis to exchange rates, leverage, stock prices, capital flows, and country credit spreads data. I first demonstrate, using nominal and real effective exchange rate data, that adverse global risk appetite shocks produce much stronger exchange rate depreciation than the appreciation caused by favorable shocks. In other words, the output response asymmetry does not seem to be driven by an exchange-rate-induced expenditure-switching based mechanism. Then, using data from the Bank for International Settlements (BIS) on cross-border credit, I demonstrate that EMEs' debt (as share of GDP) owed to international banks falls by much more in response to adverse shocks than its rise following favorable shocks. Moreover, stock prices also fall by much more in response to adverse shocks and capital outflows are much more significant following adverse shocks than capital inflows are following favorable shocks. Country credit spreads initially rise by much more in response to adverse shocks relative to their decline following favorable shocks, but this asymmetry only lasts for a year after which it reverses direction. Nevertheless, this reversal is consistent with the timing of the significantly stronger fall in leverage following adverse shocks, which exerts downward pressure on spreads. More generally, the results on leverage, stock prices, capital flows, and credit spreads generally accord with the presence of a meaningful financial accelerator mechanism that is more intense following adverse shocks, with a greater worsening of balance sheets amplifying a rise in borrowing costs and ultimate fall in investment and output.

Related Literature. Motivated by the asymmetry in U.S. business cycles observed in the data and the desire to study potential mechanisms capable of explaining this asymmetry, a fairly large theoretical (see, e.g., Chalkley and Lee (1998), Gilchrist and Williams (2000), McKay and Reis (2008), Kim and Ruge-Murcia (2009), Abbritti and Fahr (2013), Ordoez (2013), Cao and Nie (2017), and Aruoba et al. (2017)) and empirical (see, e.g., Mork (1989), Cover (1992), Koop et al. (1996), Weise (1999), Kilian and Vigfusson (2011), Tenreyro and Thwaites (2016), Barnichon and Matthes

(2018a), Barnichon and Matthes (2018b), and Barnichon et al. (2018)) literature on impulse response sign-dependency has emerged in the last 20 years or so in the context of the U.S. economy.

The corresponding literature for EMEs has been quite active on the theoretical, structural side but quite limited on the empirical, reduced form side. On the theoretical side, the literature has mainly focused on two structural mechanisms capable of producing asymmetric business cycles in EMEs. (While these two mechanisms were mostly used to study issues such as Sudden Stops and/or optimal exchange rate, capital control, and macroprudential polices, and not necessarily the potential business cycle asymmetry implied by these mechanisms, they still constitute modeling frameworks capable of producing asymmetric effects of shocks and are therefore relevant for the topic of this paper.) The first mechanism is based on financial frictions in the form of occasionally binding constraints (OBCs) (see, e.g., Mendoza (2002), Mendoza and Smith (2006), Mendoza (2006), Mendoza (2010), Jeanne and Korinek (2010), Bianchi (2011), Benigno et al. (2013), Ottonello (2015), Fornaro (2015), Devereux and Yu (2017), Bianchi and Mendoza (2018), and Bengui and Bianchi (2018)). These models can accommodate asymmetric effects of shocks through the potential binding of the collateral constraint assumed, which is usually either formulated in terms of current income (as in Mendoza (2002)) or capital (as in Mendoza (2010)). Specifically, an adverse shock that leads to a binding of the constraint leads to a much bigger fall in output than a favorable shock that maintains a non-binding constraint.[4]

In general, Sudden Stops in models with occasionally binding collateral constraints are defined as periods in which these constraints bind. It is important to stress that my empirical analysis is neither able nor is it meant to identify such episodes; rather, it seeks to capture conditional asymmetry in normal business cycles by identifying an arguably exogenous shifts in global investors' risk appetite where negative such shifts may or may not ultimately lead to a binding of borrowers' collateral constraints. Nevertheless, declines in global risk appetite are likely to produce a tightening in collateral constraints, and this makes my empirical analysis potentially informative

---

[4]Models with OBCs are also capable of producing asymmetry without the actual binding of the constraint so long that the constraint becomes sufficiently close to binding after an adverse shock such that precautionary motives start to kick in (see, e.g., Bianchi (2016).

also for models that study the implications of binding collateral constraints in addition to models emphasizing more regular business cycle related mechanisms.

The second mechanism is based on downward nominal wage rigidity, where the focus is on the shock-amplifying nature of fixed exchange rate regimes in the presence of such rigidity, with the lack of currency depreciation following an adverse shock enhancing the increase in unemployment due to lack of downward adjustment in real wages (Schmitt-Grohé and Uribe (2013, 2014, 2016)). More generally, since wage rigidity is asymmetric in these models, they can accommodate asymmetric effects of shocks on the economy where contractionary shocks' effects get amplified owing to the lack of adjustment of the nominal wage.

On the empirical side, there has been quite limited work that provided evidence on asymmetric effects of shocks in the context of EMEs. A notable exception is Edwards and Levy-Yeyati (2005), who examine the effects of positive and negative terms of trade shocks on output for a panel of 183 countries and find significantly stronger effects of negative shocks. As their general focus is on examining the shock-absorbing role of flexible exchange rate regimes, they also look at the asymmetry of the effects as a function of the type of exchange rate regime in place and find that this asymmetry is stronger when a flexible exchange rate regime is in place. An additional paper, studying the asymmetric effects of exchange rate shocks on foreign exchange (FX) reserves, is Chen and Lin (2019); they find for a panel of 13 EMEs that depreciation shocks cause stronger central bank intervention in the FX market than appreciation shocks.

From a methodological standpoint, both these papers estimate response asymmetry in line with the above-cited empirical literature on the U.S. economy in postulating a dichotomous specification that divides the shock series into positive and negative realizations and estimates the coefficients on these two separate series. Ben Zeev (2019b) has shown that such a dichotomous specification is likely to lead to significant upward bias in the estimation of the response asymmetry, this in contrast to the second-order specification used in this paper which leads to unbiased response asymmetry estimates. As such, what is done in this paper can also be viewed as a methodological contribution to the empirical literature, in addition to the contribution embodied

8

in addressing the three research questions of this paper (posed above on Page 1).

Outline. The remainder of the paper is organized as follows. In the next section, I present unconditional evidence on EMEs business cycle asymmetry, after which I present theoretical motivation for studying business cycle asymmetry in EMEs through the lens of global risk appetite shocks. Section 4 presents the data, methodology, and empirical evidence. Section 5 examines the robustness of the results to alternative specifications. Section 6 discusses the validity of the interpretation of this paper's results in relation to the asymmetric response of FBP. The final section concludes.

2   Unconditional Evidence

This section present unconditional evidence on business cycle asymmetry in EMEs by computing the first four moments of the two-year cumulative trend-adjusted output growth rates for my 42 EMEs panel sample, both for the baseline sample and associated recessionary and expansionary periods as well as a pre-2008 sample and its associated recessions and expansions. The panel is unbalanced and covers the period 1986-2017 with output measured as quarterly real GDP. (Data details are provided in Section 4.1 and Appendix A.) I focus on two-year growth rates based on the argument that two-year frequencies capture reasonably well business cycle frequencies. Output trend is accounted for by estimating cubic-trend time polynomials for each country's logged output and then computing growth rates based on the residuals of these polynomial regressions.

The Whole Sample. The first row of Table 1 shows the first four moments of the pooled distribution of two-year cumulative trend-adjusted output growth rates.[5] As evident from the computed negative skewness of -0.85 and excessive kurtosis of 8, the distribution of growth rates appears to be very non-normal. And, importantly for the focus of this paper, the meaningful

---

[5]Note that the mean *quarterly* trend-adjusted growth rate is zero by definition but the mean growth rate reported in Table 1 pertains to two-year cumulative growth rates and therefore it need not necessarily be exactly zero (it is close to zero, however).

leftward skewness suggests strong distributional asymmetry reflected in the long tail of the distribution clearly being on the left.

Recessions and Expansions. I now report the four moments separately for periods characterized by recessions and those characterized by expansions. I define recessions as periods characterized by two consecutive quarters of negative trend-adjusted output growth rates (quarter-over-quarter growth rates) with expansions defined as the periods being perfect complements to recessions. While this way of defining recessions is imperfect, it is still sufficiently reasonable for having a meaningful platform to look at distributional asymmetry across different business cycle states. Defined in this way, recessions comprise 32% of the sample.

The second and third rows present the first four moments of two-year cumulative trend-adjusted output growth rates in recessions and expansions, respectively. The mean two-year growth rates are quite far apart and asymmetric in that in absolute terms the average growth rate in recessions (1.8%) is nearly 90% higher than the corresponding growth rate for expansions (0.96%). This asymmetry in the first moment implies that recessions are periods of much sharper falls in economic activity than the corresponding rise in activity taking place in expansions. While the variance during recessions is only 7% higher than that in expansions (and recessions' kurtosis 47% higher than that of expansions), skewness in recessions is 127% higher than the skewness in expansions. This strong difference in distributional asymmetry in recessions and expansions indicates that recessions' growth rates are far more likely to obtain relatively large negative growth realizations than expansionary growth rates.

Overall, the results from the first three rows of Table 1 point to strong business cycle asymmetry in EMEs. Output growth rates at business cycle frequencies exhibit a much longer left tail

10

than a right tail with recessions being much sharper than expansions.[6] Nevertheless, I now turn to show that this asymmetry is entirely driven by the 2008-2009 global recession.

Pre-2008 Sample. The last three rows of Table 1 correspond to the first three rows only that now post-2008 observations are excluded from the analysis. It is clear that the negative skewness of the baseline sample is driven by the recent global recession as skewness values for the 1986-2007 sample and its associated pre-2008 recessions and expansions are all slightly positive.

At first pass these results would seem to suggest that the significantly negative skewness observed for the baseline sample is merely an artifact of the sheer size of the 2008-2009 global recession. However, as I argue in the remainder of this paper, both theory as well as suitable econometric analysis seem to suggest that there is more to the role of the recent global recession in producing this business cycle asymmetry than merely its sheer size. Specifically, the most plausible shock being central to this recession appears to have the potential in theory to produce meaningful business cycle asymmetry and, importantly, this potential seems to be borne out by the data. Following this reasoning, I now turn to show that basic theory can motivate studying this asymmetry through the lens of global risk appetite shocks.

3 Theoretical Motivation

In this section I present theoretical motivation for studying business cycle asymmetry in EMEs through the lens of global risk appetite shocks. Toward this end, I proceed in two steps. First, I demonstrate the asymmetric effects of a borrower's perceived riskiness in a partial equilibrium, static costly-state verification (CSV) setting. Second, I present sign-dependent impulse responses

---

[6]I have confirmed that the recessions in my sample are not strongly associated with Sudden Stops, and thus can be considered as normal business cycles, by computing the occurrence of periods in which capital inflows relative to GDP fell by more than one standard deviation. Such Sudden Stop periods were found to overlap with only 12% of the recessionary periods in my sample. Notably, only 13 and 8 countries experienced a sum of capital inflows that exceeds one standard deviation in the 2008-2009 and 2008 periods, respectively. I.e., consistent with this paper's general view that the 2008-2009 global recession can inform us about potential asymmetry in regular (non-Sudden-Stop) EMEs business cycles, the data seem to suggest that this recession is largely removed from what is commonly considered as a Sudden Stop type recession.

to risk shocks from a stochastic capital market equilibrium model that builds on the setting from the first step.

3.1 Partial Equilibrium CSV Setting

Agency Problem Between Borrower and Lender. The borrower's project is financed partly internally and partly by borrowing from risk-neutral financial intermediaries within a CSV framework á la Bernanke et al. (1999), such that her assets QK are the sum of her debt B and net worth N:

$$QK = B + N. \tag{1}$$

The gross real rate of return on capital for the borrower is $R^k = \omega R^k$ (with the gross proceeds from the borrower's production activity represented by $\omega R^k QK$), where R^k is the average, or aggregate, gross real rate of return on capital in the economy and ω is a random idiosyncratic productivity shock which is assumed to be log-normally distributed $ln\omega_{i,t} \sim N(\frac{-\sigma^2}{2}, \sigma^2)$ so that $\mathbb{E}(\omega_{i,t}) = 1$. σ can be viewed as capturing the borrower's perceived risk or alternatively the lender's risk perception which in turn dictates her risk appetite or lack thereof.

The focal assumption underlying the CSV problem is that the realization of ω is private information of the borrower and that in order to observe it the lender has to pay a monitoring cost of $\mu\omega R^k QK$, where $0 < \mu < 1$ is the monitoring cost parameter. The optimal debt contract between the borrower and the lender specifies that, in the case of no default, the former pays the lender ZB, where Z is the no-default contractual interest rate; that is, if $\omega R^k QK \geq ZB$, the borrower will pay the debt and retain any residual profit. In the case of default, i.e., $\omega R^k QK < ZB$, the lender will pay the monitoring cost and obtain $(1 - \mu)\omega R^k QK$. It is straightforward to define the default threshold value of ω, $\bar{\omega}$, as $\bar{\omega} = \frac{ZB}{R^k QK}$. As formalized below, the optimal contract will specify $\bar{\omega}$ and K as the choice variables, which is equivalent to specifying Z and B as the choice variables due to the relations $\bar{\omega} = \frac{ZB}{R^k QK}$ and $QK = B + N$.

I now turn to presenting the maximization problem that characterizes the optimal debt contract. Assuming that the lender operates in a perfectly competitive environment in which she earns, in expectation, the gross risk-free return R_t, the optimal contract problem that maximizes the borrower's expected profit subject to the lenders' zero-profit condition is

$$\max_{K,\bar{\omega}} \int_{\bar{\omega}}^{\infty} \left[\omega R^k QK - ZB \right] dF(\omega) = \left[1 - \Gamma(\bar{\omega}) \right] R^k QK$$

$$s.t \; R(QK - N) = \left[\Gamma(\bar{\omega}) - \mu G(\bar{\omega}) \right] R^k QK,$$

(2)

where $F(\omega)$ is the CDF; $\Gamma(\bar{\omega}) \equiv \int_0^{\bar{\omega}} \omega dF(\omega) + \bar{\omega} \int_{\bar{\omega}}^{\infty} dF(\omega)$; and $G(\bar{\omega}) \equiv \int_0^{\bar{\omega}} \omega dF(\omega)$. The first component of $\Gamma(\bar{\omega})$ (which is also equal to $G(\bar{\omega})$) gives the borrower's expected return in case of a default, whereas the second one gives the expected return in case of solvency; hence, the optimization constraint dictates that the expected returns of the lenders on a risky loan net of monitoring costs, given by the RHS of the constraint, be equal to the risk-free return given by the LHS of the constraint. For future reference, as in BGG, I define the external finance premium (EFP) as $s \equiv \frac{R^k}{R}$ and Leverage as $k \equiv \frac{QK}{N}$.

3.1.1 EFP-Leverage Curve and Risk

The central motivation for my focusing on the CSV setting as the conceptual framework for my analysis is based on the notion that increased risk (σ) raises EFP for a given leverage more than the reduction in EFP caused by decreased risk.[7] To show this asymmetry, I proceed in two steps. First, I provide the basic intuition for the validity of this notion. Second, I formally show that this notion is correct by looking at the EFP-leverage curve for alternative risk levels.

Basic Intuition. To provide the basic intuition underlying the asymmetric effects of risk on the EFP-leverage curve, I center my attention around the lender's expected monitoring cost, which is

---

[7]The nonlinear implications of risk in a CSV setting have also been highlighted recently in Harding and Wouters (2019), albeit in the context of the fact that the EFP-leverage elasticity is increasing in risk which has implications for the state-dependency of financial frictions but can not produce the kind of asymmetry focused on in this section.

the focal element of the CSV problem in that its existence produces a positive EFP. In particular, I aim to show mechanically that this expected cost is convex in risk. This is obtained in a mechanical way because I will treat $\bar{\omega}$ and μ as exogenous to my computation. In the second step of this section I will solve the entire CSV problem; for now I merely want to show that the mathematical term that encapsulates expected monitoring cost is convex in risk.

Recall that this expected cost is defined as $\mu G(\bar{\omega}) \equiv \mu \int_0^{\bar{\omega}} \omega dF(\omega)$. If, for reasonable values of $\bar{\omega}$ and μ, the expected monitoring cost can be shown to be convex in risk, this would mean that higher risk entails greater expected monitoring cost for lenders than the reduction in them implied by lower risk. And this, in turn, can serve as intuition for why the EFP-leverage curve shifts upward more when risk rises than downward when risk goes down.

Figure 1 shows the relation between expected monitoring cost and risk for the baseline $\bar{\omega} = 0.48$ and $\mu = 0.12$ values from BGG. This relation was obtained by forming a grid of σ that ranges between 0.23 and 0.33 with spacing of 0.001 and computing $\mu G(\bar{\omega})$ for each value in this grid. Notably, expected monitoring cost is clearly convex in risk. To see this numerically, note that rising in risk from 0.28 to 0.33 implies a rise in expected monitoring cost that is 133% greater than the rise induced by increasing risk from 0.23 to 0.28. This convexity stems from the fact that, due to the rightward skewness of the log-normal distribution, greater risk raises the expected ω conditional on being in the default range $[0, \bar{\omega}]$ more than the reduction in it induced by lower risk. While mechanical by nature in not accounting for the endogeneity of the default range, this convexity still implies that increased risk has a mechanical basis for exacerbating the agency problem between the lender and the borrower much more than the alleviation of this problem induced by decreased risk. And this consequently potentially opens the door for there being asymmetric effects of risk on EFP, as formalized by the result I turn to next.

Asymmetric Effects of Risk on EFP. I conduct the following numerical experiment. For three values of borrower's riskiness $\sigma = [0.23, 0.28, 0.33]$ (the middle value of $\sigma = 0.28$ is in line with BGG), I solve Problem (2) for a grid of s that ranges between 1.001 and 1.02 and has a spacing of 0.001, while keeping constant the monitoring cost parameter at $\mu = 0.12$ (as in BGG).

14

The results from this experiment are shown in Figure 2, where the solid line depicts the EFP-leverage curve for $\sigma = 0.28$ and the dashed and dotted lines correspond to $\sigma = 0.23$ and $\sigma = 0.33$, respectively. The logs of EFP and leverage appear on the y- and x-axis so that the slope of the curve can be considered the elasticity of EFP with respect to leverage.

We are now in position to state the main result of this section, i.e., that a rise in σ for a given leverage raises EFP by more than the corresponding EFP decline induced by an equivalent decrease in σ. This result is graphically illustrated by Figure 2 in that the vertical gap between the higher risk curve and the intermediate risk curve is larger than that between the intermediate risk curve and the lower risk curve. To see this with a simple numerical example, consider the value of logged leverage which correspond to the steady state in BGG, i.e., $lnk = 0.69$. For this leverage value, logged EFP rises by 0.0066 when σ rises from 0.28 to 0.33 while only declining by 0.0044 when σ goes down to 0.23. In other words, an increase in risk shifts the EFP-leverage curve upward by more than the corresponding downward shift induced by lower riskiness. Such asymmetry, where a rise in risk increases EFP by 50% more than the corresponding decline when risk decreases, has the potential to lead to asymmetric effects of risk shocks in a stochastic, dynamic environment. This is what I turn to formalizing next.

3.2   Stochastic Capital Market Equilibrium

This section extends the CSV setting from the previous section into a stochastic, dynamic capital market equilibrium model. The purpose of this extension is to further motivate the potentially relevant role of credit intermediation disruptions in inducing asymmetric business cycle. Granted, one can pursue a more ambitious extension to a full-blown small open economy DSGE model that incorporates BGG-type financial frictions, along the lines of Céspedes et al. (2004), Devereux et al. (2006), Elekda and Tchakarov (2007), Gertler et al. (2007), Akinci (2014), and Fernández and Gulan (2015). That said, this would go beyond the scope of this paper, which is mainly empirical, and also diminish the clarity regarding the specific asymmetry-inducing financial frictions mechanism I aim to highlight owing to the addition of various other mechanisms such a far-reaching extension

15

would introduce. Hence, I opt to keep things as simple as possible while still allowing me to establish a conceptual base upon which to build the discussion of the empirical results in the next section and to help in motivating this paper's focus on global risk appetite shocks as a source of business cycle asymmetry in EMEs.

To obtain a capital market equilibrium that is partly dependent on external funding subject to a CSV agency problem, I add capital producers and a net worth accumulation equation to a stochastic, dynamic CSV modeling version of the one introduced in the previous section.

Entrepreneurs. There is a continuum of identical, finitely-lived, and risk-neutral entrepreneurs. The i-th entrepreneur produces good $Y_{i,t}$ using the following technology:

$$Y_{i,t} = \omega_{i,t} K_{i,t}^{\alpha}, \tag{3}$$

where $\omega_{i,t}$ is a random idiosyncratic productivity shock which is assumed to be log-normally distributed $ln\omega_{i,t} \sim N(\frac{-\sigma_t^2}{2}, \sigma_t^2)$ so that $\mathbb{E}(\omega_{i,t}) = 1$; and $K_{i,t}$ is physical capital of the i-th entrepreneur.

Entrepreneurs purchase capital from capital producers in the beginning of period t at price Q_{t-1}, which they then operate in period t and resell it at the end of the period at price Q_t. The gross real rate of return on capital for the i-th entrepreneur, denoted by $R_{i,t}^k$, is the sum of the marginal profitability of capital and the capital gain:

$$R_{i,t}^k = \frac{\alpha K_{i,t}^{\alpha-1} + (1-\delta)Q_t}{Q_{t-1}}, \tag{4}$$

where δ is the rate of capital stock depreciation.

Entrepreneurs' capital purchases are financed partly internally and partly by borrowing from risk-neutral financial intermediaries within a CSV framework (as the one described in the previous section), such that the assets of entrepreneurs $Q_t K_{t+1}$ are the sum of their debt B_{t+1} and net worth

16

N_{t+1}:

$$Q_t K_{t+1} = D_{t+1} + N_{t+1}. \tag{5}$$

Since the CSV setting was already described in detail in the previous section, I skip the details here and just note that a similar version to Problem (2) is solved in order to obtain the optimal debt contract with the only difference being that aggregate uncertainty need be accounted for now. The reason for needing to account for aggregate uncertainty is that I now assume that perceived risk as measured by σ_t, the variance of entrepreneurial idiosyncratic productivity, follows the stochastic process

$$\sigma_t = \bar{\sigma}(1 - \rho) + \rho \sigma_{t-1} + \eta_t, \tag{6}$$

where $\bar{\sigma}$ is the steady state value of σ_t; $0 \leq \rho < 1$ governs the persistence of the process; and η_t is a white noise shock with standard deviation σ_η referred to as 'risk shock' (see, e.g., Christiano et al. (2014)).

The last piece of modelling the entrepreneurial sector is to lay out the dynamics of the net worth of entrepreneurs.[8] Toward this end, I make the standard assumption that entrepreneurs "die" with a constant exogenous probability in each period, $1 - v$, in which case they simply consume their entire net worth and are replaced within the period by new entrepreneurs.[9] This setting implies the following law of motion for aggregate entrepreneurial net worth:

$$N_{t+1} = v[1 - \Gamma(\bar{\omega}_t)]R_t^k Q_{t-1} K_t, \tag{7}$$

where K_t is aggregate capital stock in the economy and $[1 - \Gamma(\bar{\omega}_t)]R_t^k Q_{t-1} K_t$ is the aggregate profit of all entrepreneurs in period t, which also corresponds to the objective function in Problem (2).

---

[8]BGG show that the chosen optimal level of $\bar{\omega}_{i,t}$ is identical across borrowers. This result is important as it facilitates aggregation of net worth in the economy.

[9]This assumption guarantees that entrepreneurs will never accumulate enough net worth so as to avoid borrowing to finance their operations.

Capital Producers. There are perfectly competitive capital producers that use a linear technology to produce capital goods which are sold at the end of period t to entrepreneurs at price Q_t. They use a fraction of final goods purchased from entrepreneurs as investment goods, I_t, which are then used in conjunction with the existing capital stock to produce new capital goods, K_{t+1}. Capital producers are also subject to the convex investment adjustment cost function of Christiano et al. (2005), resulting in the following capital accumulation equation:

$$K_{t+1} = (1 - \delta)K_t - \left[1 - \Theta \left(\frac{I_t}{I_{t-1}} \right) \right] I_t, \tag{8}$$

where Θ is the adjustment cost function, with $\Theta(1) = \Theta'(1) = 0$ and $\Theta''(1) > 0$.[10] The capital producers optimization problem consists of choosing the quantity of investment to maximize the present value of their infinite stream of profits:

$$\max_{\{I_t\}_{t=0}^{\infty}} \mathbb{E}_0 \sum_{t=0}^{\infty} \frac{1}{R_t^t} Q_t \left[1 - \Theta \left(\frac{I_t}{I_{t-1}} \right) \right] I_t - I_t. \tag{9}$$

Solution and Calibration. I solve the model by taking a second order approximation of its system of equilibrium equations about the steady state values of the variables. Using a second order approximation for solving the model is necessary for properly studying the possible asymmetric effects of risk shocks. To compute the sign-dependent responses of the variables, I produce two simulations of the model where one draws a risk shock realization of 0.05 and the other a -0.05 realization.

Table 2 presents the calibration used for the model's parameters. The calibration for the parameters underlying the CSV problem and net worth accumulation (μ, $\bar{\sigma}$, and v) as well as the risk-free rate steady state level, capital share, and capital depreciation rate follows BGG. The convexity parameter of the investment adjustment cost function (φ) follows the estimated value from Christiano et al. (2005). Lastly, the persistence parameter of the risk shock process and the standard deviation of the risk shock are calibrated at 0.8 and 0.05. The former is lower than the 0.97

---

[10]I assume the following investment adjustment cost function: $\Theta \left(\frac{I_t}{I_{t-1}} \right) = \frac{\varphi}{2} \left(\frac{I_t(j)}{I_{t-1}(j)} - 1 \right)^2$.

estimated by Christiano et al. (2014) for U.S. data but is still reasonably high; Christiano et al. (2014) estimated the standard deviation of their risk shock at 0.07, or 26% of their estimated value of the steady state of σ_t, so my choice of a 0.05 risk shock standard deviation (which is less than 18% of my BGG based calibrated value for $\bar{\sigma}$) and associated shock realization for my simulations can be viewed as a conservative one.

The Asymmetric Effects of Risk Shocks. Figure 3 shows the response of the capital market model to 0.05 and -0.05 risk shock realizations. The solid line depicts the response to the positive shock and the dashed line shows the response to the negative shock, with the latter response multiplied by -1 for comparison purposes.

The impulse responses clearly demonstrate impulse response sign-dependence. While, by construction, risk responds symmetrically to the positive and negative shocks, there is a 0.4 percentage point difference between the rise in EFP following the positive risk shock and the corresponding decline induced by a negative risk shock. This directly speaks to the discussion from the previous section on the stronger upward shift in the EFP-leverage curve following a rise in risk than the corresponding downward shift induced by a decline in risk. And, importantly, this asymmetric EFP response leads to a fall in investment, price of capital, and net worth following a positive risk that is greater than the corresponding rise in these variables caused by the negative shock.[11]

In sum, Figure 3 stresses that financial frictions, as modeled here in a CSV setting, can have potentially meaningful asymmetrical implications for the behavior of the capital market in response to risk shocks. Since these types of shocks can be viewed as proxies for the risk appetite of

---

[11]Note that leverage jumps by more in the first year following the positive shock due to the stronger decline in net worth after this shock and that thereafter it goes into a deleveraging process which is weaker than the leveraging process experienced after the negative risk shock. While this differentially weaker deleveraging process is not consistent with what I find in my empirical analysis, I have found that lowering the 'death rate' of entrepreneurs goes a long way toward reversing this differential response and making the deleveraging process following the positive shock stronger than the leveraging one following the negative shock. The reason for this is that entrepreneurs' accumulation of net worth in the presence of the negative (positive) shock and such lower 'death rate' becomes more (less) persistent and thus acts to reverse the differentially stronger leveraging process that occurs in the baseline calibration after a negative shock.

lenders (see, e.g., Gilchrist and Zakrajšek (2011) and Gilchrist and Zakrajšek (2012a)), and given the strong dependence of EMEs on foreign lenders, the results of this section can serve as motivation for studying EMEs business cycle asymmetry through the lens of global risk appetite shocks.

4 Empirical Analysis

4.1 Data

Data are quarterly and cover 42 EMEs with samples that span 1986-2017. The panel is an unbalanced panel with the included countries chosen on the basis of belonging to the universe of EMEs having quarterly data on real macroeconomic aggregates with reasonable length. The starting date is dictated by the availability of the global risk appetite shock series which spans 1986-2012. I go beyond 2012 to 2017 with the outcome EMEs data because the rolling regressions structure (going up to the 5-year horizon) of my econometric approach allows to exploit outcome variables data that go up to 2017 for estimating the dynamic effects of risk appetite shocks. Appendix A contains a detailed description of the data and its sources. The primary data source I use is the International Financial Statistics (IFS) database. The main outcome variable I consider is output, defined as local currency current GDP divided by the GDP deflator. I seasonally adjusted the output variable using ARIMA X12.

The variable I use to measure global risk appetite shocks is the financial bond premium (FBP) series from Gilchrist and Zakrajšek (2011) and Gilchrist and Zakrajšek (2012a). Building on the methodology from Gilchrist and Zakrajšek (2012b), these papers use micro-level data for 193 financial intermediaries to construct a credit spread index which they decomposed into a component that captures firm-specific information on expected defaults and a residual component that they termed as FBP which represents the shifts in financial intermediaries' risk attitudes. As such, as argued in Gilchrist and Zakrajšek (2011), Gilchrist and Zakrajšek (2012a), and Gertler and Gilchrist (2018), FBP is a reasonable proxy for the level of disruption (or tranquility) of credit intermediation in the U.S. Considering the important role that U.S. credit markets play globally, using

FBP allows to identify the potentially asymmetric effects of global risk appetite shocks on EMEs.

Other outcome variables I consider to learn more about the mechanism behind the output-based results are investment, consumption, exports, imports, trade balance, exchange rates, leverage, stock prices, international capital flows, and country credit spreads. The first two are defined as gross fixed capital formation and private consumption expenditure (both in local currency) divided by the GDP deflator; exports and imports are local currency exports and imports of goods and services divided by the GDP deflator; the trade balance is nominal exports minus nominal imports (both in local currency) divided by local currency current GDP. I use nominal and real (CPI-based) effective exchange rate data to measure nominal and real exchange rates.

Leverage is the ratio of total gross claims of Bank for International Settlements (BIS) reporting banks' claims on each EME to its GDP, where the former is taken from the consolidated banking statistics database of the BIS and is converted to local currency by multiplying the dollar value of claims by the corresponding dollar exchange rate. Stock prices are market price indices of equities based on major stock exchange indices available from the IFS database. I employ data on international capital flows that consists of net outflows related to foreign direct investment, portfolio investment, and other investment. All of these items are in raw dollar values and are thus converted to local currency using the respective dollar exchange rates and then divided by local currency current GDP. I seasonally adjusted the raw variables using ARIMA X12.

The country credit spread is the stripped Emerging Markets Bond Index (EMBI) Global computed by JP Morgan, which is a composite of different U.S. dollar-denominated bonds. The stripped spread is computed as an arithmetic, market-capitalization-weighted average of bond spreads over U.S. Treasury bonds of comparable duration.

Except for exchange rates, stock prices, and country credit spreads, all EMEs outcome variables were seasonally adjusted using ARIMA X12. Apart from the trade balance and capital flows, which are measured in terms of GDP shares, I take logs of all of the variables. To extract the cyclical components of the trending variables in my sample, I estimate a cubic-trend time polynomial for each trending variable and take the associated residuals as the corresponding variables' cycli-

cal components (as in, e.g., Garcia-Cicco et al. (2010)). (I do this for all variables except the capital flows variables, for which there is no significant trend.) See Section 5.3 for the robustness of my results to using alternative detrending techniques. All outcome variables are entered in cumulative differences in the estimation Equation (12) below, except for FBP as this variable is effectively a residual from a regression of credit spreads on expected default risk; hence, I use it in raw levels both when extracting the risk shock series (see Equations (10) and (11) below) and also when I examine its sign-dependent response from Equation (12).

4.2 Methodology

I make use of the Jorda (2005) local projections method within a fixed-effects panel sign-dependent model, where a Bayesian estimation and inference procedure is performed by assuming a diffuse normal-inverse Wishart prior distribution for the local projection regressions' coefficients and residual variance. To account for correlations of the error term across EMEs and time, I apply a correction to the standard errors within my Bayesian estimation procedure, based on Driscoll and Kraay (1998) and following Auerbach and Gorodnichenko (2012)'s use of this correction in a classical setting, which accounts for arbitrary spatial and temporal correlations of the error term. In doing so I accord with the reasoning from Miranda-Agrippino and Ricco (2017), who estimate a hybrid VAR-local-projections model and follow the suggestion from Müller (2013) to increase estimation precision in the presence of a misspecified likelihood function (as in mine and their setting) by replacing the original posterior's covariance matrix with an appropriately modified one. I discuss my Bayesian estimation and inference approach in more detail below and Appendix B provides full technical details of my estimation procedure. I now turn to a general description of the estimation procedure.

Econometric Specification.   The estimation proceeds in three steps. The first step regresses monthly FBP on 12 lags of own raw and squared values as well as 12 lags of raw and squared log-first-differences of the real S&P 500 index. My controlling for past information as encapsu-

lated in lagged stock prices is meant to account for the potential presence of news shocks and thus facilitates the identification of the unanticipated shock to FBP, which is what is sought after. The second step takes the residual from this regression and regresses it on its squared value. This is done in order to purge the first step's residual of the potential presence of squared values of the global risk appetite shock, whose significance is ultimately borne out by the data as reflected by a significantly positive coefficient estimated in the second step's regression.[12] The third step runs local projection regressions of the EMEs' outcome variable of interest on raw and squared values of the standardized residual from the second step, where I convert this residual to quarterly frequency by taking averages of monthly observations.[13] The econometric framework just described can be formally presented with the following three-equation system:

$$FBP_t = \Gamma_1^{FBP} FBP_{t-1} + \Psi_1^{FBP} FBP_{t-1}^2 + ... + \Gamma_p^{FBP} FBP_{t-p} + \Psi_p^{FBP} FBP_{t-p}^2 + \quad (10)$$

$$+ \ \Gamma_1^{SP} \Delta SP_{t-1} + \Psi_1^{SP} \Delta SP_{t-1}^2 + ... + \Gamma_p^{SP} \Delta SP_{t-1} + \Psi_p^{SP} \Delta SP_{t-1}^2 + C + \epsilon_t,$$

$$\hat{\epsilon}_t = \delta + \gamma \hat{\epsilon}_t^2 + \xi_t, \quad (11)$$

$$y_{i,t+h} - y_{i,t-1} = \alpha_{i,h} + \Xi_h \hat{\xi}_t + \Phi_h \hat{\xi}_t^2 + u_{i,t+h}, \quad (12)$$

where Γ_i and Ψ_i are scalar coefficients; p denotes the number of lags, which I set to 12 in accordance with the monthly frequency of Equation (10); C is a constant; ϵ_t is the true residual from Equation (10) whose standard deviation is denoted by σ_1; $\hat{\epsilon}_t$ is the estimated residual from Equation (10) and

---

[12]A basic litmus test for the ability of the second step to truly capture the effect of the squared value of the true shock, as opposed to just erroneously pick up a potentially non-zero skewness of the true shock, is that the FBP response asymmetries from an estimation procedure that includes and excludes the second step are similar to one another. The reason for the validity of this litmus test is that an estimation that excludes the second step, while not able to identify the true shock series in the presence of true contemporaneous response asymmetry in FBP, is still able to identify the response asymmetry itself with this ability being robust to the distributional asymmetry of the true shock. Importantly, I have confirmed that such similarity is borne out by the data with estimated response asymmetries from including and excluding the second step of 16 and 17 basis points, respectively. This indicates that the second estimation step is likely to do a good job of purging the residual from the first step and getting at the true shock as opposed to merely picking up a potentially non-zero skewness of the true shock.

[13]Results are similar when the FBP regression is based on quarterly frequency. However, I opt to use FBP in its highest frequency as it raises confidence in its innovations (after properly controlling for past information) truly capturing global risk appetite shocks.

ξ_t is the true residual (i.e., global risk appetite shock) from Equation (11) whose standard deviation is denoted by σ_2; i and t index countries and time; α_i is the country fixed effect; $\hat{\xi}_t$ is the estimated residual from Equation (11), converted into quarterly frequency by taking averages of monthly values and normalized to have unit variance; Ξ_h and Φ_h are the first- and second-order effects of the global risk appetite shock, where $\Xi_h + \Phi_h$ and $\Xi_h - \Phi_h$ give the responses of the outcome variable y (say, logged output) at period h to a positive and negative one standard deviation risk shock at time t, respectively;[14] and $u_{i,t+h}$ is the residual of Equation (12) with standard deviation $\sigma_{3,h}$. For future reference, let the stacked $(p+1)$x4 $B^1 = [\Gamma_1^{FBP}, \Psi_1^{FBP}, \Gamma_1^{SP}, \Psi_1^{SP}, ..., \Gamma_p^{FBP}, \Psi_p^{FBP}, \Gamma_p^{SP}, \Psi_p^{SP}, C]'$ matrix and 2x1 $B^2 = [\gamma, \delta]'$ matrix represent the coefficient matrices from Equations (10) and (11), respectively, such that B^1 and σ_1 and B^2 and σ_2 correspond to the parameters to be estimated from these two equations.

I estimate Equations (10), (11), and (12) jointly by applying the Bayesian estimation algorithm for strong block-recursive structure put forward by Zha (1999) in the context of block-recursive VARs, where the likelihood function is broken into the different recursive blocks. In my case, I have only two blocks, where the first consists of Equations (10) and (11) and can be estimated via a two-step procedure explained below and the second corresponds to Equation (12). As shown in Zha (1999), this kind of block separation along with the standard assumption of a normal-inverse Wishart conjugate prior structure leads to a normal-inverse Wishart posterior distribution for the block-recursive Equation parameters.

Specifically, considering that the number of RHS variables in Equation (12) is 3 (raw and squared shock and the constant), let the stacked 3x1 coefficient matrix $Q_h = [\Xi_h, \Phi_h, \alpha_{i,h}]'$ represent the coefficients from Equation (12). Moreover, let $\sigma_{3,h}$ represent the standard deviation of the residual from Equation (12) at each horizon h. Hence, the parameters to be estimated from Equation (12) can be summarized by the coefficient matrix Q_h and residual variance $\sigma_{3,h}$. I assume

---

[14]All outcome variables are entered in cumulative differences, except for the capital flows variables which are entered in levels in both sides as they are effectively already first-differences of their corresponding stock variables. Note that my pre-estimation log-cubic-trend removal applied to the trending variables does not remove stochastic trends; hence, the differencing procedure is important in removing any such potential stochastic trends and making the data stationary, which is necessary for validating the local projections estimation and inference approach undertaken in this paper.

a diffuse normal-inverse Wishart prior distribution for both $[B^1, \sigma_1, B^2, \sigma_2]$ and $[Q_h, \sigma_{3,h}]$; this conjugate prior structure coupled with the assumption of a Gaussian likelihood for the data sample imply a posterior density of these parameters that is also distributed as a normal-inverse Wishart. Following the suggestion from Müller (2013) to increase estimation precision in the presence of a misspecified likelihood function (as in my setting owing to the spatial and temporal correlation in $u_{i,t+h}$), I apply a correction to $\sigma_{3,h}$ based on Driscoll and Kraay (1998) which accounts for arbitrary spatial and temporal correlations of the error term.

Operationally, for each posterior draw of the coefficients from Equation (10), I collect the estimated residual from this equation ($\hat{\epsilon}_t$) and use its raw and squared values as the outcome and explanatory variables in Equation (11), respectively, to form a posterior distribution of δ and γ conditional on $\hat{\epsilon}_t$. I then take a posterior draw of δ and γ and obtain $\hat{\xi}_t$, subsequently using its raw and squared values (converted to quarterly frequency in unit standard deviation units by dividing $\hat{\xi}_t$ by $\sqrt{3}\sigma_2$) in Equation (12) to form a posterior distribution for Ξ_h and Φ_h. I then take a posterior draw of these coefficients and estimate the sign-dependent response of the outcome variable at horizon h to positive and negative one standard deviation global risk appetite shocks as $\Xi_h + \Phi_h$ and $\Xi_h - \Phi_h$, respectively. I generate 500 such posterior draws from which I am then able to estimate the median sign-dependent impulse responses to global risk appetite shocks along with their posterior confidence bands. Appendix B contains the specific details of the posterior simulator I use to obtains these estimates.

4.3 Results

This section presents the main results of the paper. I first show the asymmetric effects of global risk appetite shocks on the U.S. economy. Then, it is established that a one standard deviation positive global risk appetite shock reduces EMEs output more than the output increase induced by an equivalent one standard deviation negative shock. In what follows after that, I turn to inspecting the asymmetric behavior of other macroeconomic variables in order to uncover the underlying mechanisms that drive the output-based results.

4.3.1 FBP and U.S. Economic Activity.

It is most natural to begin the empirical analysis with a depiction of how the U.S. economy, from which the global risk appetite shock originates, responds to this shock and whether its response is asymmetric. Toward this end, I use FBP, U.S. unemployment rate, and logged U.S. industrial production as the outcome variables in Equation (12). Here I exploit the rather rich availability of macro data in monthly frequency for the U.S. economy (as opposed to EMEs) and estimate Equation (12) in monthly frequency for all three considered variables. While the unemployment rate and logged industrial production enter Equation (12) in cumulative differences form, I insert FBP in levels in this equation as it is effectively a residual from a regression of credit spreads on expected default risk.

The results from these estimations appear in Figures 4 (FBP), 5a (unemployment rate), and 5b (industrial production). As in all subsequent figures, these figures show the corresponding variable's response to a positive and negative global risk appetite shock (both of one standard deviation size) as well as the difference between the positive shock's effect and the negative shock's effect. Specifically, responses to the shock are constructed as $\hat{\Xi}_h + \hat{\Phi}_h$ for the positive shock and as $\hat{\Xi}_h - \hat{\Phi}_h$ for the negative shock.[15] Solid lines depict the median estimates of the responses while dashed line correspond to the 68% posterior confidence bands.

FBP.   Clearly, FBP rises by more on impact in response to a positive shock than its corresponding decline following a negative shock. While the latter decline is both economically and statistically significant on impact (as implied by multiplying the response to the negative shock shown in Figure 4 by -1), exceeding 15 basis points, the corresponding increase following a positive shock is significantly stronger reaching nearly 32 basis points. At first pass, this result does not seem very sensible because FBP is the fundamental associated with global risk appetite shocks and we usually think of shocks as affecting their fundamental on impact in a symmetric way. This need

---

[15]Notably, there is no need to multiply by -1 either the positive shock's effect or the negative shock's effect in Regression (12) for comparison purposes because the estimated responses already reflect effects that go in the same direction in the absence of asymmetry.

not be necessarily the case, however, as there could be an exogenous sign-dependent mechanism by which U.S. credit markets get rattled by bad risk appetite shocks more than they get frothy after good shocks of the same size.[16] And this possibility is the reason for my including the second step in my estimation procedure involving regressing the residual from Equation (10) on its squared value. It turns out that a significant relation is borne out by this regression, consistent with the significant contemporaneous difference between the FBP response to positive and negative global risk appetite shocks.

Notwithstanding the aforementioned significant contemporaneous response difference, positive shocks' effects are significantly stronger than those of negative shocks for only one year and actually negative shocks' effects begin to be significantly stronger than those of positive shocks from the two-year mark, albeit intermittently, obtaining significance for a total of 18 months. That is, FBP seems to be more sensitive to positive shocks mainly for the short-term while negative shocks' effects appear to be more persistent with more long-lasting effects. Hence, taking into account the entire dynamics of the sign-dependent behavior of FBP, it is not clear which effects win out: the sharper and shorter-lasting positive shocks' effects or the deeper and longer-lasting ones of negative shocks. E.g., simply averaging the responses over the 60 considered horizons results in very similar average effects of positive and negative shocks of 3 and 4 basis points, respectively; and averaging over the more reasonable business cycle frequency of 3 years results in average effects of 7 and 6 basis points, respectively. This issue is crucial for the subsequent analysis as it emphasizes that any persistent asymmetry found in EMEs variables' responses can not be merely interpreted as arising from FBP response asymmetry. I shall return to this issue in Section 6 and investigate the validity of the latter statement from a structural perspective.

Unemployment and Industrial Production. Both Figure 5a and Figure 5b indicate that U.S. economic activity responds significantly more strongly to positive global risk appetite shocks than

---

[16]Granted, following standard proactive, I also assumed response symmetry in the stochastic process for the risk shock (given by Equation (6)) in the simple capital market equilibrium model from Section 3.2. The asymmetry in the impulse responses from that model would only get amplified if I allowed for a less simple stochastic process which accommodated sign-dependency.

to negative ones. The response asymmetry for the unemployment rate is somewhat shorter lived, lasting roughly 2.5 years, while that for industrial production seems to be very persistent and lasts for about 4 years. Note that both variables' response differences are much more persistent than the year-long stronger rise in FBP from Figure 4 and are therefore unlikely to merely be an artifact of this initially stronger FBP rise after positive shocks. And this argument is further validated by the reversal of the FBP response difference from roughly the two-year mark onwards.

It is noteworthy that negative global risk appetite shocks do seem capable of producing significant rises in economic activity, with the effects of these shocks on unemployment and industrial production being significant for a total of 34 and 17 months, respectively. However, positive shocks simply appear to produce much more severe declines in economic activity. Hence, even absent any financial frictions present between EMEs and foreign lenders, we should expect to see an asymmetric response of EMEs to global risk appetite shocks through a basic trade channel. What I shall establish below is that this basic trade channel, while present in the data, can not in and of itself explain the asymmetric response of EMEs in the data.

4.3.2 Asymmetric Responses of EMEs' Outcome Variables

Exports to U.S. I begin my analysis of the potentially asymmetric behavior of EMEs following global risk appetite shocks with Figure 6, which depicts the sign-dependent response of real exports to U.S. This is the first EMEs related variable I look at so as to establish the strength of the basic trade channel by which global risk appetite shocks' effects can be transmitted to EMEs.

The results from Figure 6 indicate that EMEs exports to the U.S. fall by significantly more from the 2nd to 5th quarter following positive shocks than their corresponding rise in response to negative shocks, with the response difference troughing at -3% in the 3rd quarter. But, notably, from the 7th quarter onwards, this negative response difference reverses and the effects of negative shocks become significantly stronger than those of positive shocks. This reversal is rooted in a much more persistent response of the exports-to-U.S. variable after negative shocks, which obtains significance even after fours years and is essentially always positive (as implied by multiplying

the response to negative shocks in the figure by -1) while the response to positive shocks is more transitory and actually becomes significantly positive from the 4-year mark onwards.

In sum, these results indicate that there exists a rather short-lived basic trade channel that transmits asymmetry to EMEs following global risk appetite shocks, as reflected by the transitory nature of this asymmetry and its reversal from the 7th quarter onwards. This issue is of particular importance as it can facilitate the structural interpretation of the asymmetric response of EMEs' output, whose analysis I turn to next.

Output.   Figure 7 depicts the sign-dependent response of output to global risk appetite shocks. Notably, the response difference is significantly negative for all but the last two horizons, with the trough difference taking place after 5 quarters and standing at -1.3%. That for nearly all horizons output falls by significantly more after positive shocks than its corresponding rise after negative shocks indicates that there must be an additional mechanism at work here beyond the short-lived trade channel embodied in Figure 7. What follows in the remainder of this section is an exploration of various variables' asymmetric responses to global risk appetite shocks whose underlying objective is to uncover the additional mechanism that is driving the persistent output response difference from Figure 7.

Investment, Consumption, and the Trade Balance.   Figures 8a-9 depict the responses of investment, consumption, and the GDP share of the trade balance. The results from Figure 8a, which depict the investment responses, indicate that investment responds significantly more to positive shocks than to negative ones for 16 of the 20 considered horizons, with a trough response difference of -3.4% taking place after 7 quarters. We see from Figure 8b that consumption follows a similar qualitative pattern with a trough response difference of -1.1% also after 7 quarters. I.e., both variables' asymmetric behavior closely tracks that of output, although clearly investment's asymmetric response difference is much stronger in quantitative terms.

Figure 9 presents the responses of the GDP share of the trade balance. While the trade balance response to negative shocks is largely insignificant, it is significantly positive following positive

shocks for all but two horizons. This contrast in responses across negative and positive shocks is manifested by a significantly positive response difference through horizon 18 which peaks at 0.6 percentage points after 6 quarters.

Taken together, the results for investment, consumption, and the trade balance indicate that while the first two variables' estimated response differences across positive and negative shocks go in the same direction as that of output, with investment seeming to quantitatively drive (from a mechanical national accounting standpoint) output's asymmetric response, the trade balance does not seem to be an important driver in quantitative terms of output's asymmetric response. Note that since the trade balance is considered in GDP share terms, one need be cautious in ascertaining from Figure 9 the actual direction in asymmetry in the trade balance. But the fact that relative to GDP its direction is opposite from output's is an indication that the trade balance is not likely to be driving the asymmetry we observe in output.

To better understand the asymmetric behavior of the trade balance, I separately look at real exports and real imports in Figures 10a and 10b, respectively. These figures shed light on the results for the opposite direction in trade balance (in GDP share terms) response asymmetry as imports clearly exhibit stronger negative response asymmetry than exports, with the former troughing at -3.7% after 4 quarters compared to a corresponding trough of -2.6% for exports. Furthermore, the imports response asymmetry is more persistent with its significance lasting for four more quarters than that of exports.

Note that exports response asymmetry is significant through the 7th quarter, lasting two more quarters than the corresponding asymmetry for the exports-to-U.S. variable and likely reflecting the fact that the U.S.-originated global risk appetite shock induces spillover effects on the global economy. Nevertheless, the duration of the total exports variable's response asymmetry is still much shorter than that of output's, leaving room for an additional mechanism (on top of the trade channel) to have a meaningful role in driving the output-based results.

Nominal and Real Exchange Rate.   Figures 11a and 11b present the responses of the nominal and real effective exchange rates. The exchange rate, both in nominal and real terms, exhibits a

significantly negative response asymmetry resulting from its more significant depreciation following positive shocks relative to its effectively non-existent appreciation following negative shocks (a negative response corresponds to a weakening, or depreciation, of the exchange rate). In nominal terms, the exchange rate response to a negative shock is insignificant while in response to a positive shock we see significant depreciation for a total of 13 horizons (troughing at 1.9% after 5 years).[17] In real terms, the exchange rate even significantly depreciates for a few horizons following negative shocks and depreciates significantly from the 3rd horizon onwards after positive shocks, resulting in significant negative response asymmetry from the 2nd horizon onwards.

The stronger response of the exchange rate in response to positive shocks indicates that the output-based results can not be accounted for by an exchange-rate-induced expenditure-switching mechanism. If anything, such a mechanism serves as a shock absorber in the presence of positive global risk appetite shocks more than it does so in the presence of negative shocks, and is therefore not a candidate channel that can explain the strong asymmetry in output's response.

Leverage. Given the important theoretical role of leverage in models of EMEs based on collateral constraints (see, e.g., Durdu et al. (2009), Mendoza (2010), Fornaro (2015), and Devereux and Yu (2017)) as well as those based on the Bernanke et al. (1999) financial accelerator framework (see, e.g., Fernández and Gulan (2015)), it is important to uncover the potentially asymmetric behavior of leverage to better understand the mechanism underlying the results shown so far.

Toward this end, I measure leverage using BIS-reporting banks' gross claims on an EME divided by its GDP. This debt-to-GDP measure embodies debt of all economic agents in the economy to internationally active foreign banks that report to the BIS (currently consisting of banking groups from 31 countries).[18]

Importantly, my leverage series is based on the BIS *consolidated* banking statistics and therefore excludes inter-office claims held by parent banks on their EMEs subsidiaries, this in contrast to the

---

[17]The currency depreciation is consistent with the stronger net capital outflow taking place for EMEs following adverse global risk appetite shocks (see Figure 11b, whose depiction appears below).

[18]This measure of debt is termed as '*international claims*' in the BIS dataset and excludes local currency claims of parent banks' subsidiaries in EMEs on domestic borrowers.

locational banking statistics database which includes them. This exclusion is important given that inter-office lending, which need not be considered as a true form of economic debt, is expected to behave very differently from interbank lending. Consistent with this notion, there is rather ample evidence that parent bank funding of subsidiaries can be an important source of funding in quantitative terms and, importantly, is a much more stable funding source than interbank lending to unaffiliated banks during periods of financial stress (see, e.g., Takats et al. (2011), Reinhardt and Riddiough (2015), and the references in Kerl and Niepmann (2015)).

Figure 12 presents the sign-dependent responses of the log of leverage to a global risk appetite shock. These results stress that leverage falls significantly more in response to positive shocks, i.e., there is a strong deleveraging process following these shocks that is unmatched in quantitative terms by the effectively non-existent leveraging process observed after negative shocks. Specifically, after 3 years leverage falls by 1.4% in response to the positive shock while not even rising in response to the negative shock but rather significantly declining by 1.1% (as implied by multiplying the response in the figure to negative shocks by -1).

To better understand which sectors drive the responses from Figure 12, I now turn to study the responses of leverage of the private non-financial sector, financial sector, and the public sector, all measured as the BIS-reporting banks' claims on an EME's corresponding sector divided by its GDP. These results are shown in Figures 13a-13c, from which it is apparent that private non-financial leverage undergoes the strongest relative deleveraging process while financial sector leverage also seems to exhibit a qualitatively similar response difference albeit less strong in quantitative terms. Public sector leverage does not seem to play a meaningful role in driving the asymmetric behavior of total leverage.

Importantly, the strong persistence of leverage's response asymmetry accords well with the very persistent response asymmetry observed for output, which goes far beyond the asymmetry implied by a basic trade channel. In this respect, one can interpret these findings on leverage as support for there being a meaningful asymmetric financial frictions based mechanism at work

here.[19] Below I continue to explore this potential mechanism by looking at other relevant variables.

Stock Prices. As just noted, that a more acute deleveraging process takes place in response to a positive global risk appetite shock is broadly consistent with there being an exacerbation of financial frictions in the presence of this shock that is stronger in absolute terms than the alleviation of these frictions in the presence of a negative shock. But to more forcefully make this claim one needs to also examine the behavior of the asset side of firms' balance sheets. Toward this end, I make use of stock price data which represent countries' major stock market exchange indices. The rationale behind using stock prices to measure the asset side of firms' balance sheet is based on the notion that firms' market value serves as a reasonable proxy for Tobin's q, a central variable in models with financial frictions that represents the price of capital.

Figure 14 shows the results for stock prices.[20] Clearly, stock prices decline by much more in response to positive shocks than their rise following negative ones. E.g., after three quarters, stock prices decline by 10.2% after a positive shock compared to rising by only 2.8% after a negative shock, reflecting a significant response difference of -7.4%. Such significant asymmetry obtains from the impact horizon through the 8th horizon and is consistent with there being a meaningful asymmetrical role for financial frictions in driving this paper's results.

Capital Flows. I now turn my attention to studying the behavior of international capital flows, which can be seen as complementary to the previous analysis of leverage. Figures 15a-16b depict the responses of total net capital outflows and their components: net outflows of foreign direct investment, portfolio investment, and other investment,[21] respectively. All variables are in terms of shares of GDP.

---

[19]Recall that the baseline calibration of the simple capital market model from Section 3.2 failed to produce this *differentially* stronger deleveraging process. However, as discussed in Footnote 11, this result can be obtained from calibrating higher survival rates of borrowers.

[20]Results are similar when stock prices are deflated by the gdp deflator or consumer price index.

[21]'Other investment' includes loans as well as other forms of cross-border finance such as trade credit, bank deposits, and cash.

As indicated by Figure 15a, capital flows out of EMEs in a more significant and persistent manner (a positive response of this variable implies that capital flows out of the economy) after positive shocks than its flowing in after negative shocks. The difference between the net capital outflows' response across the two shocks is significantly positive from the impact horizon to the 8th horizon, peaking at 0.8% after four quarters. These results are broadly consistent with the previous ones on leverage as they emphasize that adverse global risk appetite shocks damage international investors' confidence in domestic assets much more strongly than the improvement in confidence induced by favorable shocks.

In terms of the sub-components of the net capital outflows variable, the subsequent figures seem to indicate that the overall stronger net capital outflow in response to positive shocks is driven mainly by a stronger net outflow of foreign direct investment and other investment flows, with the latter variable's response asymmetry being consistent with the results we saw from leverage given that other investment flows consist in part of bank loans.

Country Credit Spreads. The previous results on leverage and stock prices indicate that financial frictions may have a role in driving the differential output response across positive and negative shocks. To further study this financial frictions based channel, I now focus my attention on the role of EMEs' perceived riskiness in driving this paper's results.

Perhaps the most natural empirical proxy for the level of riskiness of EMEs as perceived by international credit market participants is the Emerging Markets Bond Index (EMBI) Global variable, which is computed by JP Morgan and proxies for country credit spreads.[22] I utilize the stripped spread version of the index, which is computed as an arithmetic, market-capitalization-weighted average of bond spreads over U.S. Treasury bonds of comparable duration. As emphasized in Elekda and Tchakarov (2007) and Fernández and Gulan (2015), country credit spreads constitute a suitable proxy for the external finance premium in EMEs. As such, they encapsulate valu-

---

[22]Data on EMBI is available for 21 countries, where the longest range of the unbalanced panel is 1994:Q1-2017:Q4. More details are provided in Appendix A. I have confirmed that the baseline output-based results are robust to using the smaller EMBI-based sample. These results are presented below in the robustness Section.

able information about the magnitude of financial frictions and their potential sign-dependence. Hence, understanding the asymmetric behavior of EMBI in response to global risk appetite shocks can shed important light on whether financial frictions may play a role in driving this paper's results.

The results for logged EMBI appear in Figure 17. For the first four quarters, spreads rise significantly more in response to a positive shock than they decline in response to a negative shock. However, this positive response difference thereafter reverses to being negative from the 6th horizon onwards and significantly so from the 10th horizon onwards. This reversal stems from the very gradual and persistent response of EMBI to the negative shock which ultimately dominates the response to the positive shock. Nevertheless, the significantly stronger responsiveness of perceived riskiness in the initial periods is consistent with the notion that there is a causal role for financial frictions in driving this paper's results. And it is a clear indication that an important interplay between the type of shock (i.e., adverse or favorable) and financial frictions takes place following global risk appetite shocks, where adverse shocks exacerbate financial frictions much more than the alleviation in them caused by favorable shocks. Notably, that EMBI is more responsive to negative shocks from the 6th quarter onwards is consistent with the timing of the stronger deleveraging process observed for positive shocks from Figure 12, as basic theory implies that such lowering of the leverage should also lower credit spreads and explain the lesser response of EBMI to positive shocks observed at more advanced horizons.

5   Robustness Checks

This section examines the robustness of the baseline results along four dimensions: considering different sub-samples; examining an alternative measure of global risk appetite shocks; using alternative detrending techniques; and controlling for size-dependence of impulse responses. In all checks I consider output as the outcome variable.

5.1 Various Sub-Samples

I consider in this section the robustness of my results to various sub-samples: sample that ends in 2007; sample covered by the EMBI variable; sample that excludes the BRIC economies (Brazil, Russia, India, and China); and sample that begins in 2000.

The first sample is worthwhile examining because (as argued at the start of the introduction) this paper tries to make a case about asymmetry in *normal* business cycles, while one can make the argument that the 2008-2009 global recession was somewhat abnormal due to the large shocks that produced it. The second sample is useful to consider to ensure that the baseline results hold also when using the sample that corresponds to that covered by the EMBI variable. The merit of examining the third sample lies in the fact that, from an identification standpoint, part of the appealingness of the econometric framework I use in this paper rests on the notion that global risk appetite shocks are exogenous to small open economies. The BRIC economies constitute the largest EMEs in my sample and, more generally, have the potential of violating the small open economy assumption. It is thus important to confirm that these relatively large economies are not driving the baseline results. The final sample is worthwhile considering because the leverage variable used in this paper only starts in 2000; hence, confirming that the baseline results for output carry over to this shorter sample is valuable.

Pre-2008 Sample. Figure 18a presents the results for the pre-2008 sample. Importantly, the effects of positive shocks continue to be significantly stronger than those of negative shocks, with a trough response difference of -0.4% taking place after 7 quarters and a total of 6 quarters for which the response difference is significantly negative. Granted, it is clear that the results for the pre-2008 sample are quantitatively less strong than the baseline ones. This mirrors the notion that including the 2008 large global risk appetite shocks in the baseline sample has much merit from an identification standpoint, enabling to better estimate the true effects of positive shocks. Nevertheless, the still meaningful significance of the response asymmetry from Figure 17 is encouraging in that it indicates that the main message of this paper does not merely stem from these large 2008

36

shocks.

EMBI Sample. Figure 18b presents the results for the EMBI sample. Appendix A gives details about this sample, which includes a total of 21 countries. Clearly, this much reduced sample still produces results that are very similar to the baseline one, with positive shocks' effects exceeding those of negative shocks by a significant margin for nearly all horizons (with this margin troughing at 1.1% after 5 quarters). Since EMBI serves as an informative variable in my analysis for uncovering the meaningfulness of financial frictions in inducing the asymmetric effects of global risk appetite shocks, it is rather encouraging that the output-based baseline results remain intact also when the baseline sample is reduced to the EMBI one.

Excluding BRIC Economies. Figure 19a presents the results for the sample that excludes the four BRIC economies. Here too the results are very similar to the baseline ones, indicating that the inclusion of the relatively large four BRIC economies is not driving the baseline results of this paper.

Post-2000 Sample. Figure 19b presents the results for the post-2000 sample. Clearly, the main message of the paper is robust to using the much reduced sample (along the time dimension). And, with similar reasoning to the EMBI case, these results are encouraging because they are based on the sample corresponding to the leverage variable, which is also a central variable in my attempt to uncover the importance of financial frictions in driving this paper's results.

5.2 Alternative Global Risk Appetite Shock Measure

My choice to measure global risk appetite shocks with FBP follows the reasoning from Gilchrist and Zakrajšek (2011), Gilchrist and Zakrajšek (2012a), and Gertler and Gilchrist (2018), who argue that FBP is a good proxy for the level of disruption (or tranquility) of credit intermediation in the U.S. The main underlying cause for this reasoning is that the excess bond premium for financial

firms (i.e., FBP) captures the level of financial distress among lenders and this in turn should represent these lenders' willingness to take on risk-bearing lending activity.

An alternative measure of such risk appetite shocks can also be arguably based on the excess bond premium (EBP) series from Gilchrist and Zakrajšek (2012b). From a methodological standpoint, FBP and EBP are extracted from equivalent procedures only that the former pertains to financial firms excess bond premium and the latter to non-financial ones. While the two series are connected, their correlation of 0.76 still points to there being a meaningful wedge between them. To better understand the source of this wedge, it is useful to look at their behavior during the bankruptcy of Lehman Brothers in September 2008 (the precise bankruptcy date being September 15), which is generally considered the epicenter of the recent financial crisis and therefore constitutes the ideal embodiment of a positive global risk appetite shock. During this month, FBP obtained a value of 281 basis points compared to just 150 basis points for EBP.[23] In other words, FBP captures the purest adverse risk appetite shock in the sample in a more timely manner than EBP. In October 2008, FBP and EBP reach 331 and 296 basis points, respectively. That the gap between the two series is so large during the actual default of Lehman and then becomes much narrower (albeit still non-negligible) in October is an indication that EBP (being linked to non-financial firms' spreads) represents a less direct measure of global risk appetite shocks than FBP.

Nevertheless, examining the results from replacing FBP with EBP still serves as a worthwhile robustness check that can further bolster the reliability of this paper's results. The EBP series is regularly updated[24] and begins in 1973 in monthly frequency, available from Favara et al. (2016). The sample I use for EBP is 1973-2017, resulting in my using EMEs output data that extends back to 1974 given that the EBP-based risk appetite shock series begins in 1974 after accounting for lagged EBP and stock prices when extracting the shock series. (Effectively, this extension results in only a modest rise in sample size as the only countries with available data that goes further

---

[23]Notably, the two series have similar variances and means, with the latter being very negligible given that these series are averages of residuals from regressions of firm-specific bond yields on expected default risk.

[24]The permanent link for the updated EBP series is https://www.federalreserve.gov/econresdata/notes/feds-notes/2016/files/ebp_csv.csv.

back than 1986 are Mexico, Philippines, South Africa, and South Korea.) Figure 20 presents the results from replacing FBP with EBP. Clearly, positive shocks continue to produce much bigger output declines than the output increases induced by negative shocks. The results are similar to the baseline ones, with the trough response difference being -0.8% after 8 quarters.

5.3   Alternative Detrending Filters

As explained at the end of Section 4.1, I detrend the trending variables in my data by fitting to them a third-order polynomial time trend prior to estimation. The objective of this procedure is to extract the cyclical component of the series which is taken to be the residual of the latter cubic polynomial time trend regression.[25] Much of the motivation for this detrending choice came from my noticing that cumulative growth rates of output at business cycle frequencies (e.g., two-year growth rates) for most of the countries in my sample appear to have significant linear- and quadratic-trend terms, thus implying a cubic-trend polynomial representation of log-levels of output.

Nevertheless, there are other alternatives for extracting the cyclical component of trending data whose deterministic trend is not a simple log-linear trend but rather a higher-order polynomial time trend. I consider three such alternatives. First, the standard HP-filer. Second, the detrending procedure proposed by Hamilton (2018). And third, a log-quadratic time trend polynomial instead of the baseline log-cubic trend polynomial. Moreover, for completeness, I also show results from a log-linear detrending procedure which is also equivalent to simply inserting log-cumulative-differences of the raw output variable in Equation (12).[26]

HP-Filter.   A recent paper by Hamilton (2018) advises against using the HP-filter, arguably the most popular detrending tool used in empirical macroeconomic research, on the grounds that its

---

[25]This amounts to estimating the following equation for the outcome variable in question y_t (say, logged output), $y_t = a + bt + ct^2 + dt^3 + \varepsilon_t$, and taking ε_t to be the corresponding cyclical component of the series.

[26]While results are similar also when a simple log-linear detrending filter is applied, the bias from doing this can be material given the significance of the higher order trend terms prevalent in the data. Specifically, not accounting for these higher order trend terms results in a misspecified model where part of the estimated effects are likely driven by higher order deterministic trends taking place in the sample's EMEs.

cyclical component has a tendency to be characterized by spurious behavior. This point is also demonstrated by Phillips and Jin (2015), who develop a limit theory for the HP-filter for various classes of stochastic and deterministic trends. Nevertheless, Sakarya and de Jong (2017) show that the HP-filer can at least asymptotically extract the cyclical component of trend polynomials of less than order 4. Overall, while recent work does suggest taking caution in choosing the HP-filer as a detrending method, it still seems worthwhile to examine the robustness of my results to estimating a specification in which the log of output is detrended using the HP filter prior to taking its cumulative differences.

Results from this exercise appear in Figure 21a. It is apparent that positive shocks continue to induce stronger effects, with response differences being significant for all horizons troughing at -0.9% after 5 quarters. This suggests that the baseline output-based results are robust to HP-filtering the output data instead of using a cubic trend polynomial.

Detrending Method from Hamilton (2018). Hamilton (2018) not only argues against using the HP-filer but also proposes an alternative detrending method which regresses the variable at date $t + h$ on the four most recent values as of date t, where the residual from this regression is taken to be the estimated cyclical component of the variable. Hamilton (2018) makes the case that, in contrast to the HP-filter, this detrending method does not suffer from the drawback of having spuriousness in its cyclical component. However, a recent paper by Schuler (2018) provides theoretical and empirical insights on the attributes of the Hamilton (2018) filter, arguing that although not subject to the exact same drawbacks as the HP filter, Hamilton's filter still modifies the original cyclical structure of economic time series and its performance naturally depends on the choice of h.

Nevertheless, I view as important checking that using Hamilton's regression filter in my estimations yields similar results given that it is an additional dimension along which to further enhance my results' reliability. Toward this end, I choose $h = 16$, which means that my cyclical component is obtained from regressing 4-year-ahead logged output on current and three lags of logged output. This cyclical component can be thought of as output variation caused by shock

components that do not persist longer than h periods. One may argue that taking a longer h is sensible for my setting as global risk appetite shocks may have rather persistent effect on output but I make a compromise here between this issue and avoiding losing too many observations in the estimation done after detrending the data.

Results from this exercise appear in Figure 21b. Importantly, output continues to fall by significantly more in response to positive shocks than its rise after negative shocks, with the response difference reaching a trough of -1.5% after 9 quarters. These results further increase confidence in the robustness of my results to filtering the data differently from the baseline procedure.

Log-Quadratic Detrending. While, as discussed above, my output data generally exhibits a significant log-cubic trend component in addition to a significant log-quadratic trend component, it is still important to ensure that my results are insensitive to lowering the trend polynomial's order by one and consider a log-quadratic trend polynomial. This second-order trend polynomial detrending is quite common for extracting the cyclical component of macro data (see, e.g., Uribe and Schmitt-Grohé (2017)). Results from log-quadratic detrending are shown in Figure 22a, indicating that output response differences from log-quadratic detrending are similar to those from log-cubic detrending.

Log-Linear Detrending. For completeness, notwithstanding the likely bias resulting from ignoring higher-order trend terms in output when detrending it, I end this section with results from log-linear detrending. These results are shown in Figure 22b, indicating that output response differences from log-linear detrending are also similar to the baseline ones.

5.4   Controlling for Impulse Response Size-Dependence

The analysis of this paper is conducted for a *given* shock size (specifically, one standard deviation shock size) for both the positive and negative shock so as to only focus on sign-dependency and leave aside the issue of size-dependency. More generally, my focus on including only an

even higher-order power (i.e., 2) in my baseline second-order specification while conditioning the results on a given shock size can serve the purpose of quantifying sign-dependency in parallel to remaining consciously silent on size-dependency. Nevertheless, one may argue for the possibility that it is the sheer size of the 2008 adverse risk shock realizations pushing this paper's results as opposed to true response asymmetry. To address this concern, I have also experimented with adding a cubed term of the global risk appetite shock in Equation (12) (similar to Tenreyro and Thwaites (2016), although they include only a linear and cubed terms in their cubed-shock-augmented regressions) to inspect the potential effect of shock size on my results.

The results from this estimation appear in Figure 23. Relative to the baseline case of constructing the impulse responses to positive and negative shocks, I simply added the coefficient on the cubed shock term for the former and subtracted it for the latter. Clearly, results are very similar to the baseline ones, reflecting the negligible and insignificant coefficients on the cubed shock term at essentially all horizons. These results further reinforce the central notion of this paper that global risk appetite shocks have asymmetric implications for EMEs business cycles that go beyond the relatively large size of the 2008 adverse risk shock realizations.

6 Discussion

On Page 27 I made the argument that the results from Figure 4 regarding the FBP response to positive and negative global risk appetite shocks did not necessarily imply that positive shocks are more detrimental for FBP than the extent to which negative shocks are favorable for it. More specifically, I emphasized that although positive shocks generate a bigger effect on FBP for the first year after the shock, this differential effects mostly reverses in the periods thereafter to the point where the average effects on FBP of positive and negative shocks over the reasonable business cycle frequency of a three year horizon are very similar at 7 and 6 basis points, respectively.

Notably, simply altering the standard deviation of the negative shock so as to eliminate FBP's impact response asymmetry is misguided for two reasons. First, such rescaling would introduce

size-dependence into the estimation thus not allowing for the isolation of sign-dependent effects which is facilitated by this paper's choice of looking at one standard deviation realizations for both positive and negative shocks (also see related discussion on Page 41). Second, such rescaling ignores the entire dynamics of FBP's response asymmetry by considering only a very limited portion of it and thus likely leads to a bias in the estimated impulse response sign-dependency.

To illustrate why this issue of the overall direction of asymmetry in the FBP response is especially important for the structural interpretation of this paper's results, consider two opposing arguments potentially arising from the results from Figure 4. The first is that the much stronger impact response of FBP to positive shocks that lasts also throughout the first year suggests that the results of this paper are not driven by endogenous sign-dependency related to EMEs financial frictions but rather by exogenous sign-dependency related to the sign-dependent nature of the stochastic process underlying FBP. The second argument is that one need not look at just the impact horizon or even the first-year horizon when trying to ascertain the overall asymmetry in the FBP response; rather, the whole dynamics of FBP need to be considered by accounting for the more persistent response of FBP to negative shocks. In what follows, I use the model from Section 3.2 to demonstrate that the second argument stands on much firmer ground than the first by conducting two experiments: first, an experiment that computes sign-dependent responses to risk shocks when accounting for the more persistent effect of negative shocks on FBP and, second, an experiment that computes these response when shutting down this greater persistence.

First Experiment: Accounting for the Whole Asymmetric Dynamics of FBP. In the first experiment I solve a slightly modified version of the model from Section 3.2 which replaces the stochastic process for risk (Equation (6)) with the one implied by the impulse responses from Figure 4. Specifically, I compute quarterly averages of the monthly effects from this Figure and let the risk variable be driven by a second-order moving average process containing the coefficients implied by the responses from Figure 4. I.e., I use the following process for risk:

$$\sigma_t = \bar{\sigma} + \alpha_1 \eta_t + \beta_1 \eta_t^2 + \alpha_2 \eta_{t-1} + \beta_2 \eta_{t-1}^2 + \ldots + \alpha_{20} \eta_{t-1} + \beta_{20} \eta_{t-20}^2, \tag{13}$$

43

where the α's and β's are taken from the quarterly averages of the estimated monthly effects from Figure 4. I normalize the effects of the positive and negative realizations such that absent asymmetry risk would rise (decline) by 0.05 on impact in response to a positive (negative) shock (as in the baseline case).

Second Experiment: Shutting Down the Stronger Persistence of the Negative Shock. In the second experiment I assign zeroes to $\beta_6, \beta_7, ..., \beta_{20}$ on the premise that the reversal in the differential response of FBP to positive shocks begins to take place from the 6th horizon. In other words, I impose on σ to respond symmetrically to positive and negative shocks from the 6th horizon onwards, which in turn enables me to examine how this shutting down of the stronger persistence of the negative shock alters the model's response asymmetry.

Results from the Two Experiments. Figures 24a and 24b present the sign-dependent impulse responses from the experiment where the more persistent effects of the negative shock are accounted for (the first experiment) and from the experiment where they are shut down (the second experiment), respectively. Clearly, accounting for this persistence has considerable implications for the asymmetry in the model's responses: all endogenous variables respond much more strongly to the negative shock when its stronger persistence is accounted for relative to when this differential persistence is shut down, with the most notable difference relating to investment. This variable, which represents the central real variable in this model, only responds more strongly to the positive shock than to the negative shock on impact and very moderately so (with the negative shock's effects clearly dominating those of the positive shock from the 3rd to 14th horizon) when the stronger persistence of the negative shock is accounted for, while responding much more strongly in quantitative terms and for much longer (3 years) when this differential persistence is shut down.

In other words, from a structural standpoint, the asymmetric behavior of FBP in the data serves as an exogenous amplification mechanism for the effects of negative shocks relative to positive shocks' effects. This suggests that the empirical results of this paper need not be interpreted as

arising from an exogenous sign-dependent mechanism underlying the FBP process. Rather, if anything, such exogenous mechanism is expected to go in the other direction of pushing negative shocks' effects to be stronger than positive shocks' effects so that there are likely to be additional (endogenous) sign-dependent mechanisms pushing this paper's results in the other direction. My analysis highlighted financial frictions as such endogenous sign-dependent mechanism and the results of this section further validate the relevance of this interpretation of my results.

7 Conclusion

This paper has presented two sets of results consistent with there being meaningful business cycle asymmetry in EMEs. First, EMEs trend-adjusted output growth at business cycle frequencies was documented to have strong negative skewness as well as much greater output losses in recessions than output gains in expansions for the baseline 1986-2017 sample; excluding post-2008 observations, however, completely eliminated the aforementioned negative skewness, raising the possibility that the shocks which were central to the recent global recession may have the potential of inducing meaningful asymmetric effects on EMEs. Second, I studied this unconditional asymmetry through the lens of global risk appetite shocks, using a suitable Bayesian sign-dependent econometric framework and building on the theoretical insight that positive risk appetite shocks raise credit spreads more then the decline in them that is induced by negative shocks. My results indicate that positive global risk appetite shocks lower output significantly more than the corresponding output increase induced by negative shocks.

Importantly, my analysis was able to deduce that this conditional asymmetry is far too persistent to be solely explained by a basic trade channel by which EMEs output behavior simply inherits its asymmetry from the U.S. economy's asymmetric response to these global risk appetite shocks. Exploring various other variables in the analysis, I uncovered a meaningful role for financial frictions in producing this asymmetry.

The results of this paper have two main implications. First, they can serve as a guide for

45

SOE model builders in stressing that business cycle asymmetry in EMEs can result not only as an outcome of Sudden Stops but also in the confines of more normal business cycles. Second, they indicate that EMEs policymakers may need to construct asymmetric policy measures when trying to alleviate business cycle fluctuations, responding more aggressively to adverse shocks than to favorable shocks.

References

Abbritti, M. and Fahr, S.: 2013, Downward wage rigidity and business cycle asymmetries, *Journal of Monetary Economics* **60**(7), 871 – 886.

Akinci, O.: 2014, Financial frictions and macroeconomic fluctuations in emerging economies, *International Finance Discussion Papers, Board of Governors of the Federal Reserve System* (1120).

Aruoba, S. B., Bocola, L. and Schorfheide, F.: 2017, Assessing dsge model nonlinearities, *Journal of Economic Dynamics and Control* **83**, 34 – 54.

Auerbach, A. J. and Gorodnichenko, Y.: 2012, *Fiscal Multipliers in Recession and Expansion*, University of Chicago Press, pp. 63–98.

Barnichon, R. and Matthes, C.: 2018a, Functional approximation of impulse responses, *Journal of Monetary Economics* **99**, 41 – 55.

Barnichon, R. and Matthes, C.: 2018b, Understanding the size of the government spending multiplier: It's in the sign, *Technical report*, CEPR Discussion Papers.

Barnichon, R., Matthes, C. and Ziegenbein, A.: 2018, Are the effects of financial market disruptions big or small?, *Technical report*.

Ben Zeev, N.: 2017, Capital controls as shock absorbers, *Journal of International Economics* **109**(Supplement C), 43–67.

Ben Zeev, N.: 2019a, Global credit supply shocks and exchange rate regimes, *Journal of International Economics* **116**, 1–32.

Ben Zeev, N.: 2019b, Identification of sign-dependency of impulse responses, *Manuscript*, Ben-Gurion University.

Bengui, J. and Bianchi, J.: 2018, Macroprudential policy with leakages, *Working Paper 25048*, National Bureau of Economic Research.

Benigno, G., Chen, H., Otrok, C., Rebucci, A. and Young, E. R.: 2013, Financial crises and macro-prudential policies, *Journal of International Economics* **89**(2), 453–470.

Benigno, G., Foerster, A., Otrok, C. and Rebucci, A.: 2017, Estimating macroeconomic models of financial crises: An endogenous regime switching approach, *Technical report*, London School of Economics.

Bernanke, B. S., Gertler, M. and Gilchrist, S.: 1999, The financial accelerator in a quantitative business cycle framework, *Handbook of macroeconomics* **1**, 1341–1393.

Bianchi, J.: 2011, Overborrowing and systemic externalities in the business cycle, *American Economic Review* **101**(7), 3400–3426.

Bianchi, J.: 2016, Efficient bailouts?, *American Economic Review* **106**(12), 3607–59.

Bianchi, J. and Mendoza, E. G.: 2018, Optimal time-consistent macroprudential policy, *Journal of Political Economy* **126**(2), 588–634.

Binning, A. and Maih, J.: 2017, Modelling occasionally binding constraints using regime-switching, *Technical report*, Centre for Applied Macro-and Petroleum economics (CAMP), BI Norwegian .

Bräuning, F. and Ivashina, V.: 2019, US monetary policy and emerging market credit cycles, *Journal of Monetary Economics (forthcoming)* .

Caballero, R. J. and Kamber, G.: 2019, On the global impact of risk-off shocks and policy-put frameworks.

Calvo, G. A., Izquierdo, A. and Talvi, E.: 2006, Sudden stops and phoenix miracles in emerging markets, *American Economic Review* **96**(2), 405–410.

Calvo, G. A. and Reinhart, C. M.: 2000, When capital inflows come to a sudden stop: Consequences and policy options, *in* P. B. Kenen and A. K. Swoboda (eds), *Reforming the International Monetary and Financial System*, International Monetary Fund, pp. 175–201.

Cao, D. and Nie, G.: 2017, Amplification and asymmetric effects without collateral constraints, *American Economic Journal: Macroeconomics* **9**(3), 222–66.

Carrire-Swallow, Y. and Cspedes, L. F.: 2013, The impact of uncertainty shocks in emerging economies, *Journal of International Economics* **90**(2), 316 – 325.

Cesa-Bianchi, A., Ferrero, A. and Rebucci, A.: 2018, International credit supply shocks, *Journal of International Economics* **112**, 219 – 237.

Céspedes, L. F., Chang, R. and Velasco, A.: 2004, Balance sheets and exchange rate policy, *American Economic Review* **94**(4), 1183–1193.

Chalkley, M. and Lee, I. H.: 1998, Learning and asymmetric business cycles, *Review of Economic Dynamics* **1**(3), 623 – 645.

Chang, C., Chen, K., Waggoner, D. F. and Zha, T.: 2015, *Trends and Cycles in China's Macroeconomy*, University of Chicago Press, pp. 1–84.

Chen, S.-S. and Lin, T.-Y.: 2019, Do exchange rate shocks have asymmetric effects on reserve accumulation? evidence from emerging markets, *The Scandinavian Journal of Economics (forthcoming)*.

Christiano, L., Eichenbaum, M. and Evans, C.: 2005, Nominal rigidities and the dynamic effects of a shock to monetary policy, *Journal of Political Economy* **113**(1), 1–45.

Christiano, L. J., Motto, R. and Rostagno, M.: 2014, Risk shocks, *American Economic Review* **104**(1), 27–65.

Cover, J. P.: 1992, Asymmetric effects of positive and negative money-supply shocks, *The Quarterly Journal of Economics* **107**(4), 1261–1282.

Devereux, M. B., Lane, P. R. and Xu, J.: 2006, Exchange rates and monetary policy in emerging market economies, *The Economic Journal* **116**(511), 478–506.

Devereux, M. and Yu, C.: 2017, Exchange rate adjustment in financial crises, *IMF Economic Review,* *(forthcoming)* .

Driscoll, J. C. and Kraay, A. C.: 1998, Consistent covariance matrix estimation with spatially dependent panel data, *Review of economics and statistics* **80**(4), 549–560.

Durdu, C. B., Mendoza, E. G. and Terrones, M. E.: 2009, Precautionary demand for foreign assets in sudden stop economies: An assessment of the new mercantilism, *Journal of development Economics* **89**(2), 194–209.

Edwards, S. and Levy-Yeyati, E.: 2005, Flexible exchange rates as shock absorbers, *European Economic Review* **49**(8), 2079 – 2105.

Elekda, S. and Tchakarov, I.: 2007, Balance sheets, exchange rate policy, and welfare, *Journal of Economic Dynamics and Control* **31**(12), 3986 – 4015.

Favara, G., Gilchrist, S., Lewis, K. F. and Zakrajsek, E.: 2016, Updating the Recession Risk and the Excess Bond Premium, *FEDS Notes 2016-10-06*, Board of Governors of the Federal Reserve System (U.S.).

Fernández, A. and Gulan, A.: 2015, Interest rates, leverage, and business cycles in emerging economies: The role of financial frictions, *American Economic Journal: Macroeconomics* **7**(3), 153–88.

Ferretti, G. M. M. and Razin, A.: 2000, Current account reversals and currency crises: Empirical regularities, *in* P. Krugman (ed.), *Currency Crises*, University of Chicago Press, pp. 285–323.

Fornaro, L.: 2015, Financial crises and exchange rate policy, *Journal of International Economics* **95**(2), 202–215.

Garcia-Cicco, J., Pancrazi, R. and Uribe, M.: 2010, Real business cycles in emerging countries?, *American Economic Review* **100**(5), 2510–31.

Gertler, M. and Gilchrist, S.: 2018, What happened: Financial factors in the great recession, *Journal of Economic Perspectives* **32**(3), 3–30.

Gertler, M., Gilchrist, S. and Natalucci, F. M.: 2007, External constraints on monetary policy and the financial accelerator, *Journal of Money, Credit and Banking* **39**(2-3), 295–330.

Gilchrist, S. and Williams, J. C.: 2000, Puttyclay and investment: A business cycle analysis, *Journal of Political Economy* **108**(5), 928–960.

Gilchrist, S. and Zakrajšek, E.: 2011, Monetary policy and credit supply shocks, *IMF Economic Review* **59**(2), 195–232.

Gilchrist, S. and Zakrajšek, E.: 2012a, Credit supply shocks and economic activity in a financial accelerator model, *Rethinking the Financial Crisis* **1**, 37–72.

Gilchrist, S. and Zakrajšek, E.: 2012b, Credit spreads and business cycle fluctuations, *American Economic Review* **102**(4), 1692–1720.

Guerrieri, L. and Iacoviello, M.: 2015, Occbin: A toolkit for solving dynamic models with occasionally binding constraints easily, *Journal of Monetary Economics* **70**, 22–38.

Hamilton, J. D.: 2018, Why you should never use the hodrick-prescott filter, *The Review of Economics and Statistics (forthcoming)* .

Harding, M. and Wouters, R.: 2019, Risk and state-dependent financial frictions, *Manuscript*, DIW Berlin.

Holden, T. D.: 2016, Computation of solutions to dynamic models with occasionally binding constraints, *Technical report*, ZBW-German National Library of Economics.

Jeanne, O. and Korinek, A.: 2010, Excessive volatility in capital flows: A pigouvian taxation approach, *American Economic Review* **100**(2), 403–07.

Jorda, O.: 2005, Estimation and inference of impulse responses by local projections, *American Economic Review* **95**(1), 161–182.

Kerl, C. and Niepmann, F.: 2015, What determines the composition of international bank flows?, *IMF Economic Review* **63**(4), 792–829.

Kilian, L. and Vigfusson, R. J.: 2011, Are the responses of the u.s. economy asymmetric in energy price increases and decreases?, *Quantitative Economics* **2**(3), 419–453.

Kim, J. and Ruge-Murcia, F. J.: 2009, How much inflation is necessary to grease the wheels?, *Journal of Monetary Economics* **56**(3), 365 – 377.

Koop, G., Pesaran, M. and Potter, S. M.: 1996, Impulse response analysis in nonlinear multivariate models, *Journal of Econometrics* **74**(1), 119 – 147.

Korinek, A. and Mendoza, E.: 2014, From sudden stops to fisherian deflation: Quantitative theory and policy, *Annual Review of Economics* **6**, 299–332.

Lan, H. and Meyer-Gohde, A.: 2013, Solving dsge models with a nonlinear moving average, *Journal of Economic Dynamics and Control* **37**(12), 2643 – 2667.

McKay, A. and Reis, R.: 2008, The brevity and violence of contractions and expansions, *Journal of Monetary Economics* **55**(4), 738 – 751.

Mendoza, E. G.: 2002, *Credit, Prices, and Crashes: Business Cycles with a Sudden Stop*, University of Chicago Press, pp. 335–392.

Mendoza, E. G.: 2006, Lessons from the debt-deflation theory of sudden stops, *American Economic Review* **96**(2), 411–416.

Mendoza, E. G.: 2010, Sudden stops, financial crises, and leverage, *American Economic Review* **100**(5), 1941–66.

Mendoza, E. G. and Smith, K. A.: 2006, Quantitative implications of a debt-deflation theory of sudden stops and asset prices, *Journal of International Economics* **70**(1), 82–114.

Miranda-Agrippino, S. and Ricco, G.: 2017, The transmission of monetary policy shocks, *Technical report*, Observatoire Francais des Conjonctures Economiques (OFCE).

Mork, K. A.: 1989, Oil and the macroeconomy when prices go up and down: An extension of hamilton's results, *Journal of Political Economy* **97**(3), 740–744.

Müller, U. K.: 2013, Risk of bayesian inference in misspecified models, and the sandwich covariance matrix, *Econometrica* **81**(5), 1805–1849.

Ordoez, G.: 2013, The asymmetric effects of financial frictions, *Journal of Political Economy* **121**(5), 844–895.

Ottonello, P.: 2015, Optimal exchange rate policy under collateral constraints and wage rigidity, *manuscript, Columbia University* .

Phillips, P. and Jin, S.: 2015, Business cycles, trend elimination, and the hp filter, *Technical report*, Cowles Foundation for Research in Economics, Yale University.

Reinhardt, D. and Riddiough, S. J.: 2015, The two faces of cross-border banking flows, *IMF Economic Review* **63**(4), 751–791.

Sakarya, N. and de Jong, R. M.: 2017, A property of the hodrick-prescott filter and its application, *Technical report*, The Ohio State University.

Schmitt-Grohé, S. and Uribe, M.: 2013, Downward nominal wage rigidity and the case for temporary inflation in the eurozone, *Journal of Economic Perspectives* **27**(3), 193–212.

Schmitt-Grohé, S. and Uribe, M.: 2014, *Pegs, Downward Wage Rigidity, and Unemployment: The Role of Financial Structure*, Central Bank of Chile, Santiago, Chile, pp. 69–95.

Schmitt-Grohé, S. and Uribe, M.: 2016, Downward nominal wage rigidity, currency pegs, and involuntary unemployment, *Journal of Political Economy* **124**(5), 1466–1514.

Schuler, Y. S.: 2018, On the cyclical properties of Hamiltons regression filter, *Technical report*, Deutsche Bundesbank.

Takats, E. et al.: 2011, Cross-border bank lending to emerging market economies, *BIS Papers chapters* **54**, 11–29.

Tenreyro, S. and Thwaites, G.: 2016, Pushing on a string: Us monetary policy is less powerful in recessions, *American Economic Journal: Macroeconomics* **8**(4), 43–74.

Townsend, R. M.: 1979, Optimal contracts and competitive markets with costly state verification, *Journal of Economic theory* **21**(2), 265–293.

Uhlig, H.: 1994, What macroeconomists should know about unit roots: A bayesian perspective, *Econometric Theory* **10**(3/4), 645–671.

Uribe, M. and Schmitt-Grohé, S.: 2017, *Open Economy Macroeconomics*, Princeton University Press.

Weise, C. L.: 1999, The asymmetric effects of monetary policy: A nonlinear vector autoregression approach, *Journal of Money, Credit and Banking* pp. 85–108.

Zha, T.: 1999, Block recursion and structural vector autoregressions, *Journal of Econometrics* **90**(2), 291–316.

Appendix A   Data

A.1   Output, Investment, Consumption, and the Trade Balance

Variables Definitions.   Output is defined as local currency nominal GDP divided by the GDP deflator; investment is local currency gross private capital formation divided by the GDP deflator; consumption is defined as local currency nominal household consumption divided by the GDP deflator; and the trade balance is the difference between local currency exports and imports divided by local currency nominal GDP. All series were seasonally adjusted using ARIMA X12 and downloaded from the International Financial Statistics (IFS) database, which is published by the International Monetary Fund, except for China for which data from Chang et al. (2015) was collected from the Atlanta Fed website.

Sample.   My panel for these variables consists of a total of 3771 observations. I use quarterly data for the following countries (42 in total) and periods: Argentina 1993:Q1-2017:Q4; Armenia 1999:Q4-2017:Q4; Bolivia 1990:Q1-2017:Q4; Brazil 1995:Q1-2017:Q4; Bulgaria 1996:Q1-2017:Q4; Chile 1990:Q1-2017:Q4; China 1992:Q1-2017:Q4; Colombia 1994:Q1-2017:Q1; Costa Rica 1991:Q1-2017:Q4; Croatia 1997:Q1-2017:Q4; Czech Republic 1994:Q1-2017:Q4; Ecuador 1991:Q1-2017:Q3; Egypt 2002:Q1-2013:Q4; Estonia 1995:Q1-2017:Q4; Georgia 1996:Q1-2017:Q4; Guatemala 2001:Q1-2016:Q4; Hungary 1995:Q1-2017:Q4; India 2004:Q1-2017:Q4; Indonesia 1997:Q1-2017:Q4; Iran 1988:Q1-2007:Q4; Korea 1986:Q1-2017:Q4; Kyrgyz 2000:Q1-2017:Q3; Latvia 1990:Q1-2017:Q4; Lithuania 1995:Q1-2017:Q4; Macedonia 1995:Q1-2017:Q4; Malaysia 1991:Q1-2017:Q4; Mauritius 2000:Q1-2017:Q4; Mexico 1986:Q1-2017:Q4; Moldova 2000:Q1-2008:Q4; Paraguay 1994:Q1-2016:Q4; Peru 1994:Q2-2017:Q1; Philippines 1986:Q1-2016:Q4; Poland 1995:Q1-2017:Q4; Romania 1998:Q1-2017:Q4; Russia 1995:Q1-2017:Q4; Serbia 1995:Q1-2017:Q4; Slovakia 1995:Q1-2017:Q4; Slovenia 1995:Q1-2017:Q4; South Africa 1986:Q1-2017:Q3; Thailand 1993:Q1-2017:Q4; Turkey 1987:Q1-2017:Q4; Ukraine 2001:Q1-2017:Q4.

A.2 Global Risk Appetite Shock

Variable Definition. To measure global risk appetite shocks, I make use of the financial bond premium (FBP) series from Gilchrist and Zakrajšek (2011) and Gilchrist and Zakrajšek (2012a). Building on the methodology from Gilchrist and Zakrajšek (2012b), these papers use micro-level data for 193 financial intermediaries to construct a credit spread index which they decomposed into a component that captures firm-specific information on expected defaults and a residual component that they termed as FBP which represents the shifts in financial intermediaries' risk attitudes. The series is in monthly frequency and runs from 1985:Q1 through 2012:Q4 and was downloaded from Simon Gilchrist's Webpage.[27]

A.3 Exchange Rates

Variables Definitions. The exchange rate data consist of nominal and real effective exchange rate series downloaded from the IFS, where the real effective exchange rate is CPI-based. Since the IFS source missed data for several countries, I complemented it with the Bank for International Settlements (BIS) nominal and real effective exchange rate dataset.

Sample. My panel for these variables consists of a total of 3165 observations. I use quarterly data for 35 countries in total, with the missing ones being Egypt, Ecuador, Guatemala, Kyrgyz, Mauritius, Serbia, and Slovenia. Except for Thailand and Turkey, whose exchange rate data begin one year later than their corresponding output data, the exchange rate sample corresponds to the baseline output one in terms of the covered periods.[28]

---

[27]http://people.bu.edu/sgilchri/Data/data.htm.

[28]To be completely consistent with the exact coverage of the output-based sample, I remove dates covered by the exchange rate data that are not covered by output (this is also done for all other variables where necessary).

A.4   Leverage

Variable Definition.   The leverage data is defined as the ratio of total BIS-reporting banks' international claims on each country to its GDP. I also make use of the three sub-compoenents of the total claims series: claims on private non-financial sector, claims on financial sector, and claims on public sector; the sectoral leverage variables are also divided by GDP. All claims series are taken from the BIS consolidated banking statistics database. Raw claims are in dollar terms and are therefore converted to local currency terms using the average quarter dollar exchange rate from each country taken from the IFS database. The BIS claims data exclude intragroup positions and are currently reported to the BIS by banking groups from 31 countries.

Sample.   The panel for leverage consists of a total of 2685 observations. The data is quarterly and covers the 42 countries that correspond to the output-based sample of countries for the sample period 2000-2017.

A.5   Stock Prices

Variable Definition.   The stock price data is based on countries' major stock market exchange indices, downloaded from the IFS.

Sample.   The panel for stock prices consists of a total of 2336 observations. This panel covers 28 countries, with the following omitted countries relative to those covered by the output variable: Armenia, Bolivia, Colombia, Costa Rica, Ecuador, Egypt, Georgia, Guatemala, Kyrgyz, Macedonia, Moldova, Paraguay, Romania, and Serbia.

A.6   Balance of Payments

Variables Definitions.   The balance of payments data consists of the GDP shares of local currency net capital outflows of foreign direct investment, portfolio investment, and other invest-

ment.[29] All variables were available in dollar values in raw form and were thus converted to local currency values by using the dollar exchange rate. All raw series were seasonally adjusted using ARIMA X12 and downloaded from the IFS.

Sample. My panel for these variables consists of a total of 3280, 3208, and 3280 observations for foreign direct investment, portfolio flows, and other investment, respectively. This panel corresponds to the countries covered by the output variable except for Ecuador, Egypt, Estonia, Malaysia, and Paraguay. The total capital flows variable (whose results appear in Figure 15a) is defined as the sum of the GDP shares of the three capital flow types.

A.7   EMBI Spread

Variable Definition. I use the Emerging Markets Bond Index (EMBI) Global computed by JP Morgan as a measure of country credit spreads. This index is a composite of different U.S. dollar-denominated bonds. The Stripped Spread is computed as an arithmetic, market-capitalization-weighted average of bond spreads over U.S. Treasury bonds of comparable duration and downloaded from Datastream. Quarterly values are average of corresponding raw spread daily values.

Sample. My panel for EMBI consists of a total of 1679 observations. I use quarterly data for the following countries (21 in total) and periods: Argentina 1994:Q1-2017:Q4; Brazil 1994:Q3-2017:Q4; Bulgaria 1994:Q3-2014:Q1; Chile 1999:Q2-2017:Q4; China 1994:Q1-2017:Q4; Colombia 1997:Q1-2017:Q4; Ecuador 1995:Q1-2017:Q4; Egypt 2001:Q3-2017:Q4; Hungary 1999:Q1-2017:Q4; Indonesia 2004:Q2-2017:Q4; Korea 1994:Q1-2004:Q2; Kyrgyz 1999:Q1-2017:Q4; Malaysia 1996:Q4-2016:Q4; Mexico 1994:Q1-2017:Q4; Peru 1997:Q1-2017:Q4; Philippines 1994:Q1-2017:Q4; Poland 1994:Q1-2017:Q4; Russia 1997:Q4-2017:Q4; South Africa 1994:Q4-2017:Q4; Thailand 1997:Q2-2006:Q1; Turkey 1996:Q3-2017:Q4.

---

[29]'Other investment' includes loans as well as other forms of cross-border finance such as trade credit, bank deposits, and cash.

Appendix B   Posterior Distribution of Parameters

Since the Bayesian estimation of Equations (10), (11), and (12) is done sequentially, estimating each conditional on the estimation of the previous equation, I present here the estimation for each equation separately while taking as given the residual from the previous equation (except for Equation (10) which starts the procedure).

Estimation of Equation (10).   Drawing on the notation from Page 24, Equation (10) can be written in matrix notation as follows:

$$F = GB^1 + V, \tag{14}$$

where $F = [FBP_1, ..., FBP_T]'$, $G = [G_1, ..., G_T]'$, $G_t = [FBP_{t-1}, FBP^2_{t-1}, \Delta SP_{t-1}, \Delta SP^2_{t-1}, ..., FBP_{t-p},$ $FBP^2_{t-p}, \Delta SP_{t-p}, \Delta SP^2_{t-p}, 1]'$, $B^1 = [\Gamma^{FBP}_1, \Psi^{FBP}_1, \Gamma^{SP}_1, \Psi^{SP}_1, ..., \Gamma^{FBP}_p, \Psi^{FBP}_p, \Gamma^{SP}_p, \Psi^{SP}_p, C]'$; p is the number of lags; and $V = [\epsilon_1, ..., \epsilon_T]'$. B^1 here represents the coefficient matrix of Equation (10) and σ^2_1 is the variance of ϵ_t. I follow the conventional approach of specifying a normal-inverse Wishart prior distribution for B^1 and Σ^2_1:

$$vec(B^1) \mid \sigma_1 \quad \sim \quad N(vec(\bar{B}^1_0), \sigma_1 \times N^{-1}_0) \tag{15}$$

$$\sigma_1 \quad \sim \quad IW_k(v_0 S_0, v_0) \tag{16}$$

where N_0 is a $4p$x$4p$ positive definite matrix, S_0 is a variance scalar, and $v_o > 0$. As shown by Uhlig (1994), the latter prior implies the following posterior distribution:

$$vec(B^1) \mid \sigma_1 \quad \sim \quad N(vec(\bar{B}^1_T), \sigma_1 \times N^{-1}_T) \tag{17}$$

$$\sigma_1 \quad \sim \quad IW_k(v_T S_T, v_T) \tag{18}$$

where $v_T = T + v_0$, $N_T = N_0 + G'G$, $\bar{B}^1_T = N^{-1}_T(N_0\bar{B}^1_0 + G'G\hat{B}^1)$, $S_T = \frac{v_0}{v_T}S_0 + \frac{T}{v_T}\hat{\sigma}_1 + \frac{1}{v_T}(\hat{B}^1 - \bar{B}^1_0)'N_0 N^{-1}_T G'G(\hat{B}^1 - \bar{B}^1_0)$, $\hat{B}^1 = (G'G)^{-1}G'F$,

and $\hat{\sigma}_1 = (F - G\hat{B}^1)'(F - G\hat{B}^1)/T$.

I use a weak prior, i.e., $v_0 = 0$, $N_0 = 0$, and arbitrary S_0 and $\bar{B}_0^1$. This implies that the prior distribution is proportional to $|\sigma_1|^{-1}$ and that $v_T = T$, $S_T = \hat{\sigma}_1$, $\bar{B}_T^1 = \hat{B}^1$, and $N_T = G'G$. Thus, the posterior simulator for B^1 and σ_1 can be described as follows:

1. Draw σ_1 from an $IW_k(T\hat{\sigma}_1, T)$ distribution.

2. Draw B^1 from the conditional distribution $MN(\hat{B}^1, \sigma_1 \times (G'G)^{-1})$.

Once I have these draws at hand, I compute $\hat{\epsilon}_t$ and feed it into the estimation of Equation (11, as described next.

Estimation of Equation (11).   The Bayesian estimation of Equation (11), from a technical standpoint, is equivalent to that of Equation (10) just described only that the outcome variable is now $\hat{\epsilon}_t$, obtained from a posterior draw via Steps 1 and 2, and the explanatory variable is $\hat{\epsilon}_t^2$. Since the technical details of the two estimation procedures are effectively the same, I directly skip to showing the posterior simulator for B^2 and σ_2, the coefficient matrix and residual variance of Equation (11) (see notation from Page 24):

3. Draw σ_2 from an $IW_k(T\hat{\sigma}_2, T)$ distribution.

4. Draw B^2 from the conditional distribution $MN(\hat{B}^2, \sigma_2 \times (X'X)^{-1})$.

Once I have these draws at hand, I compute $\hat{\zeta}_t$ (the estimated residual from Equation (11)) and transform it into quarterly frequency by taking averages of monthly observations within each quarter while standardizing the resulting quarterly shock series to have unit standard deviation at quarterly frequency. I.e., the shock series I feed into the estimation of Equation (12), as described below, is defined as $\hat{\zeta}_{t,q} \equiv \frac{\hat{\zeta}_t}{\sqrt{3}\sigma_2}$, where the multiplication of the drawn σ_2 by $\sqrt{3}$ is done to produce a unit standard deviation shock series at the quarterly frequency.

Estimation of Equation (12). Drawing on the notation from Page 24, let the set of the parameters (coefficients matrix and residual standard deviation) to be estimated from Equation (12) be given by Q_h and $\sigma_{3,h}$. Equation (12) can then be written in companion form as follows:

$$Y_{i,h} = X_{i,h}Q_{i,h} + U_{i,h} \tag{19}$$

where i indexes countries, with $i = 1, ..., 42$; h is the regression's rolling horizon with $h = 1, ..., 20$; $Y_{i,h} = [y_{i,h} - y_{i,0}, y_{i,h+1} - y_{i,1}, ..., y_{i,T} - y_{i,T-h-1}]'$, with T being the time dimension of the sample; $X_{i,h} = [X_{i,1}, ..., X_{i,T-h}]'$, with $X_{i,t} = [\hat{\xi}_{i,t,q}, \hat{\xi}^2_{i,t,q}, 1]';$[30] $Q_h = [\Xi_h, \Phi_h, \alpha_{i,h}]'$; and $U_{i,h} = [u_{i,p-1+h}, ..., u_T]'$. Q_h here represents the coefficient matrix of Equation (12) and $\sigma^2_{3,h}$ is the variance of $u_{i,t+h}$.

I assume the following normal-inverse Wishart prior distribution for these parameters:

$$vec(Q_h) \mid \sigma^2_{3,h} \quad \sim \quad N(vec(\bar{Q}_{0,h}), \sigma^2_{3,h} \times N_0^{-1}), \tag{20}$$

$$\sigma^2_{3,h} \quad \sim \quad IW_k(v_0 S_{0,h}, v_0), \tag{21}$$

where N_0 is a $3(1+42)$ x $3(1+42)$ positive definite matrix; S_0 is a variance scalar; and $v_o > 0$. As shown by Uhlig (1994), the latter prior implies the following posterior distribution:

$$vec(Q_h) \mid \sigma^2_{3,h} \quad \sim \quad N(vec(\bar{Q}_h), \sigma_{3,h} \times N_h^{-1}), \tag{22}$$

$$\sigma^2_{3,h} \quad \sim \quad IW_k(v_h S_h, v_h), \tag{23}$$

where $v_h = 42 \times (T-h) + v_0$; $N_h = N_0 + \sum_i X'_{i,h}X_{i,h}$; $\bar{Q}_h = N_h^{-1}(N_0\bar{Q}_{0,h} + \sum_i X'_{i,h}X_{i,h}\hat{Q}_h)$; $S_h = \frac{v_0}{v}S_{0,h} + \frac{42\times(T-h+1)}{v_h}\hat{\sigma}^2_{3,h} + \frac{1}{v_h}(\hat{Q}_h - \bar{Q}_{0,h})'N_0N_h^{-1}\sum_i X'_{i,h}X_{i,h}(\hat{Q}_h - \bar{Q}_{0,h})$, where $\hat{Q}_h = (\sum_i X'_{i,h}X_{i,h})^{-1}(\sum_i X_{i,h})'Y$ and $\hat{\sigma}^2_{3,h} = \sum_i(Y_{i,h} - X_{i,h}\hat{Q}_h)'(Y_{i,h} - X_{i,h}\hat{Q}_h)/(42\times(T-h))$.

I use a weak prior, i.e., $v_0 = 0$, $N_0 = 0$, and arbitrary $S_{0,h}$ and $\bar{Q}_{0,h}$. This implies that the prior distribution is proportional to $\sigma^2_{3,h}$ and that $v_h = 42 \times (T-h)$, $S_h = \hat{\sigma}^2_{3,h}$, $\bar{Q}_h = \hat{Q}_h$, and

---

[30]Note that $\hat{\xi}_{i,t,q}$, in denoting the global risk appetite shock series, is identical across the different i's. Nevertheless, keeping with the cross-sectional based notation is still of value here so as to remain consistent with the cross-sectional nature of the outcome variable and the fixed effects.

$N_h = \sum_i X'_{i,h} X_{i,h}$. Due to the spatial and temporal correlations of the error term $u_{i,t+h}$, the likelihood function is misspecified which in turn requires that the residual variance estimate $\hat{\sigma}^2_{3,h}$ be appropriately modified so as to improve estimation precision (Müller (2013)). Toward this end, I apply a correction to $\hat{\sigma}^2_{3,h}$ based on Driscoll and Kraay (1998) which accounts for arbitrary spatial and temporal correlations of the error term and denote the corrected variance estimate by $\hat{\sigma}^2_{hac,3,h}$.

We are now in position to lay out the posterior simulator for Q_h and $\sigma^2_{3,h}$, which accounts for uncertainty in the estimation of the global risk appetite shock series $\hat{\xi}^q_t$ and can be described as follows:

1. Do Steps 1 and 2 from the posterior simulator of Equation (10) and obtain $\hat{\epsilon}_t$.

2. Using $\hat{\epsilon}_t$, do Steps 3 and 4 from the posterior simulator of Equation (11) and obtain $\hat{\xi}_t$ (whose raw and squared values are to be used as explanatory variables for the next two steps).

3. Draw $\sigma_{3,h}$ from an $IW_k(42 \times (T-h+1)\hat{\sigma}^2_{hac,3,h}, 42 \times (T-h+1))$ distribution.

4. Draw Q_h from the conditional distribution $MN(\hat{Q}_h, \sigma^2_{3,h} \times \sum_i (X'_{i,h} X_{i,h})^{-1})$.

5. Repeat Steps 1-4 a large number of times and collect the drawn Q_h's and $\sigma^2_{3,h}$'s.

Table 1: **Unconditional Evidence on Business Cycle Asymmetry: Moments of Two-Year Cumulative Output Growth Rates**.

	Mean	Standard Deviation	Skewness	Kurtosis
Full Sample	0.06%	5.82%	-0.85	7.51
Recessions	-1.80%	5.92%	-1.33	9.36
Expansions	0.96%	5.55%	-0.58	6.38
Pre-2008 Sample	-0.01%	4.80%	0.17	7.71
Pre-2008 Recessions	-0.82%	4.84%	0.11	6.92
Pre-2008 Expansions	0.43%	4.72%	0.30	8.50

Notes: This table presents the mean, standard deviation, skewness, and kurtosis of the trend-adjusted two-year cumulative growth rates of output for my 42 EMEs panel sample. The trend is estimated for each country from cubic-trend time polynomial regressions with their residuals used to compute output growth rates. The first row computes the moments for the full sample, while the second and third rows report moments for recessions and expansions. The former are defined as periods with two consecutive negative quarter-over-quarter growth rates and the latter are defined as the former's perfect complements. The last three rows correspond to the first three only that only pre-2008 observations underlie the numbers presented in these rows.

Table 2: **Model Parameterization**.

Parameter	Description	Value
$\bar{R}$	Steady State Gross Risk-Free Rate	1.01
α	Capital Share	0.35
ω	Convexity Parameter of Investment Adjustment Cost Function	2.5
δ	Depreciation Rate	0.025
υ	Entrepreneurs' Survival Rate	0.9728
μ	Monitoring Cost	0.12
$\bar{\sigma}$	Steady State S.D. of Idiosyncratic Productivity	0.28
ρ	Risk Shock Persistence	0.8
σ_{η}	Standard Deviation of Risk Shock	0.05

Notes: This table consists of the parameters' values used for the model of Section 3.2.

Figure 1: **Expected Monitoring Cost and Risk**.
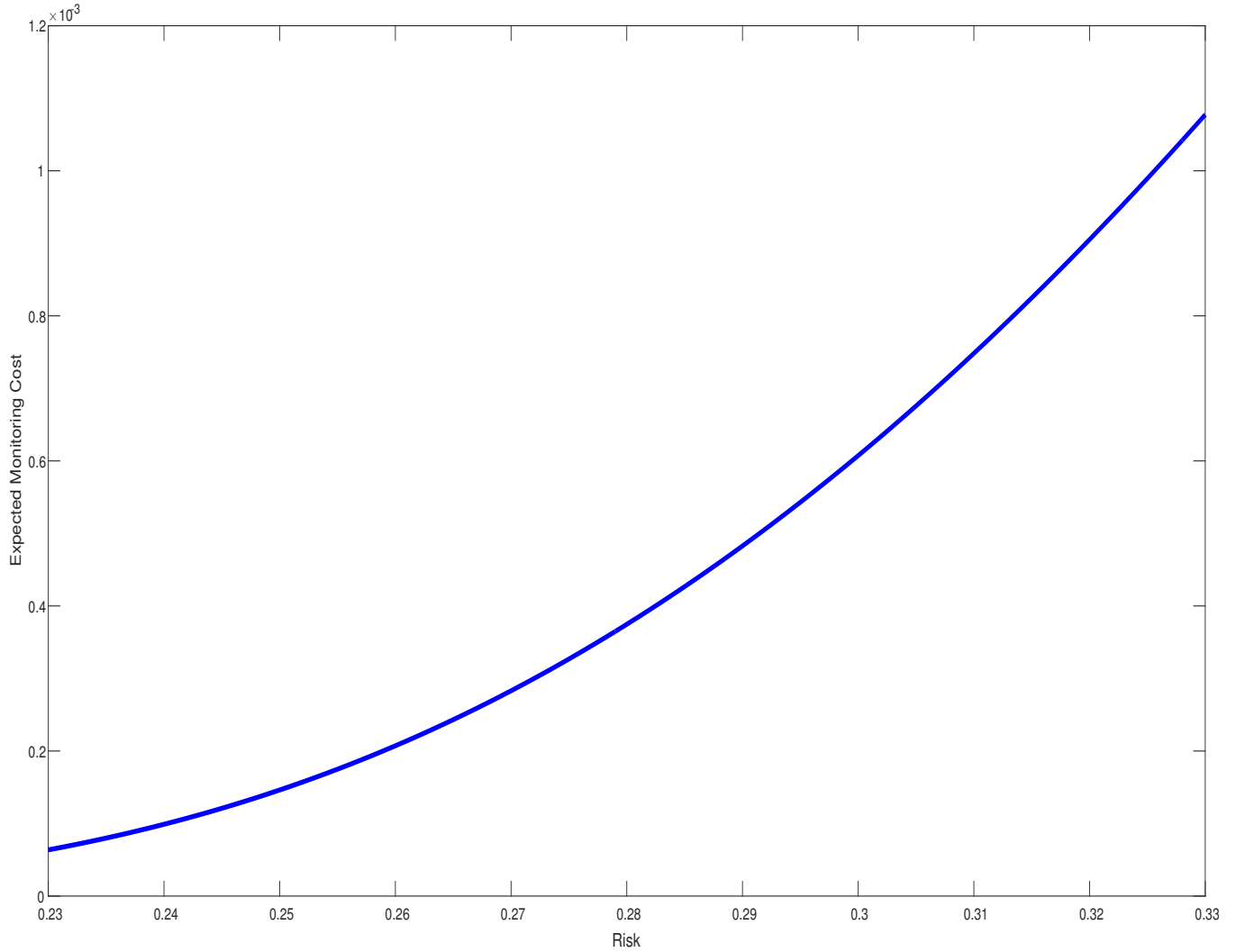
Notes: This figure presents the relation between expected monitoring cost and risk (as defined in relation to the CSV problem from Section 3.1), which is obtained as follows: For the baseline values from BGG of $\bar{\omega} = 0.48$ and $\mu = 0.12$, I compute the expected monitoring cost for a grid of σ that ranges between 0.23 and 0.33 and has a spacing of 0.001. The solid line is the curve depicting this computation. Risk (σ) appears on the x-axis and Expected monitoring cost ($\mu G(\bar{\omega})$) is on the y-axis.

Figure 2: **EFP-Leverage Curve and Risk**.
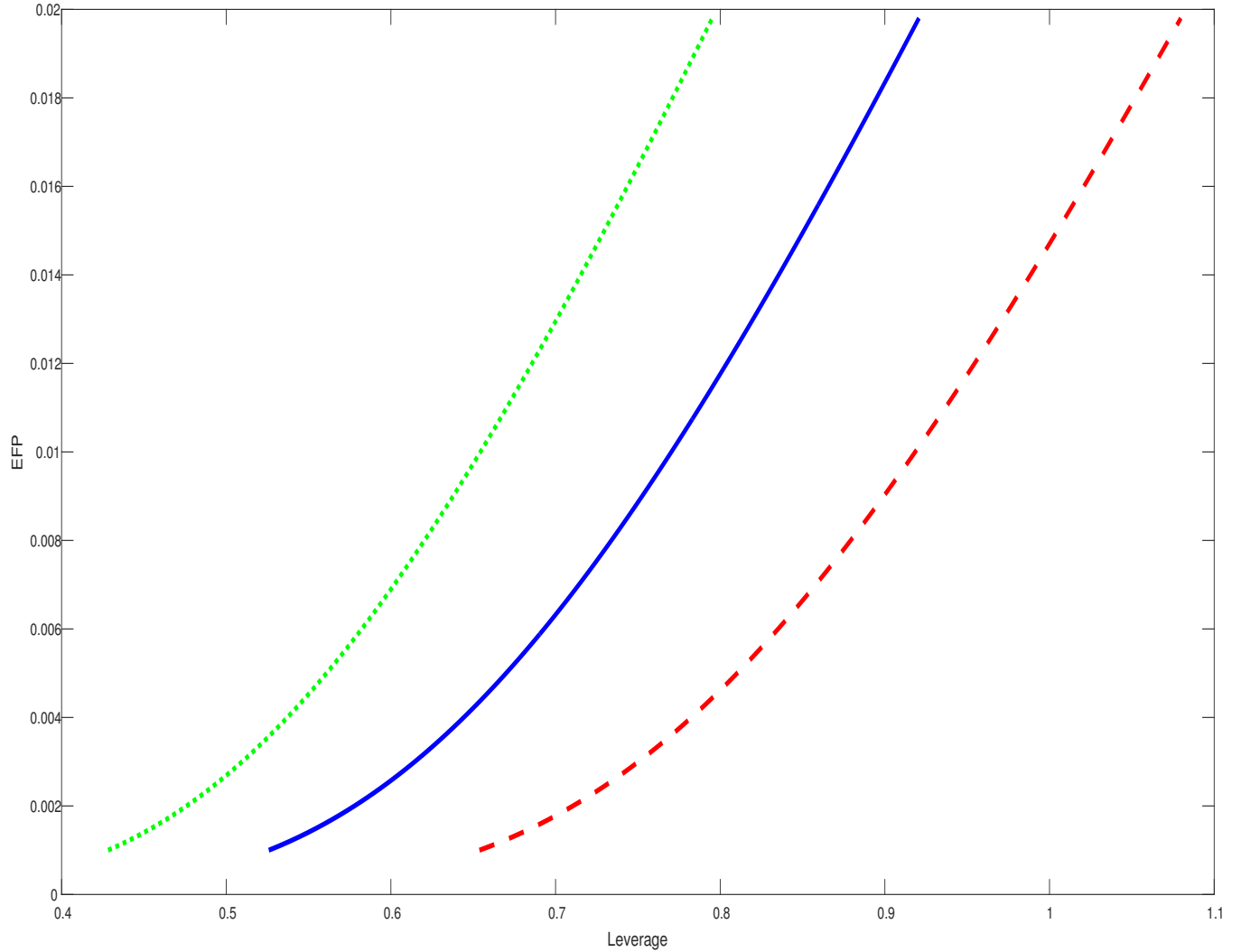
Notes: This figure presents the EFP-leverage curve for the CSV problem from Section 3.1, which is obtained as follows: For three values of borrower's riskiness $\sigma = [0.23, 0.28, 0.33]$ (the middle value of $\sigma = 0.28$ is in line with BGG), I solve Problem (2) for a grid of s (i.e., EFP) that ranges between 1.001 and 1.02 and has a spacing of 0.001, while keeping constant the monitoring cost parameter at $\mu = 0.12$ (as in BGG). The solid line is the EFP-leverage curve for $\sigma = 0.28$, the dashed line corresponds to $\sigma = 0.23$, and the dotted line corresponds to $\sigma = 0.33$. Logged leverage appears on the x-axis and logged EFP is on the y-axis.

Figure 3: **Sign-Dependent Impulse Responses to Risk Shocks**.
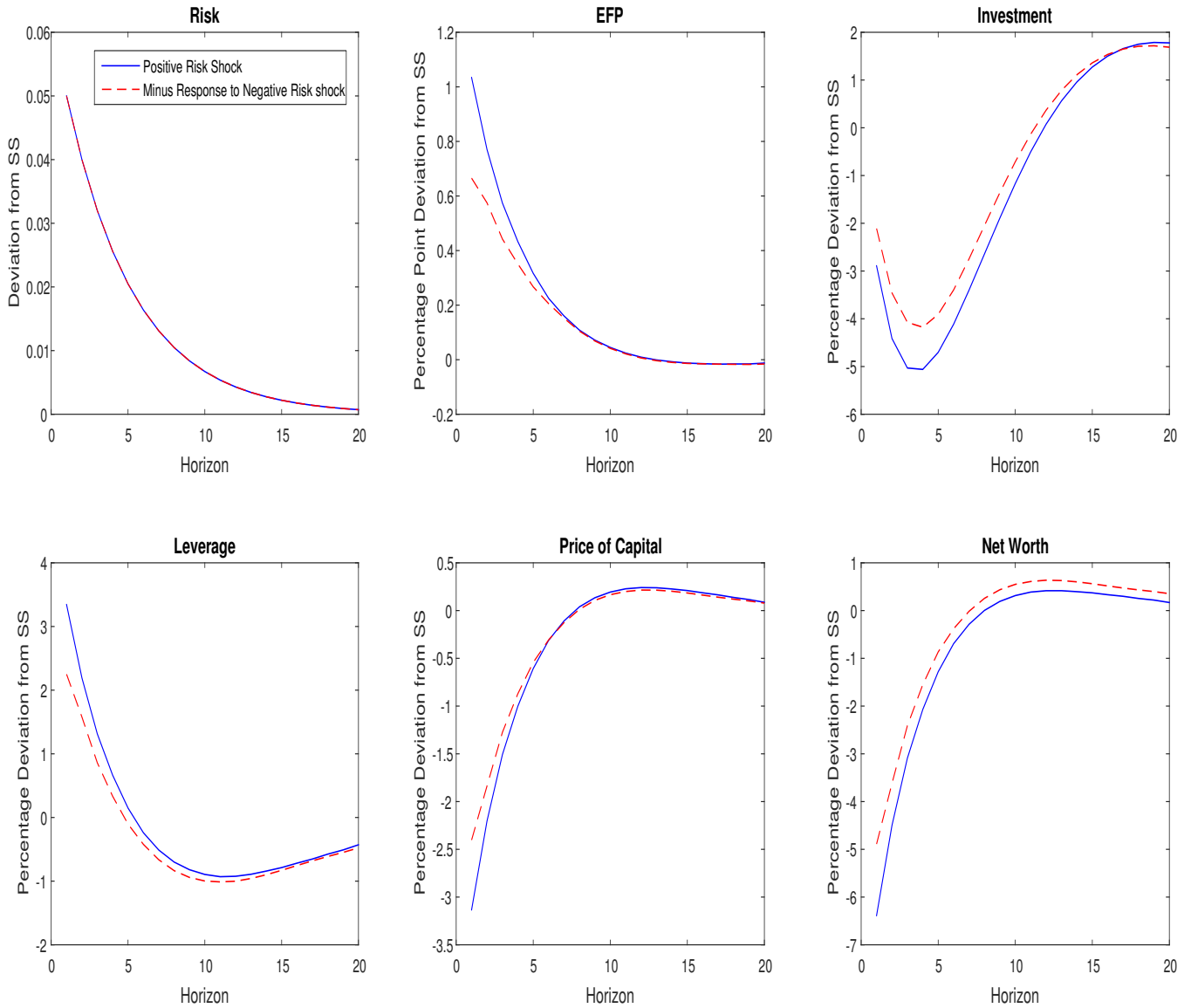
Notes: This figure presents the impulse responses to a positive and negative risk shock from the model presented in Section 3.2. The responses are shown in terms of percentage deviations from steady state values (except for risk and EFP, whose responses are shown in terms of raw deviation and percentage point deviation, respectively). Solid lines depict responses to a positive risk shock, whereas dashed lines present responses to a negative shock (multiplied by -1 for comparison purposes). Horizon is in quarters.

Figure 4: **Sign-Dependent Effects of Global Risk Appetite Shocks on FBP**.
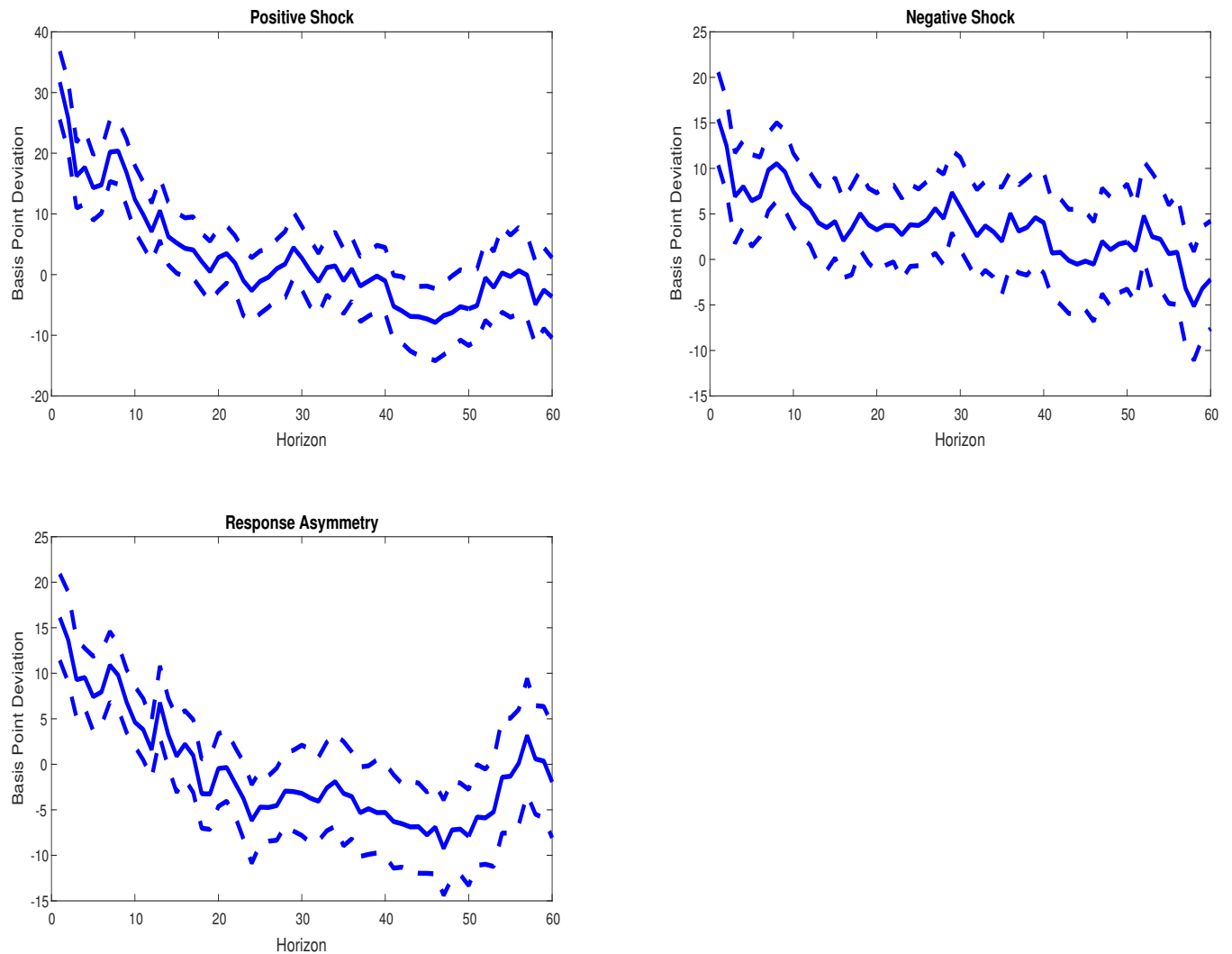
Notes: This figure presents the sign-dependent impulse responses of FBP to positive and negative one standard deviation risk appetite shocks as well as the difference between the responses to the shocks. Solid lines depict median estimates and dashed lines correspond to the 68% posterior confidence bands. Responses are in terms of basis point deviations from pre-shock values. Horizon is in months.

Figure 5: **U.S. Economy's Sign-Dependent Response to Global Risk Appetite Shocks: (a) Unemployment Rate; (b) Industrial Production.**
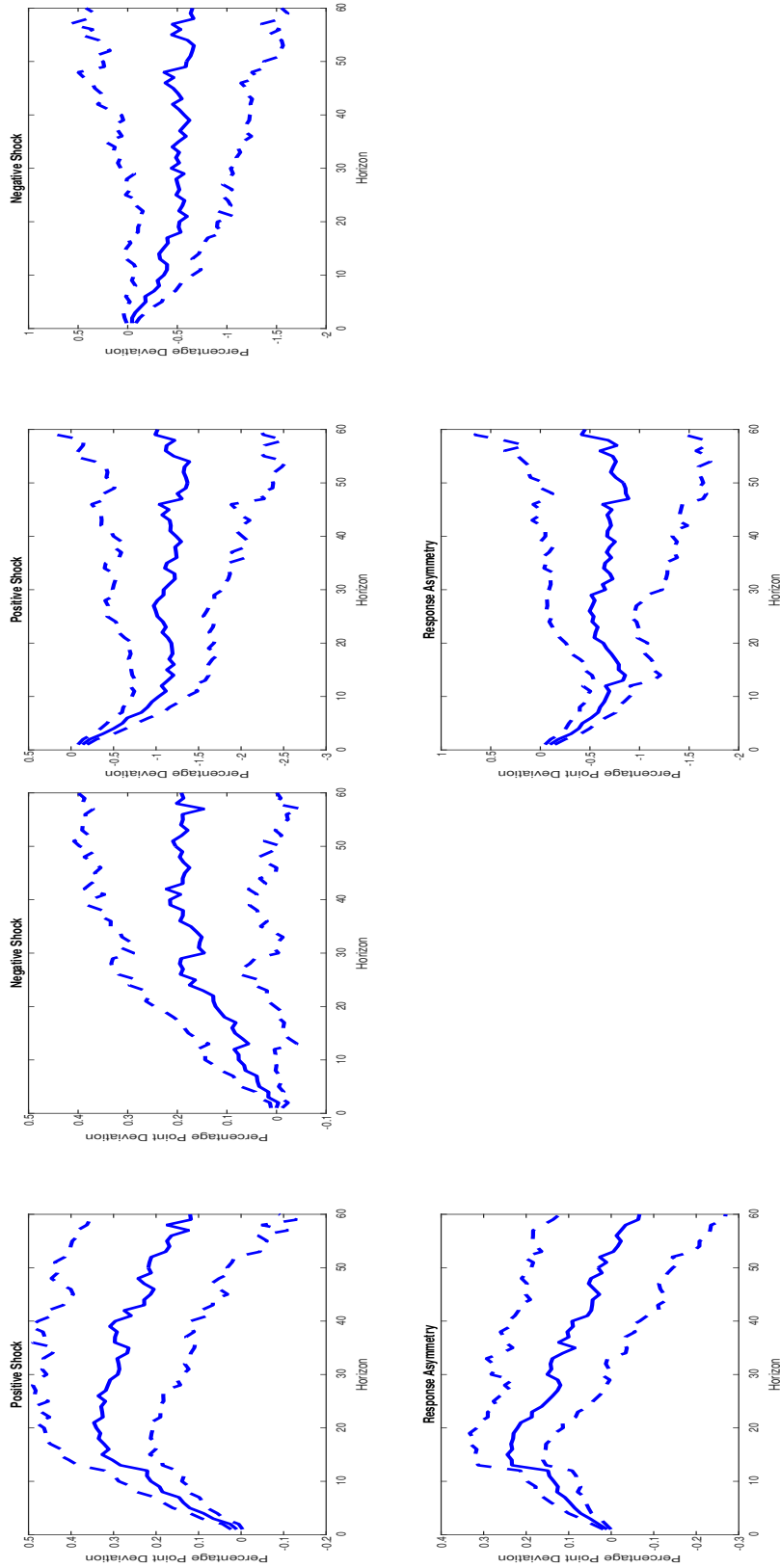
(a) Sign-Dependent Impulse Responses to a One Standard Deviation Global Risk Appetite Shock (Unemployment Rate).

(b) Sign-Dependent Impulse Responses to a One Standard Deviation Global Risk Appetite Shock (Industrial Production).

Notes: Panel (a): This figure presents the sign-dependent impulse responses of U.S. unemployment rate to positive and negative one standard deviation global risk appetite shocks as well as the difference between these two shocks' effects. Solid lines depict median estimates and dashed lines correspond to the 68% posterior confidence bands. Responses are in terms of percen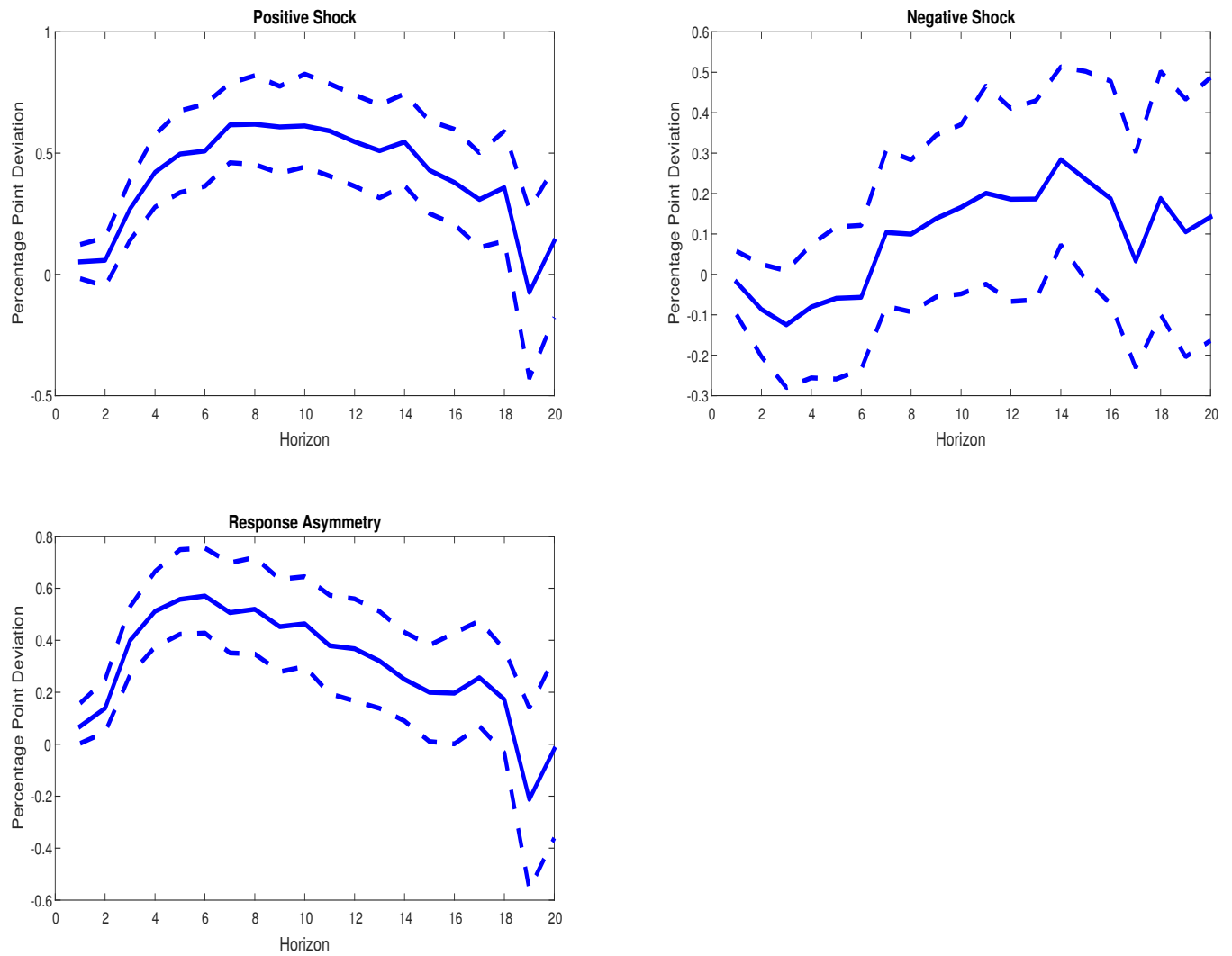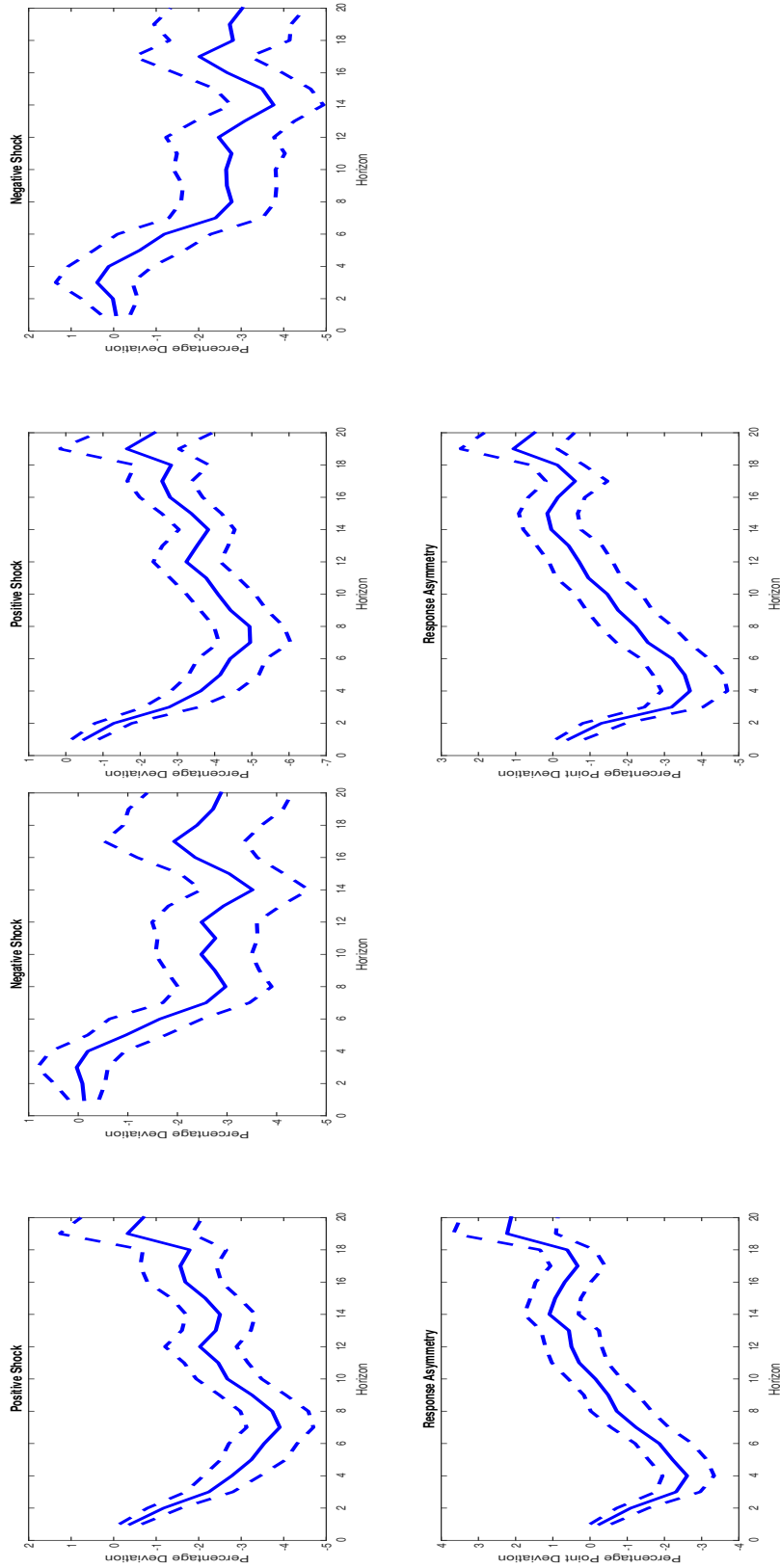tage point deviations from pre-shock values. Horizon is in months. Panel (b): This figure presents the sign-dependent impulse responses of U.S. industrial production to positive and negative one standard deviation global risk appetite shocks as well as the difference between these two shocks' effects. Solid lines depict median estimates and dashed lines correspond to the 68% posterior confidence bands. Responses are in terms of percentage deviations from pre-shock values. Horizon is in months.

Figure 6: **Sign-Dependent Effects of Global Risk Appetite Shocks on EMEs Exports to U.S.**
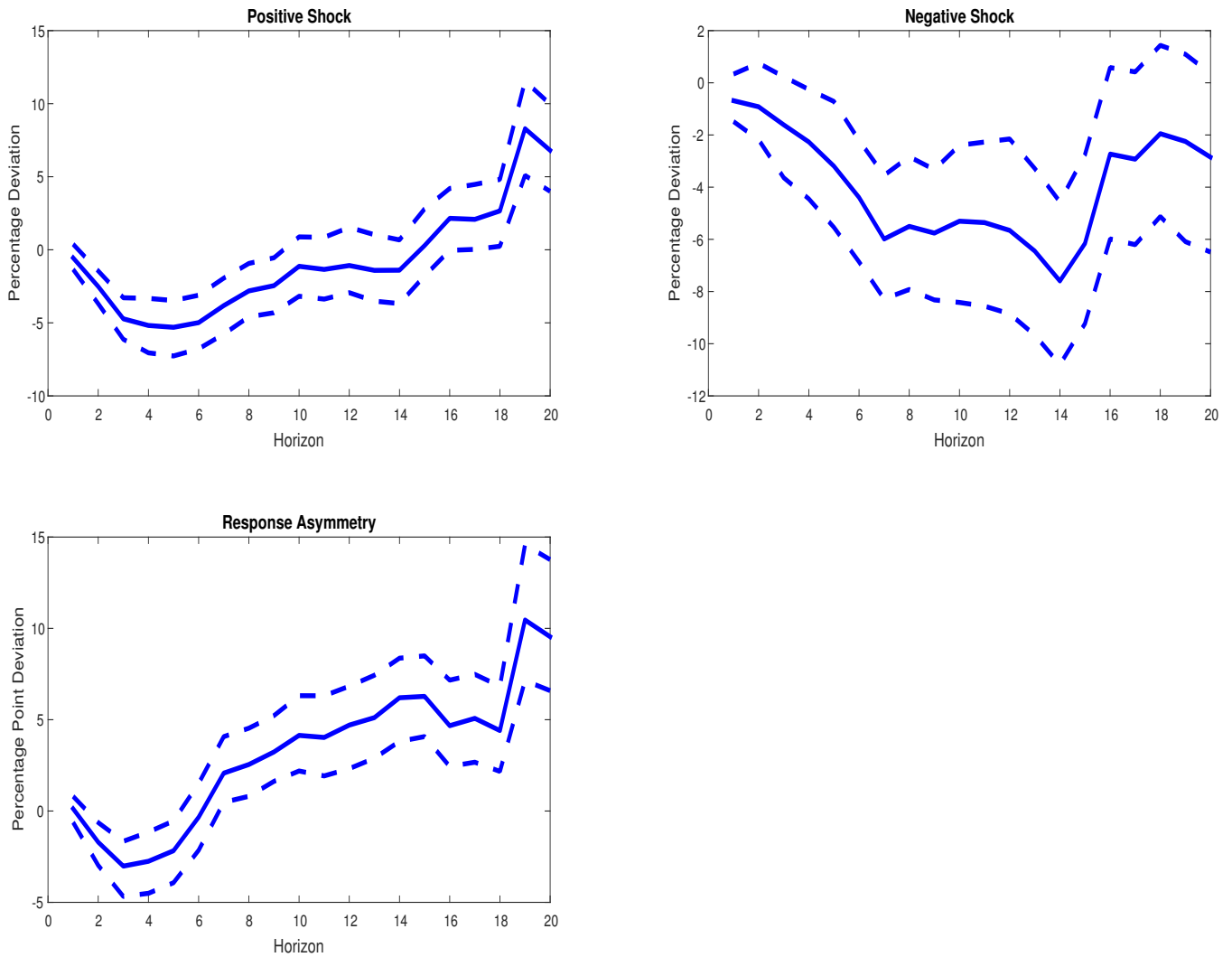
Notes: This figure presents the sign-dependent impulse responses of real exports to U.S. (nominal exports are deflated by GDP deflator) to positive and negative one standard deviation global risk appetite shocks as well as the difference between the responses to the shocks. Solid lines depict median estimates and dashed lines correspond to the 68% posterior confidence bands. Responses are in terms of percentage deviations from pre-shock values. Horizon is in quarters.

Figure 7: **Sign-Dependent Effects of Global Risk Appetite Shocks on Output**.
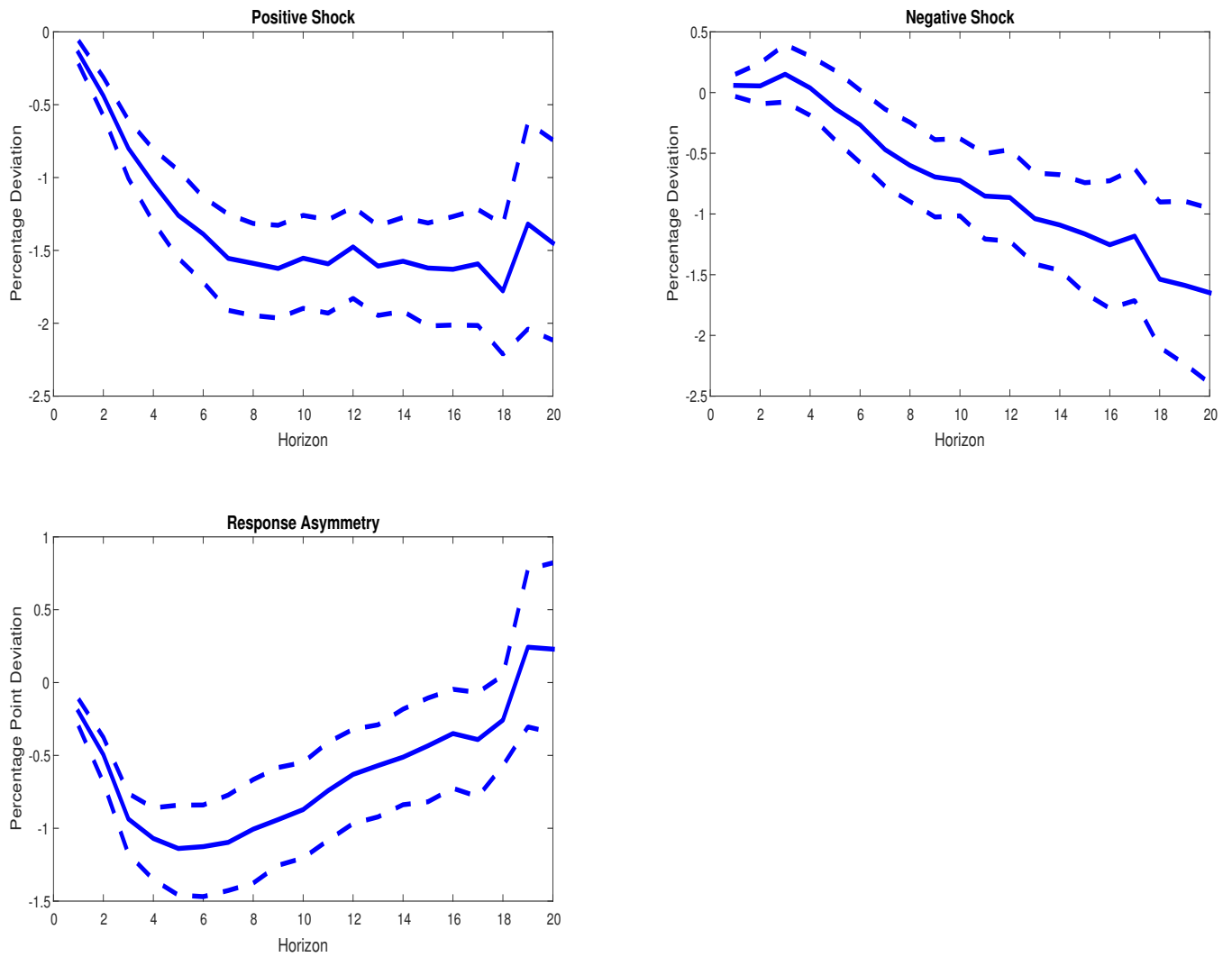
Notes: This figure presents the sign-dependent impulse responses of output to positive and negative one standard deviation global risk appetite shocks as well as the difference between the responses to the shocks. Solid lines depict median estimates and dashed lines correspond to the 68% posterior confidence bands. Responses are in terms of percentage deviations from pre-shock values. Horizon is in quarters.

Figure 8: **Sign-Dependent Response of Investment and Consumption to Global Risk Appetite Shocks: (a) Investment; (b) Consumption.**
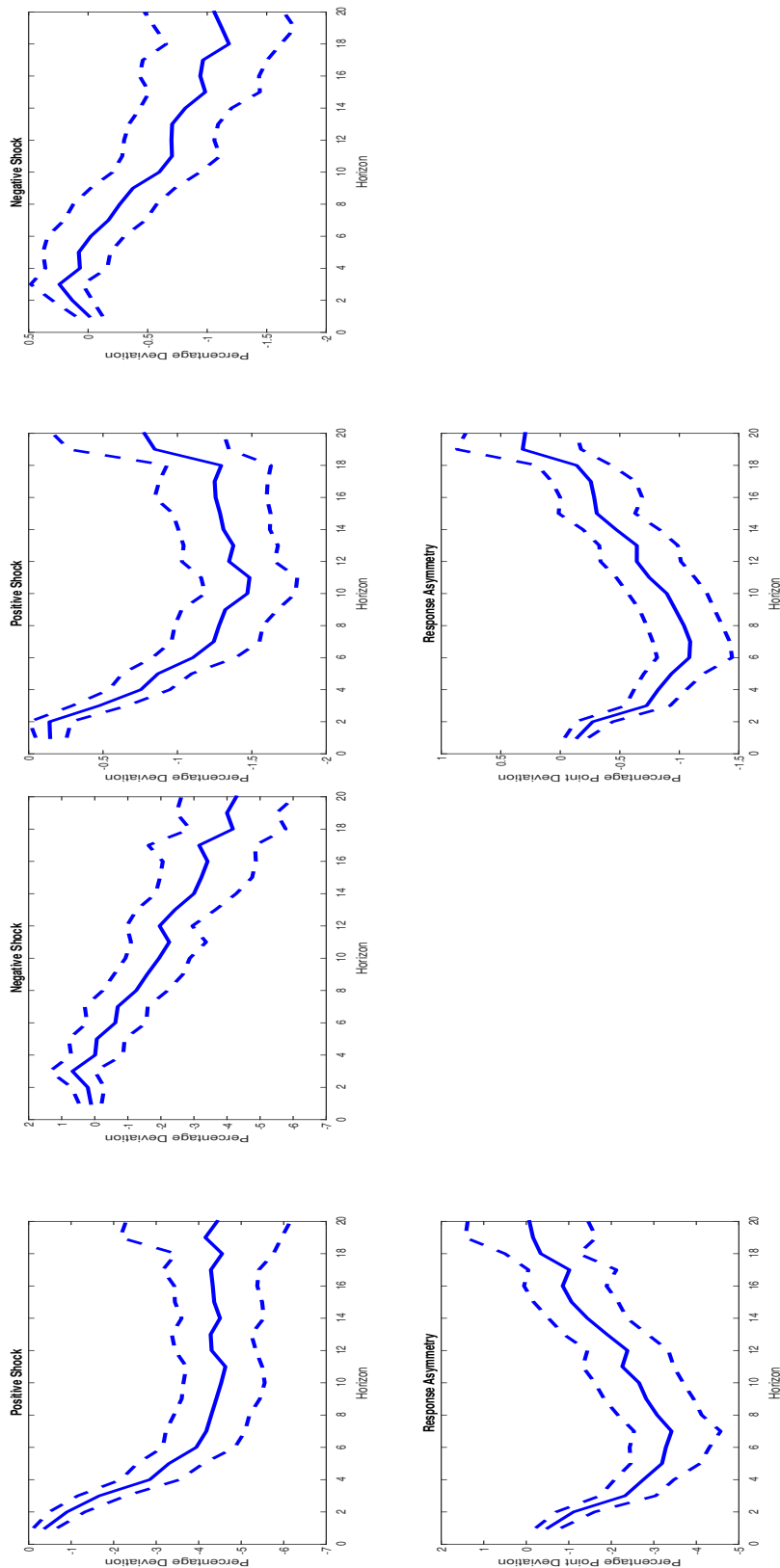
(a) Sign-Dependent Impulse Responses to a One Standard Devia-
tion Global Risk Appetite Shock (Investment).

(b) Sign-Dependent Impulse Responses to a One Standard Devia-
tion Global Risk Appetite Shock (Consumption).

Notes: Panel (a): This figure presents the sign-dependent impulse responses of investment to positive and negative one standard deviation global risk appetite shocks as well as the difference between these two shocks' effects. Solid lines depict median estimates and dashed lines correspond to the 68% posterior confidence bands. Responses are in terms of percentage deviations from pre-shock values. Horizon is in quarters. Panel (b): This figure presents the sign-dependent impulse responses of consumption to positive and negative one standard deviation global risk appetite shocks as well as the difference between these two shocks' effects. Solid lines depict median estimates and dashed lines correspond to the 68% posterior confidence bands. Responses are in terms of percentage deviations from pre-shock values. Horizon is in quarters.

71

Figure 9: **Sign-Dependent Effects of Global Risk Appetite Shocks on the Trade Balance**.

Notes: This figure presents the sign-dependent impulse responses of the GDP share of the trade balance to positive and negative one standard deviation global risk appetite shocks as well as the difference between the responses to the shocks. Solid lines depict median estimates and dashed lines correspond to the 68% posterior confidence bands. Responses are in terms of percentage point deviations from pre-shock values. Horizon is in quarters.
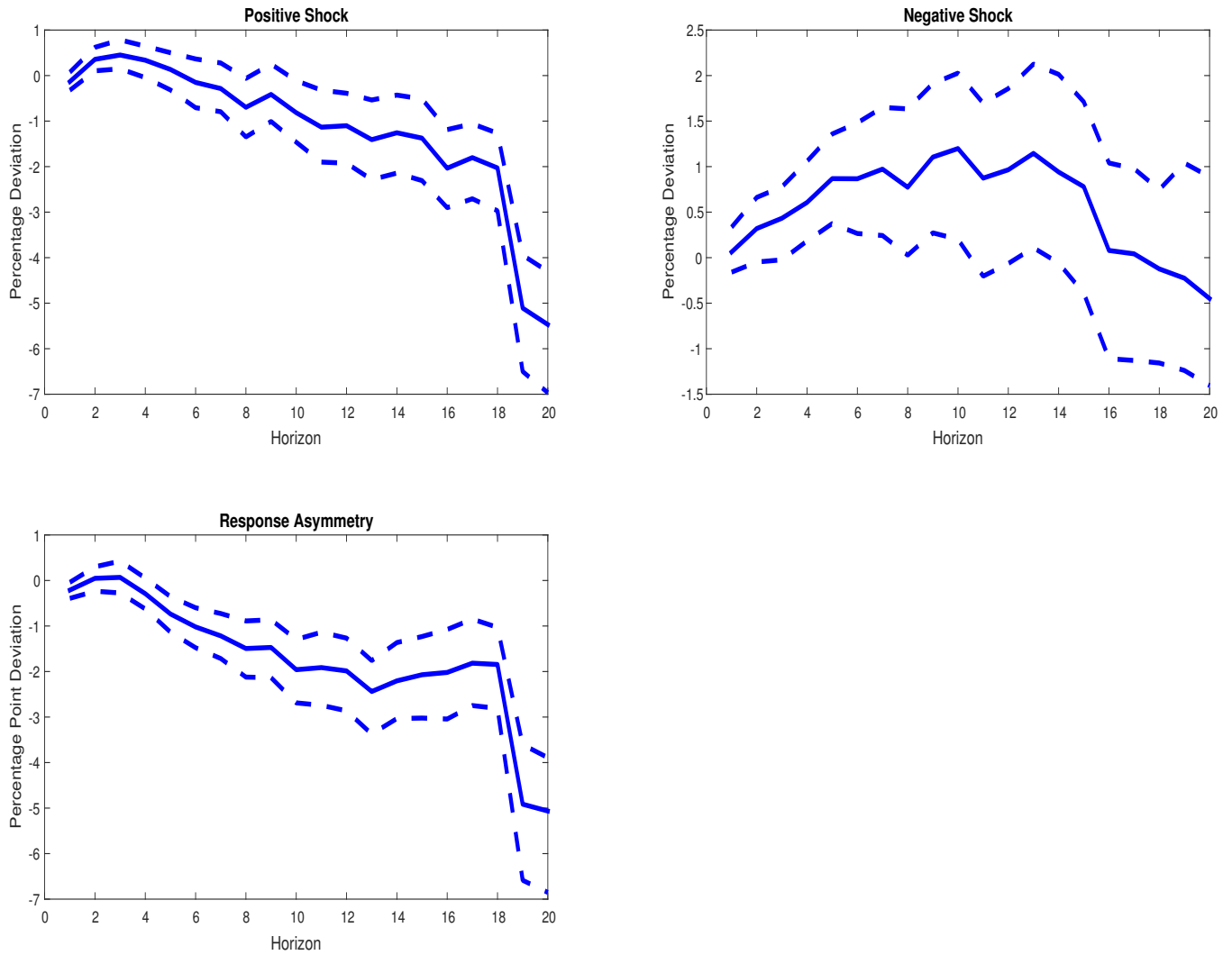
Figure 10: **Sign-Dependent Response of Exports and Imports to Global Risk Appetite Shocks: (a) Exports; (b) Imports.**

(a) Sign-Dependent Impulse Responses to a One Standard Deviation Global Risk Appetite Shock (Exports).

(b) Sign-Dependent Impulse Responses to a One Standard Deviation Global Risk Appetite Shock (Imports).

Notes: Panel (a): This figure presents the sign-dependent impulse responses of real exports to positive and negative one standard deviation global risk appetite shocks as well as the difference between these two shocks' effects. Solid lines depict median estimates and dashed lines correspond to the 68% posterior confidence bands. Responses are in terms of percentage deviations from pre-shock values. Horizon is in quarters. Panel (b): This figure presents the sign-dependent impulse responses of real imports to positive and negative one standard deviation global risk appetite shocks as well as the difference between these two shocks' effects. Solid lines depict median estimates and dashed lines correspond to the 68% posterior confidence bands. Responses are in terms of percentage deviations from pre-shock values. Horizon is in quarters.

Figure 11: **Sign-Dependent Response of Exchange Rate to Global Risk Appetite Shocks: (a) Nominal Exchange Rate; (b) Real Exchange Rate.**
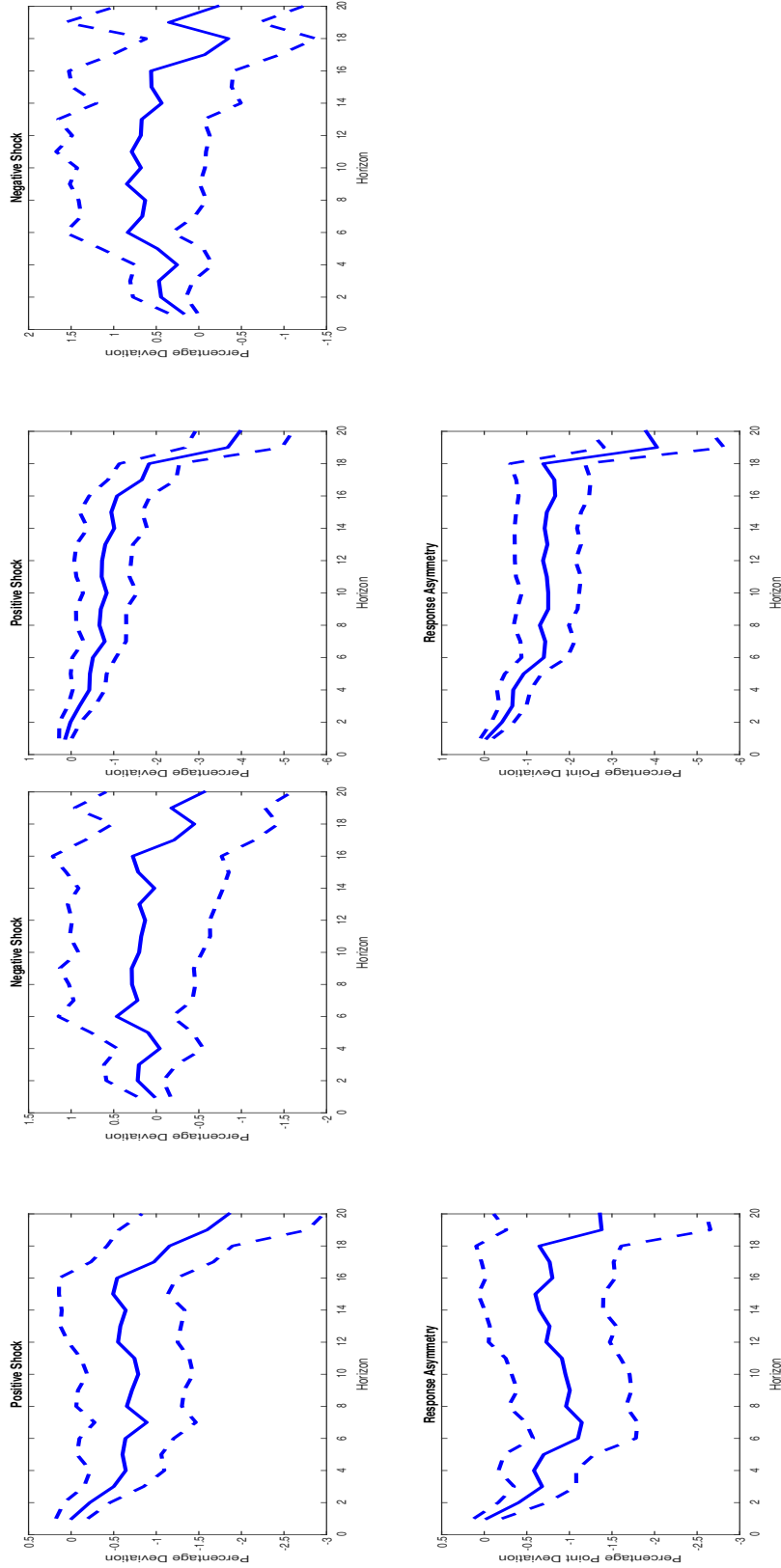
(a) Sign-Dependent Impulse Responses to a One Standard Devia- (b) Sign-Dependent Impulse Responses to a One Standard Devia-
tion Global Risk Appetite Shock (Nominal Exchange Rate). **tion Global Risk Appetite Shock (Real Exchange Rate).**

Notes: Panel (a): This figure presents the sign-dependent impulse responses of the nominal effective exchange rate to positive and negative one standard deviation global risk appetite shocks as well as the difference between these two shocks' effects. Solid lines depict median estimates and dashed lines correspond to the 68% posterior confidence bands. Responses are in terms of percentage deviations from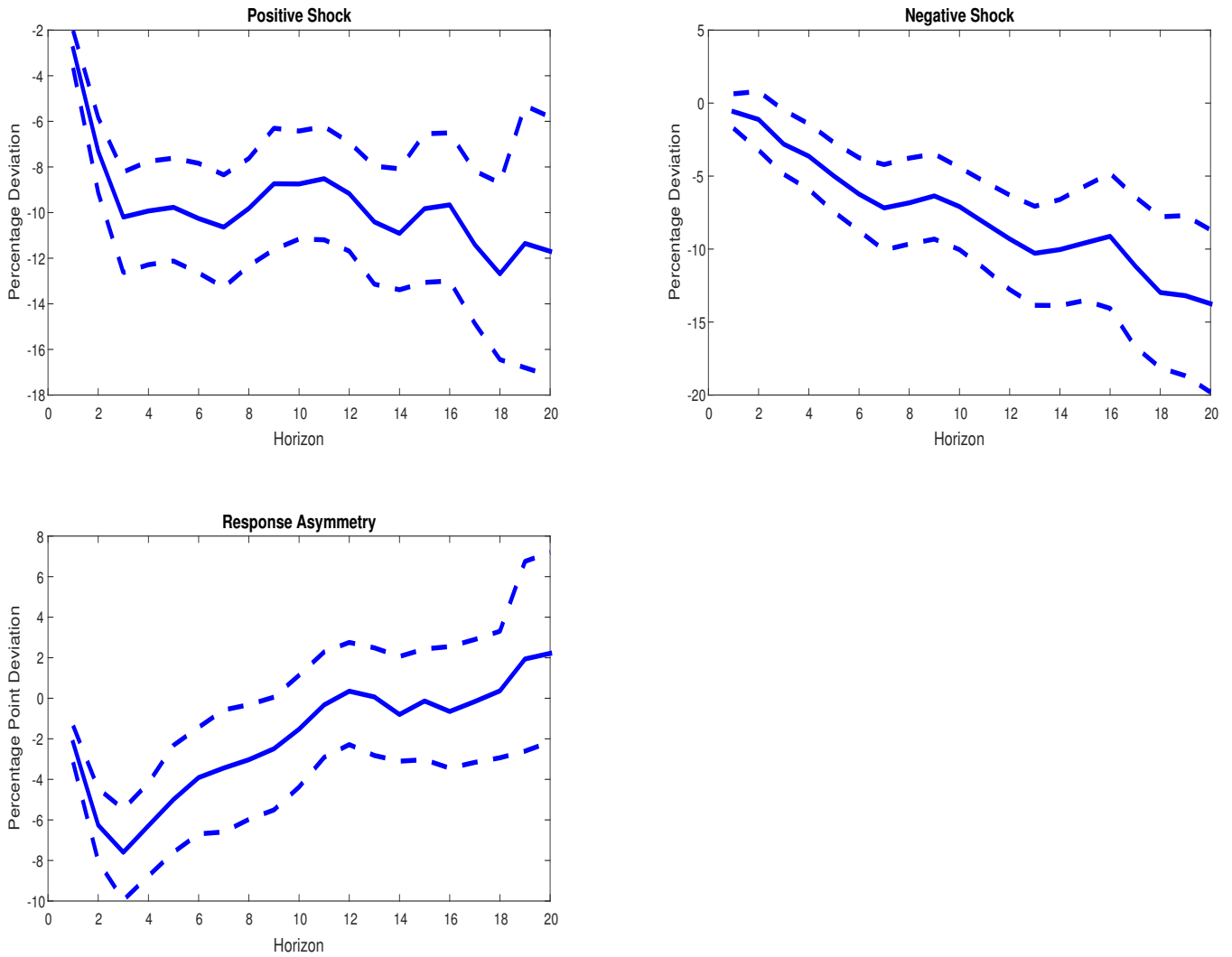 pre-shock values. Horizon is in quarters. Panel (b): This figure presents the sign-dependent impulse responses of the real effective exchange rate to positive and negative one standard deviation global risk appetite shocks as well as the difference between these two shocks' effects. Solid lines depict median estimates and dashed lines correspond to the 68% posterior confidence bands. Responses are in terms of percentage deviations from pre-shock values. Horizon is in quarters.

Figure 12: **Sign-Dependent Effects of Global Risk Appetite Shocks on Leverage**.

Notes: This figure presents the sign-dependent impulse responses of leverage to positive and negative one standard deviation global risk appetite shocks as well as the difference between the responses to the shocks. Solid lines depict median estimates and dashed lines correspond to the 68% posterior confidence bands. Responses are in terms of percentage deviations from pre-shock values. Horizon is in quarters.

Figure 13: **Sign-Dependent Response of Sectoral Leverage to Global Risk Appetite Shocks: (a) Private Non-Financial Sector's Leverage; (b) Financial Sector's Leverage; (c) Public Sector's Leverage.**
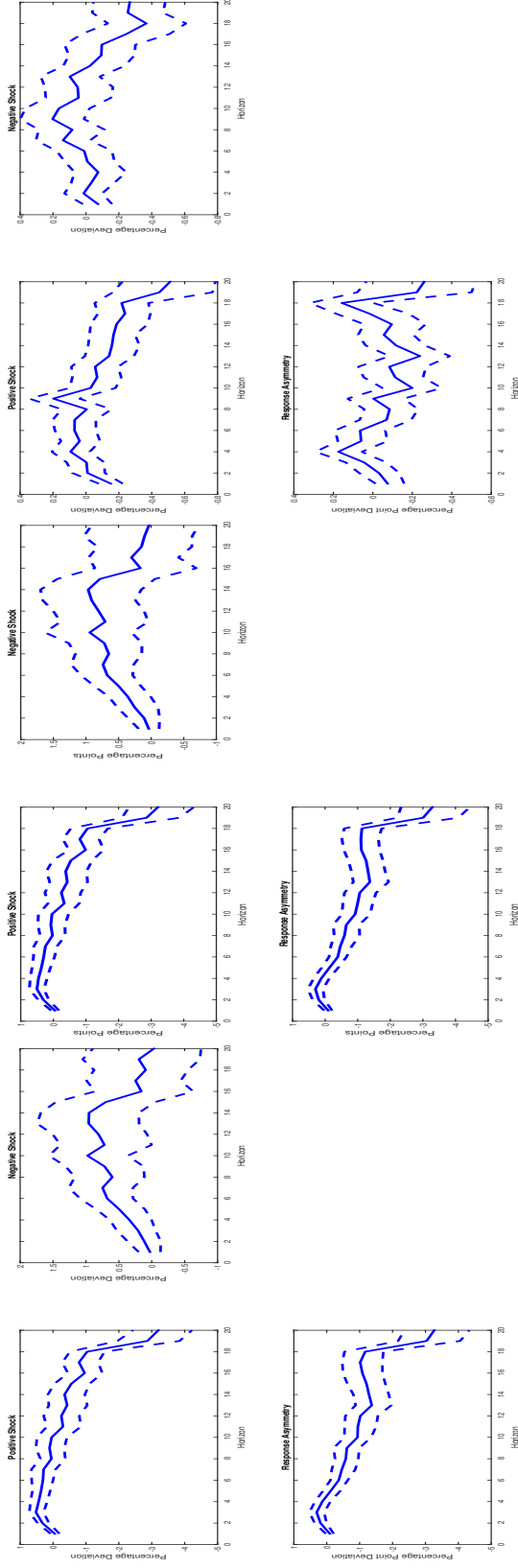
(a) **Sign-Dependent Impulse Responses to a (b)** One Standard Deviation Global Risk Appetite Shock (Private Non-Financial Sector's Leverage).

(b) **Sign-Dependent Impulse Responses to a One Standard Deviation Global Risk Appetite Shock (Financial Sector's Leverage).**

(c) **Sign-Dependent Impulse Responses to a One Standard Deviation Global Risk Appetite Shock (Public Sector's Leverage).**

Notes: Panel (a): This figure presents the sign-dependent impulse responses of private non-financial sector's leverage to positive and negative one standard deviation global risk appetite shocks. Solid lines depict median estimates and dashed lines correspond to the 68% posterior confidence bands. Responses are in terms of percentage deviations from pre-shock values. Horizon is in quarters. Panel (b): This figure presents the sign-dependent impulse responses of financial sector's leverage to positive and negative one standard deviation global risk appetite shocks. Solid lines depict median estimates and dashed lines correspond to the 68% posterior confidence bands. Responses are in terms of percenta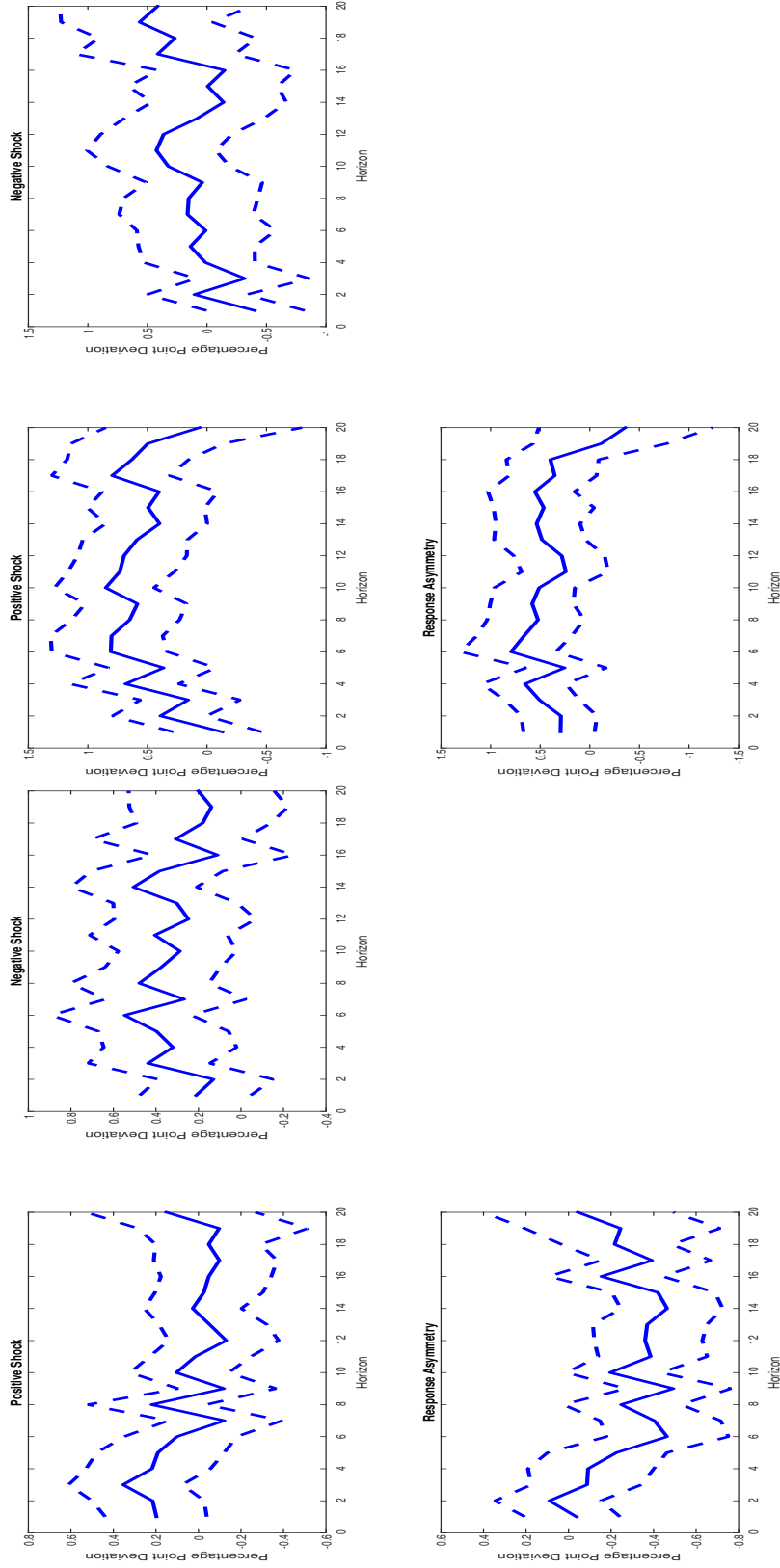ge deviations from pre-shock values. Horizon is in quarters. Panel (c): This figure presents the sign-dependent impulse responses of public sector's leverage to positive and negative one standard deviation global risk appetite shocks. Solid lines depict median estimates and dashed lines correspond to the 68% posterior confidence bands. Responses are in terms of percentage deviations from pre-shock values. Horizon is in quarters.

Figure 14: **Sign-Dependent Effects of Global Risk Appetite Shocks on Stock Prices**.

Notes: This figure presents the sign-dependent impulse responses of stock prices to positive and negative one standard deviation global risk appetite shocks as well as the difference between the responses to the shocks. Solid lines depict median estimates and dashed lines correspond to the 68% posterior confidence bands. Responses are in terms of percentage deviations from pre-shock values. Horizon is in quarters.

Figure 15: **Sign-Dependent Responses of Total Capital Flows and Foreign Direct Investment Flows to Global Risk Appetite Shocks: (a) Total Capital Flows; (b) Foreign Direct Investment.**
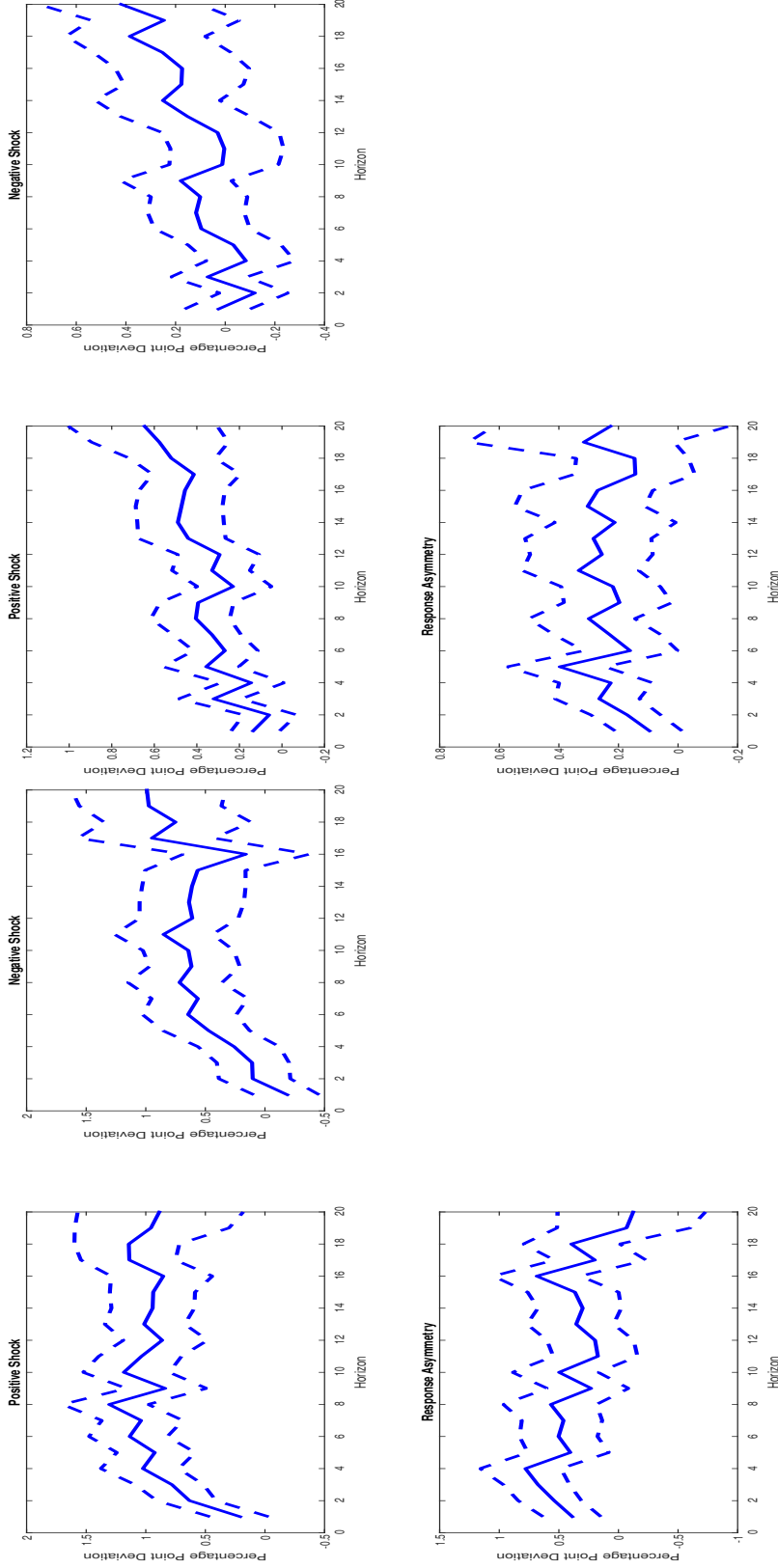
(a) Sign-Dependent Impulse Responses to a One Standard Devia- **(b) Sign-Dependent Impulse Responses to a One Standard Devi-**
tion Global Risk Appetite Shock (Total Capital Flows). **ation Global Risk Appetite Shock (Foreign Direct Investment Flows).**

Notes: Panel (a): This figure presents the sign-dependent impulse responses of the GDP share of total net capital outflows to positive and negative one standard deviation global risk appetite shocks. Solid lines depict median estimates and dashed lines correspond to the 68% posterior confidence bands. Responses are in terms of percentage point deviations from pre-shock values. Horizon is in quarters. Panel (b): This figure presents the sign-dependent impulse responses of the GDP share of net foreign direct investment outflows to positive and negative one standard deviation global risk appetite shocks. Solid lines depict median estimates and dashed lines correspond to the 68% posterior confidence bands. Responses are in terms of percentage point deviations from pre-shock values. Horizon is in quarters.

Figure 16: **Sign-Dependent Responses of Portfolio Flows and Other Investment Flows to Global Risk Appetite Shocks: (a) Portfolio Flows; (b) Other Investment Flows.**

(a) Sign-Dependent Impulse Responses to a One Standard Devia- (b) Sign-Dependent Impulse Responses to a One Standard Devia-
tion Global Risk Appetite Shock (Portfolio Flows). tion Global Risk Appetite Shock (Other Investment Flows).

Notes: Panel (a): This figure presents the sign-dependent impulse responses of the GDP share of net portfolio outflows to positive and negative one standard deviation global risk appetite shocks. Solid lines depict median estimates and dashed lines correspond to the 68% posterior confidence bands. Responses are in terms of percentage point deviations from pre-shock values. Horizon is in quarters. Panel (b): This figure presents the sign-dependent impulse responses of the GDP share of net other investment outflows (these include loans as well as other forms of cross-border finance such as trade credit, bank deposits, and cash) to positive and negative one standard deviation risk appetite shocks. Solid lines depict median estimates and dashed lines correspond to the 68% posterior confidence bands. Responses are in terms of percentage point deviations from pre-shock values. Horizon is in quarters.
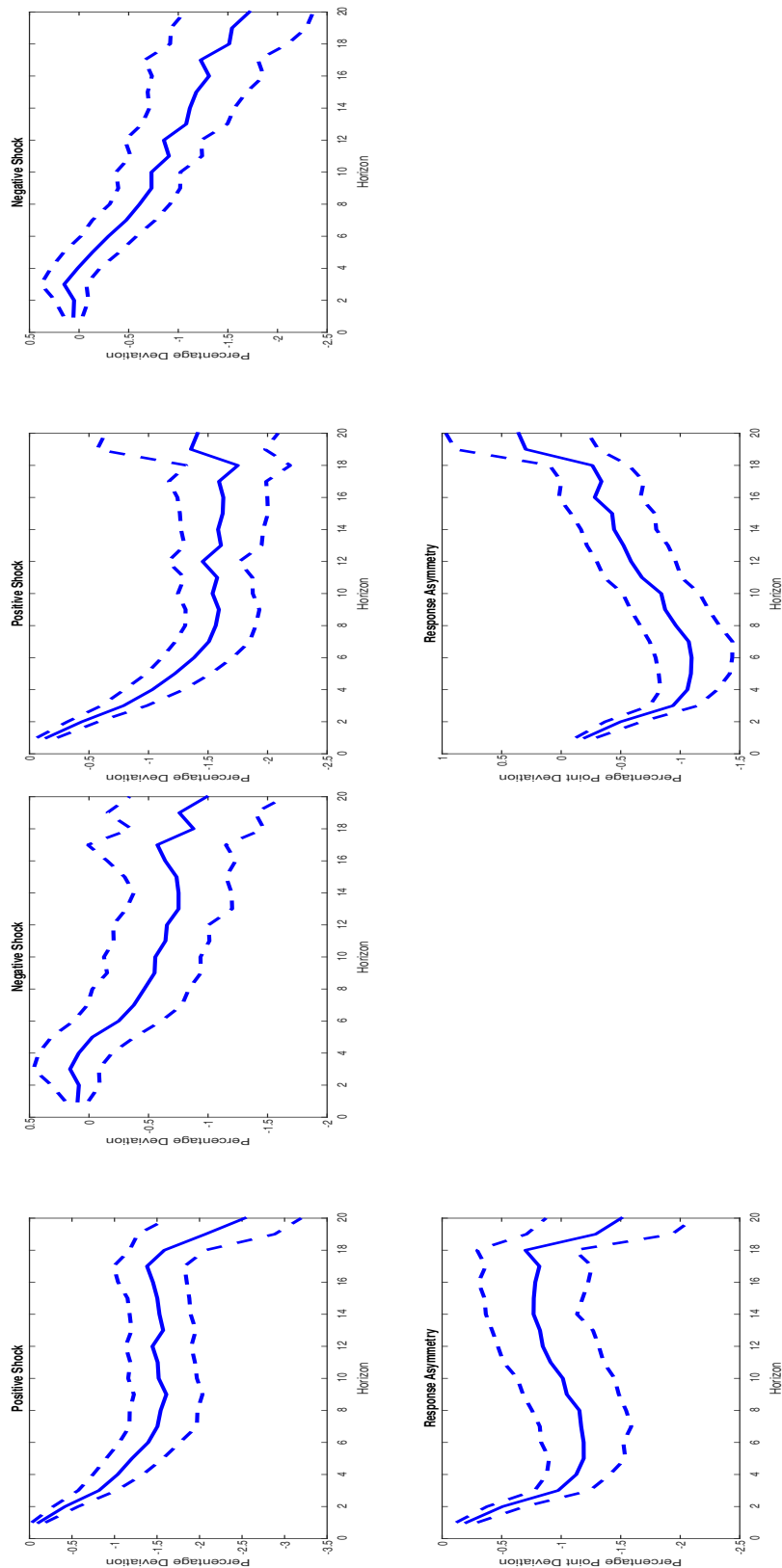
Figure 17: **Sign-Dependent Effects of Global Risk Appetite Shocks on EMBI**.
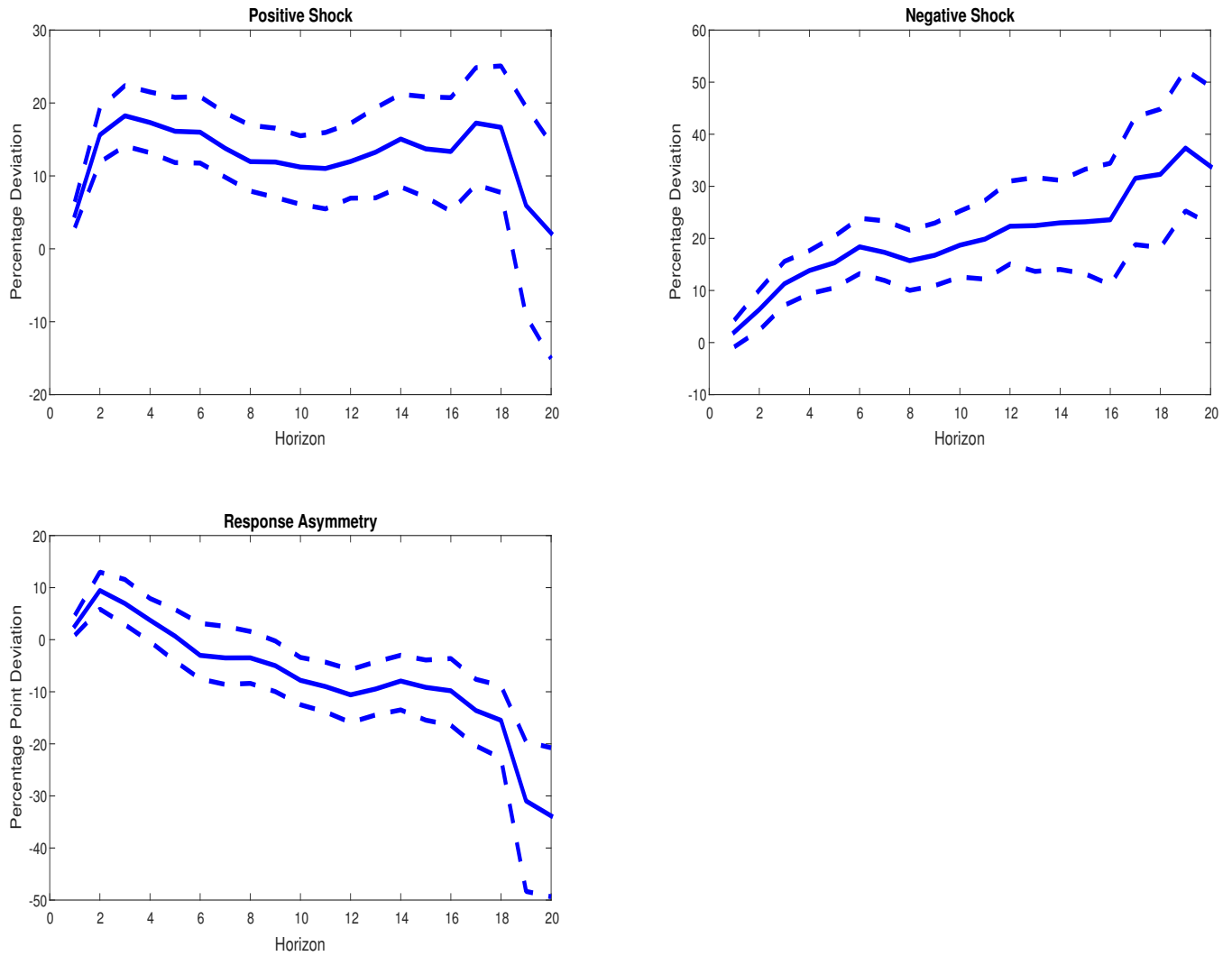
Notes: This figure presents the sign-dependent impulse responses of EMBI (country credit spreads) to positive and negative one standard deviation risk appetite shocks as well as the difference between the responses to the shocks. Solid lines depict median estimates and dashed lines correspond to the 68% posterior confidence bands. Responses are in terms of percentage deviations from pre-shock values. Horizon is in quarters.

Figure 18: **Sign-Dependent Responses of Output to Global Risk Appetite Shocks: (a) Pre-2008 Sample; (b) EMBI Sample.**
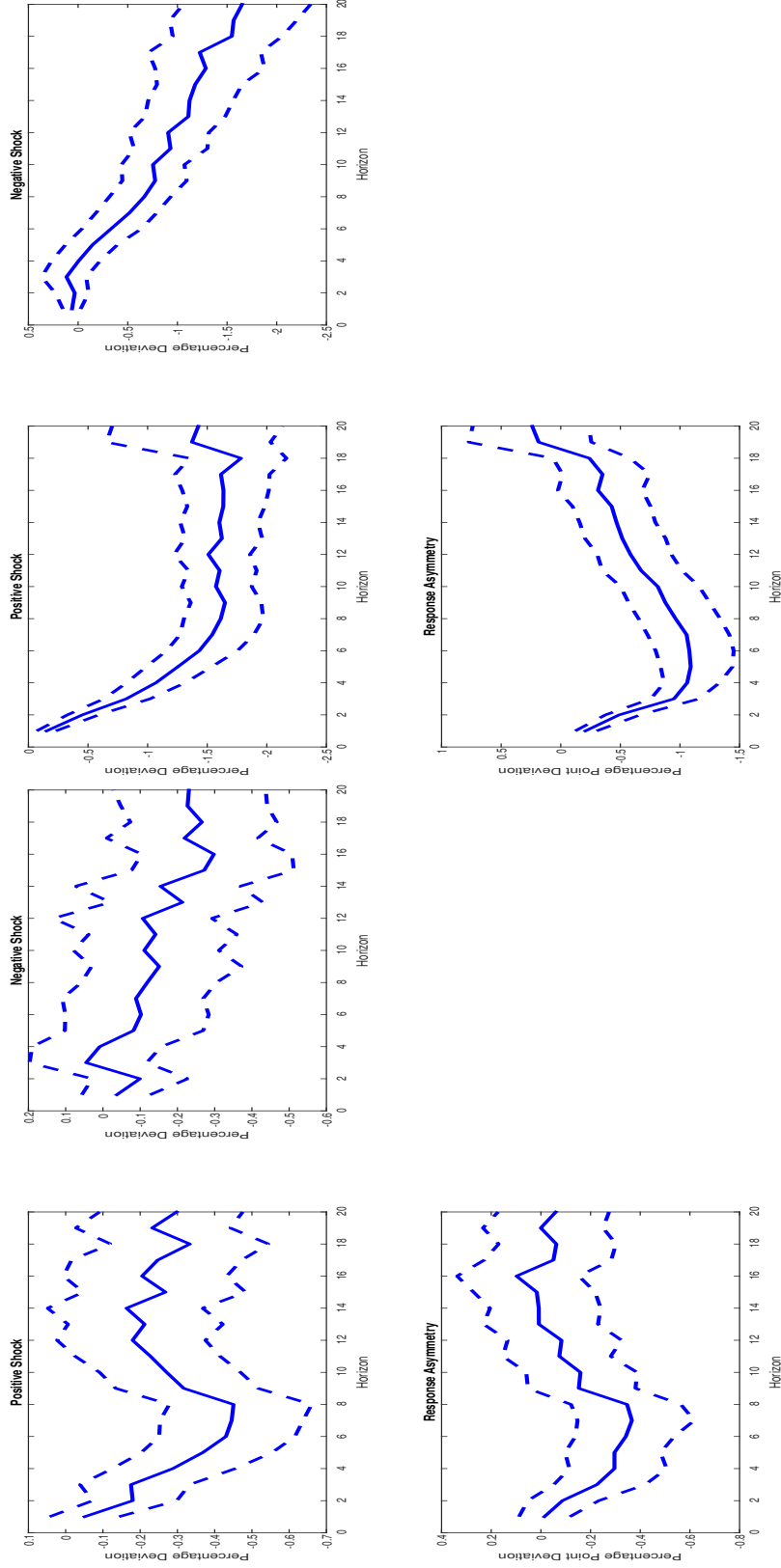
(a) Sign-Dependent Impulse Responses of Output to a One Standard Deviation Global Risk Appetite Shock (Pre-2008 Sample).

(b) Sign-Dependent Impulse Responses of Output to a One Standard Deviation Global Risk Appetite Shock (EMBI Sample).

Notes: Panel (a): This figure presents the sign-dependent impulse responses of output to positive and negative one standard deviation global risk appetite shocks from truncating the baseline sample at 2007:Q4. Solid lines depict median estimates and dashed lines correspond to the 68% posterior confidence bands. Responses are in terms of percentage deviations from pre-shock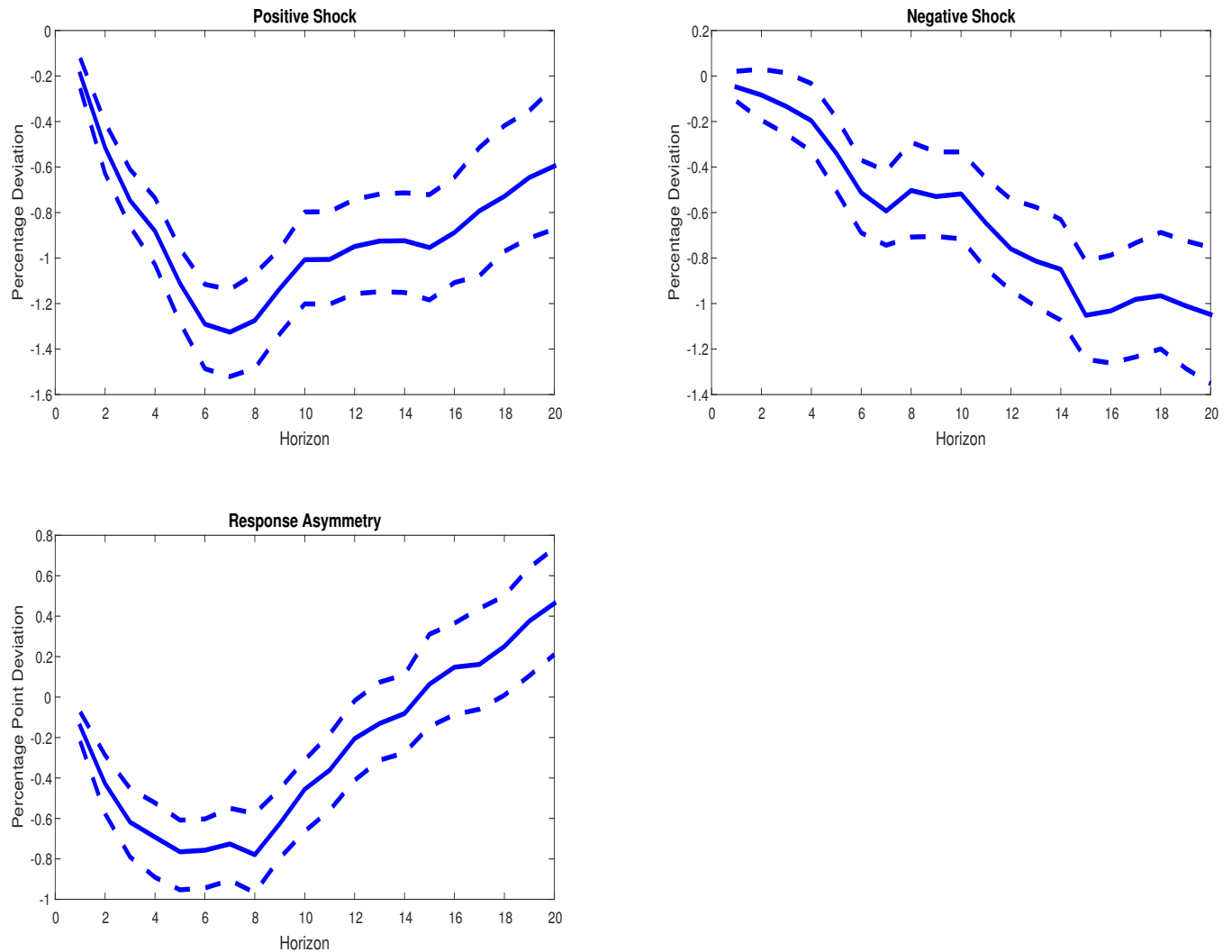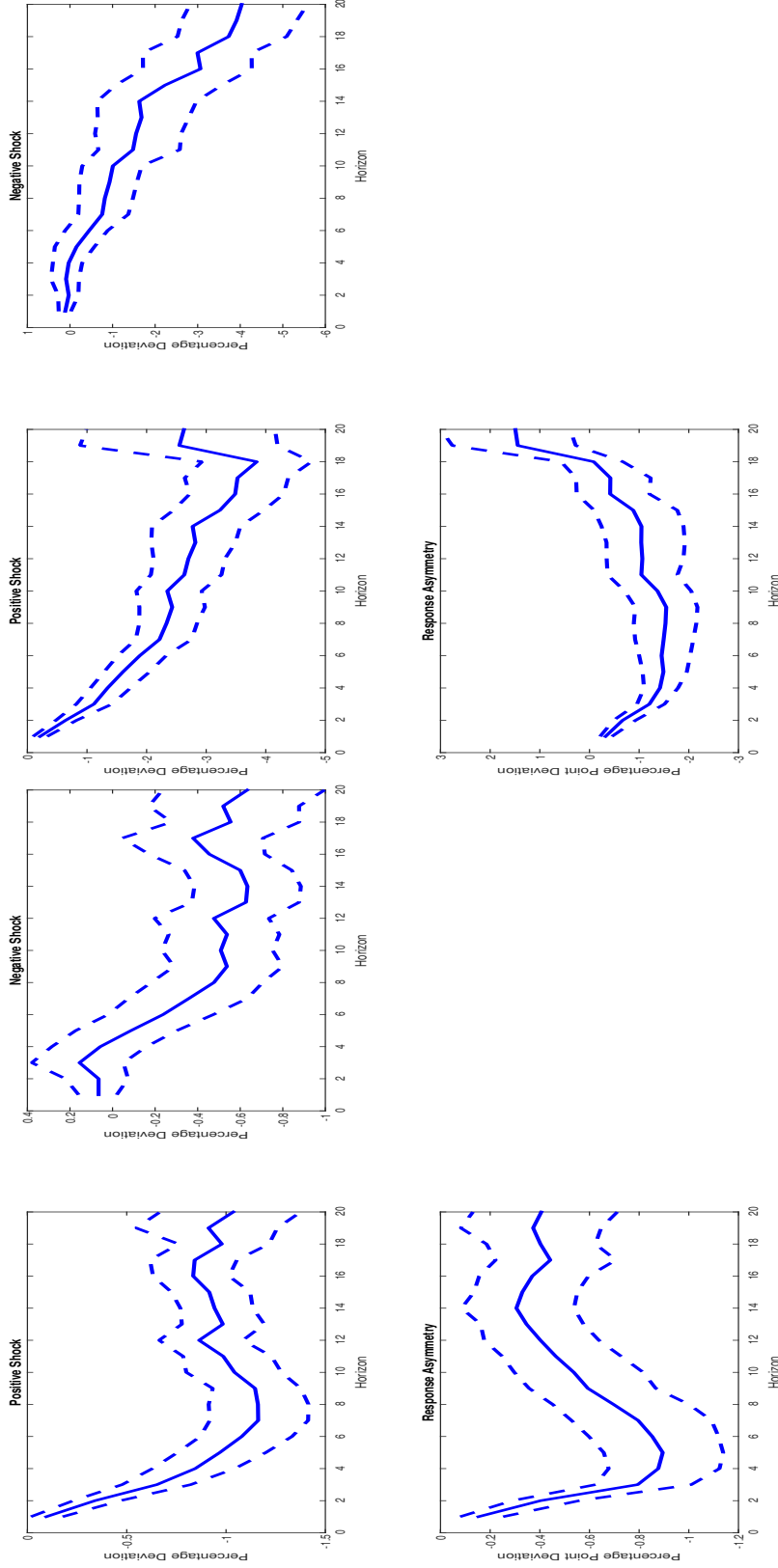 values. Horizon is in quarters. Panel (b): This figure presents the sign-dependent impulse responses of output to positive and negative one standard deviation risk appetite shocks from a sample that corresponds to the EMBI sample (which includes 21 countries, as detailed in Appendix A). Solid lines depict median estimates and dashed lines correspond to the 68% posterior confidence bands. Responses are in terms of percentage deviations from pre-shock values. Horizon is in quarters.

Figure 19: **Sign-Dependent Responses of Output to Global Risk Appetite Shocks: (a) Post-2000 Sample; (b) Excluding BRIC Economies.**

(a) **Sign-Dependent Impulse Responses of Output to a One Standard Deviation Global Risk Appetite Shock (Post-2000 Sample).**

(b) **Sign-Dependent Impulse Responses of Output to a One Standard Deviation Global Risk Appetite Shock (Excluding BRIC Economies).**

Notes: Panel (a): This figure presents the sign-dependent impulse responses of output to positive and negative one standard deviation global risk appetite shocks from removing pre-2000 observations from the baseline sample. Solid lines depict median estimates and dashed lines correspond to the 68% posterior confidence bands. Responses are in terms of percentage deviations from pre-shock values. Horizon is in quarters. Panel (b): This figure presents the sign-dependent impulse responses of output to positive and negative one standard deviation global risk appetite shocks from a removing the BRIC (Brazil, Russia, India, China) economies from the baseline sample. Solid lines depict median estimates and dashed lines correspond to the 68% posterior confidence bands. Responses are in terms of percentage deviations from pre-shock values. Horizon is in quarters.

Figure 20: **Sign-Dependent Effects of Global Risk Appetite Shocks on Output: Alternative Risk Appetite Shock Measure**.

Notes: This figure presents the sign-dependent impulse responses of output to positive and negative one standard deviation global risk appetite shocks from replacing FBP with the EBP series from Gilchrist and Zakrajšek (2012b). Solid lines depict median estimates and dashed lines correspond to the 68% posterior confidence bands. Responses are in terms of percentage deviations from pre-shock values. Horizon is in quarters.
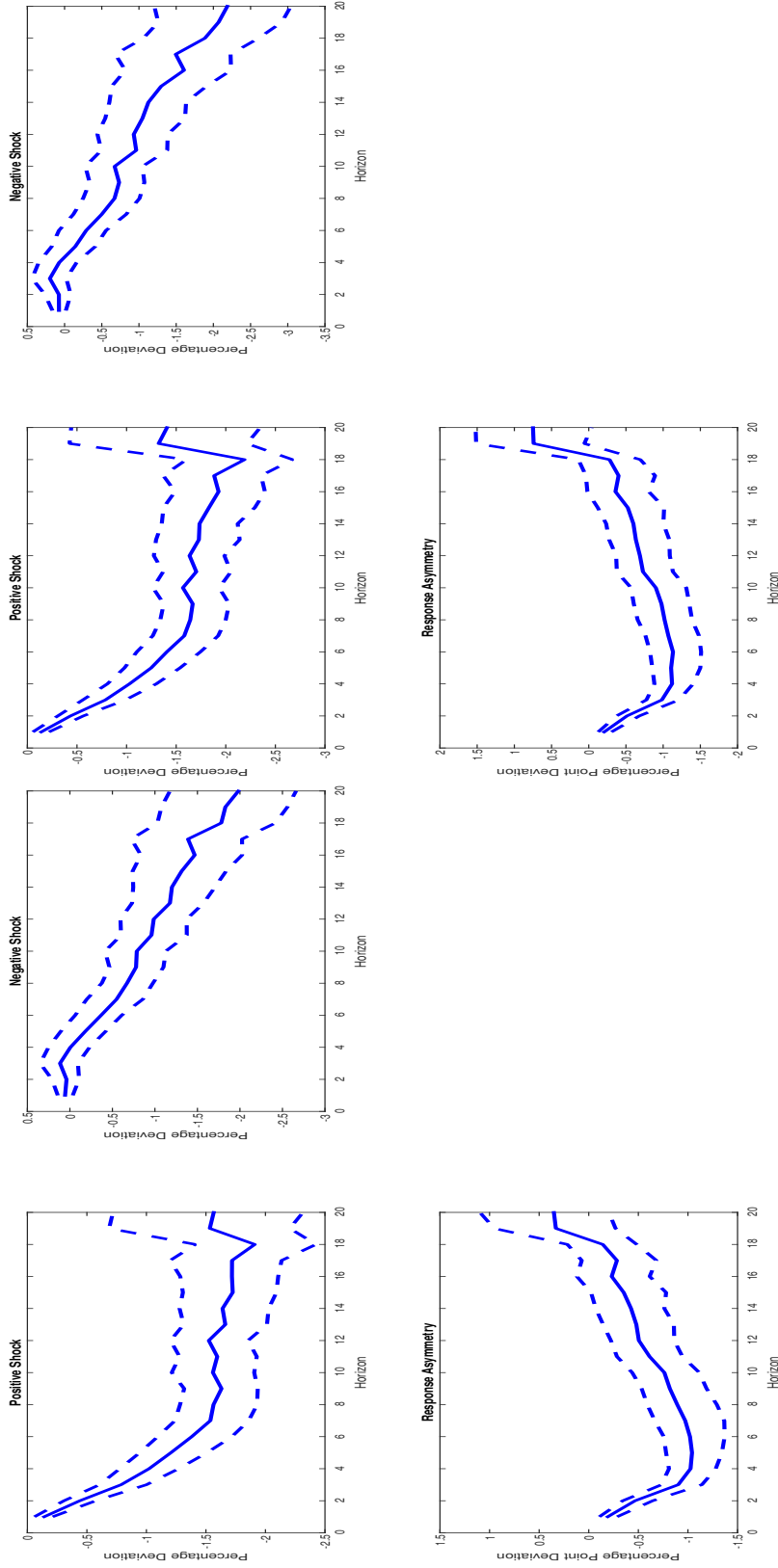
Figure 21: **Sign-Dependent Responses of Output to Global Risk Appetite Shocks: (a) HP-Filter; (b)** Hamilton (2018)′ **Detrending Method.**

(a) Sign-Dependent Impulse Responses of Output to a One Stan-
      dard Deviation Global Risk Appetite Shock (HP-Filter Sample).
(b) Sign-Dependent Impulse Responses of Output to a One Stan-
      dard Deviation Global Risk Appetite Shock (Hamilton (2018)′
      Detrending Method).

Notes: Panel (a): This figure presents the sign-dependent impulse responses of output to positive and negative one standard deviation global risk appetite shocks from extracting the cyclical component of output using an HP-filter. Solid lines depict median estimates and dashed lines correspond to the 68% posterior confidence bands. Responses are in terms of percentage deviations from pre-shock values. Horizon is in quarters. Panel (b): This figure presents the sign-dependent impulse responses of output to positive and negative one standard deviation global risk appetite shocks from extracting the cyclical component of output using Hamilton (2018)'s method. Solid lines depict median estimates and dashed lines correspond to the 68% posterior confidence bands. Responses are in terms of percentage deviations from pre-shock values. Horizon is in quarters.
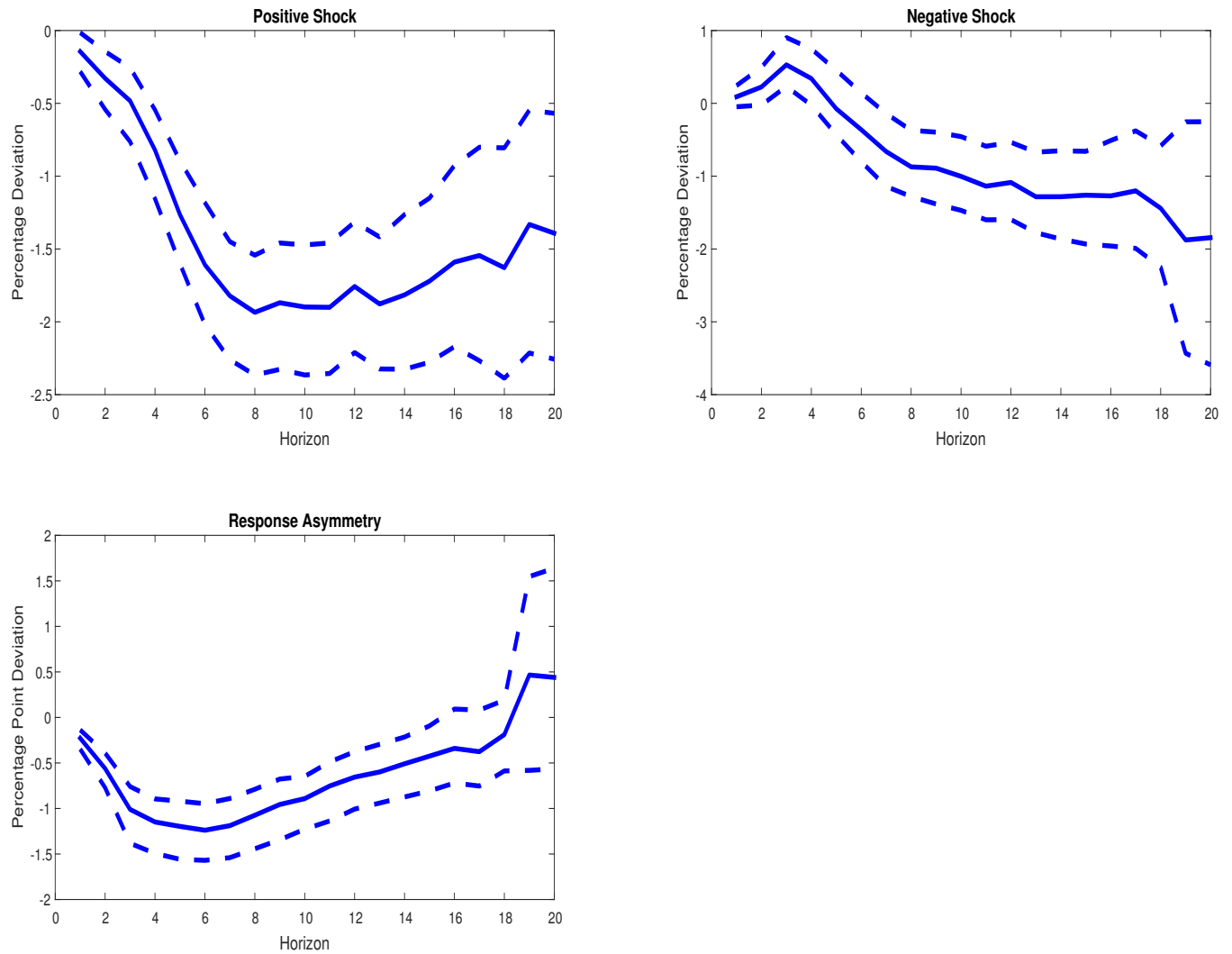
Figure 22: **Sign-Dependent Responses of Output to Global Risk Appetite Shocks: (a) Log-Quadratic Detrending; (b) Log-Linear Detrending.**

(a) **Sign-Dependent Impulse Responses of Output to a One Standard Deviation Global Risk Appetite Shock (Log-Quadratic Detrending).**

(b) **Sign-Dependent Impulse Responses of Output to a One Standard Deviation Global Risk Appetite Shock (Log-Linear Detrending).**

Notes: Panel (a): This figure presents the sign-dependent impulse responses of output to positive and negative one standard deviation global risk appetite shocks from extracting the cyclical component of output using log-quadratic detrending. Solid lines depict median estimates and dashed lines correspond to the 68% posterior confidence bands. Responses are in terms of percentage deviations from pre-shock values. Horizon is in quarters. Panel (b): This figure presents the sign-dependent impulse responses of output to positive and negative one standard deviation global risk appetite shocks from extracting the cyclical component of output using log-linear detrending. Solid lines depict median estimates and dashed lines correspond to the 68% posterior confidence bands. Responses are in terms of percentage deviations from pre-shock values. Horizon is in quarters.

Figure 23: **Sign-Dependent Effects of Global Risk Appetite Shocks on Output: Controlling for Size-Dependence**.

Notes: This figure presents the sign-dependent impulse responses of output to positive and negative one standard deviation global risk appetite shocks from adding a cubed shock term to Equation (12). Solid lines depict median estimates and dashed lines correspond to the 68% posterior confidence bands. Responses are in terms of percentage deviations from pre-shock values. Horizon is in quarters.

Figure 24: **Sign-Dependent Responses to Risk Shocks: (a) Accounting for Stronger Persistence of Negative Shocks; (b) Shutting Down the Stronger Persistence of Negative Shocks.**
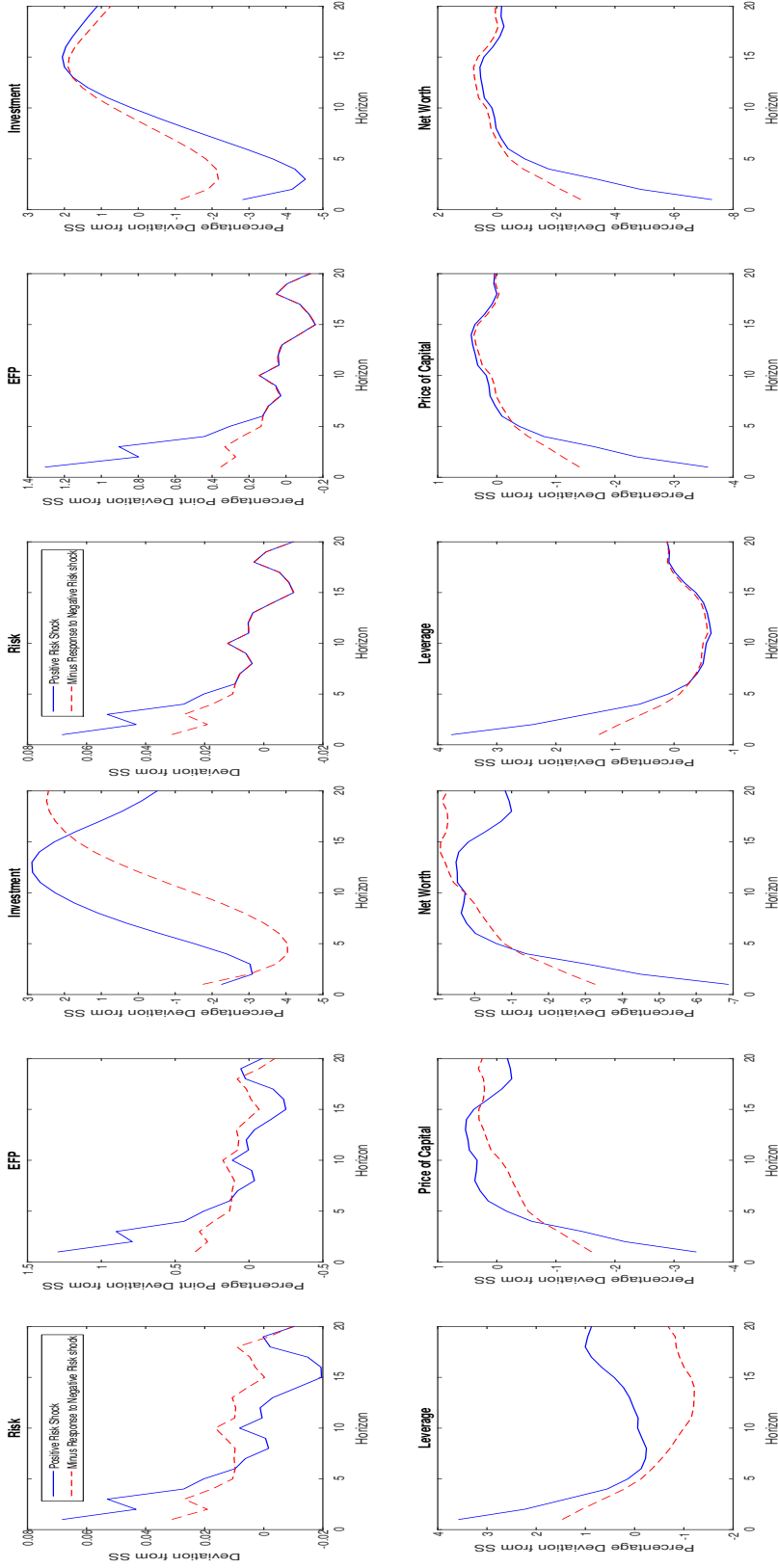
(a) Sign-Dependent Impulse Responses to Risk Shocks (Account- **(b) Sign-Dependent Impulse Responses to Risk Shocks (Shutting ing for Stronger Persistence of Negative Shocks).** **Down the Stronger Persistence of Negative Shocks).**

Notes: Panel (a): This figure presents the impulse responses to a positive and negative risk shock from the model presented in Section 3.2 where the exogenous process for risk was replaced by a second-order moving average process that admits the coefficients implied by the sign-dependent responses of FBP in the data. Panel (b): This figure presents the impulse responses to a positive and negative risk shock from the model presented in Section 3.2 where the exogenous process for risk was replaced by the second-order moving average process underlying Figure 24a up the 6th horizon, from that point forward imposing symmetry on the effects of positive and negative shocks. For both figures, the responses are shown in terms of percentage deviations from steady state values (except for risk and EFP, whose responses are shown in terms of raw deviation and percentage point deviation, respectively). Solid lines depict responses to a positive risk shock, whereas dashed lines present responses to a negative shock (multiplied by -1 for comparison purposes). Horizon is in quarters.